UHASSELT
KNOWLEDGE IN ACTION

Maastricht University

Faculteit Geneeskunde en Levenswetenschappen
School voor Levenswetenschappen

master in de biomedische wetenschappen

Masterthesis

Vegetation exposed to traffic exhaust: a dual study of chlorophyll fluorescence kinetics in Platanus x acerifolia and antioxidative responses in Brassica oleracea var. italica

Mathias Lenaers

Scriptie ingediend tot het behalen van de graad van master in de biomedische wetenschappen, afstudeerrichting milieu en gezondheid

PROMOTOR :

Prof. dr. Roland VALCKE

BEGELEIDER :

De heer Dimitri DAUWE

2017
2018

De transnationale Universiteit Limburg is een uniek samenwerkingsverband van twee universiteiten in twee landen: de Universiteit Hasselt en Maastricht University.

UHASSELT
KNOWLEDGE IN ACTION

www.uhasselt.be
Universiteit Hasselt
Campus Hasselt:
Martelarenlaan 42 | 3500 Hasselt
Campus Diepenbeek:
Agoralaan Gebouw D | 3590 Diepenbeek

UHASSELT
KNOWLEDGE IN ACTION

Maastricht University

Faculteit Geneeskunde en Levenswetenschappen

School voor Levenswetenschappen

master in de biomedische wetenschappen

Masterthesis

Vegetation exposed to traffic exhaust: a dual study of chlorophyll fluorescence kinetics in Platanus x acerifolia and antioxidative responses in Brassica oleracea var. italica

Mathias Lenaers

Scriptie ingediend tot het behalen van de graad van master in de biomedische wetenschappen, afstudeerrichting milieu en gezondheid

PROMOTOR :

Prof. dr. Roland VALCKE

BEGELEIDER :

De heer Dimitri DAUWE

ACKNOWLEDGEMENTS

This internship has been a great opportunity for me to experience first-hand how to think and conduct experiments as a researcher. This master in particular, has taught me step by step how to discuss and interpret scientific literature all the way up to designing my own experiments and dealing with matters concerning the financial part of science and scientific integrity. As a bachelor in biology, I do not regret my decision to follow this master as it has provided me the skills and attitudes for my future endeavors.

Foremost, I would like to thank my supervisor, **Dimitri Dauwe**, who has provided excellent guidance throughout my Senior Practical Training. Dimitri was always prepared to make time to answer questions, or go through the data I obtained. Furthermore, I could always count on his support, both when developing my research proposal and during my practical training, and I am grateful to have worked with him.

In addition to my supervisor, I would like to thank my promotor, **prof. dr. Roland Valcke**. Even though he retired at the start of the academic year, he still managed to make time to visit the campus regularly, and to discuss my results and provide input on my analyses. Moreover, I am grateful for the necessary funding he provided to perform this research.

With regard to the sampling campaign in Hasselt during August and September, I would like to thank **Nico Vanuytrecht** and the community landscaping services of the city of Hasselt for scheduling and arranging a height worker to collect our samples. Furthermore, my thanks also go to **Carine Put** for performing the ICP-OES analysis on our collected samples. Additionally, I would like to thank **Charlotte Vanpoucke** of IRCEL for providing the air pollution data of our sampling points in Hasselt.

In addition to the summer campaign, there are several people I would like to thank who have guided me throughout the course of my Senior Practical Training.

First, my thanks go to **dr. Hanne Vercampt** for providing input on the total antioxidative capacity analysis, as well as answering my questions during the data analysis afterwards. Then, my thanks go to **Karolien Bijnens** and the **zoology department** of Hasselt University for providing the protocol and materials for the hydrogen peroxide analysis, as well as the reagents for the Bradford protein assay. Next, I would like to thank **dr. Nick Smisdom** for the time and effort put into the confocal microscopy measurements, and the data analysis afterward. Subsequently, my thanks also go to **dr. Els Keunen**, **dr. Heidi Gielen**, and in particular **Sophie Hendrix**, for their valuable input and guidance throughout the gene expression analysis. Furthermore, I would like to thank the **oxidative stress department** for providing the reagents to perform this experiment.

In addition, I would like to thank **Erin Dobrange** for her work on antioxidant enzyme activities during her bachelor thesis, as well as for providing the schematic drawing of the diesel engine set-up.

Finally, I would like to thank everyone else who has contributed to the completion of this thesis.

ABSTRACT

PART I: The impact of traffic-related air pollution on chlorophyll fluorescence kinetics in London Plane (*Platanus x acerifolia*)

Air pollution worldwide is increasing, and it is considered the largest environmental threat to human health. Cities, in particular, have been experiencing worsening air quality, a direct consequence of further urbanization accompanied with an increased traffic load. Urban vegetation is directly exposed to the present air pollution, and has the potential to serve as a bioindicator for poor air quality. Recent studies focus on changes in plant physiology, specifically chlorophyll fluorescence kinetics, to monitor air quality. This study carried out a comparison of Hasselt's busy inner ring road, and Kapermolen Park outside the city center. We hypothesized that leaves of London Planes near Hasselt inner ring road showed altered physiological and structural characteristics compared to those near Kapermolen Park. Results showed a significantly higher presence of Cu, Fe and Pb in leaves from Hasselt inner ring road compared to the reference site, which are all related to traffic exposure. Moreover, these leaves also show a significantly higher performance index and electron transport rate, a finding that correlates with previous work and indicates a stress-induced increase in plant performance. Finally, a correlation analysis of the investigated parameters showed a significant association between the specific leaf area and heat dissipation, and the relative chlorophyll content and Cu, Zn, and Ni with some of the parameters of the chlorophyll fluorescence kinetics, the latter of which are all involved in processes of photosynthesis or plant growth and development. We conclude that trees near Hasselt inner ring road indicate a higher overall performance and show more deposition of traffic-related heavy metals.

PART II: Antioxidative responses in *Brassica oleracea* var. *italica* induced by diesel exhaust exposure

Plants are continuously exposed to their environment, and respond to a variety of stressors in their immediate surroundings. Among these stressors, air pollutants have been shown to cause various responses, including changes in plant performance and growth. Effects on plant antioxidant defences have been little studied, but might lie at the root of the responses at higher organization levels. Diesel exhaust in particular, could induce damaging effects because it contains relatively high amounts of combustion gasses and particulates. Therefore, it serves as an interesting tool to study the defence mechanisms of plants against traffic emissions. We hypothesized that leaves of broccoli exposed to diesel exhaust showed altered antioxidative responses. Results indicated that exposed leaves have a significantly lower total antioxidative capacity, which could indicate that antioxidant resources are being depleted. This finding is confirmed by lower $(NADH + H^+)/NAD^+$ and $FADH_2/FAD$ ratios in exposed leaves, suggesting that these plants show an altered cellular redox state. Moreover, an overall higher amount of H_2O_2 was observed in exposed leaves, demonstrating the adverse impact of diesel exhaust on the physiology of broccoli leaves. Finally, a general trend of fewer transcripts of antioxidative enzymes was observed in exposed plants. This indicates a stress-induced downregulation in contrast to higher antioxidant enzyme activities found in a previous study. Based on this, we suggest that plants rather optimize the use of available enzymes than invest in the production of more. We conclude that plants are affected by diesel exhaust which leads to antioxidant depletion, a change in their cellular redox state and altered antioxidant gene expression.

SAMENVATTING

Deel I: De impact van verkeersgerelateerde luchtvervuiling op de chlorofylfluorescentiekinetiek in de Gewone plataan (*Platanus x acerifolia*)

Luchtvervuiling is wereldwijd aan het stijgen, en wordt beschouwd als het grootste gezondheidsrisico voor de mens. Vooral steden hebben te kampen met almaar slechtere luchtkwaliteit, wat een direct gevolg is van doorgedreven verstedelijking met een bijbehorende stijging in verkeersdrukte. Stadsvegetatie is van nature blootgesteld aan luchtvervuiling, en kan bijgevolg dienen als bioindicator van slechte luchtkwaliteit. Recent onderzoek focust op veranderingen in plantenfysiologie, specifiek op chlorofylfluorescentiekinetiek, om luchtkwaliteit te monitoren. Dit onderzoek voerde een vergelijking uit tussen de Kleine Ring in Hasselt, de drukke verkeersring, en Kapermolen Park net buiten het centrum. Onze veronderstelling was dat bladeren van platanen nabij de Kleine Ring, veranderde fysiologische en structurele karakteristieke vertoonden vergeleken met bladeren van platanen uit Kapermolen Park. Onze resultaten toonden een verhoogde aanwezigheid van Cu, Fe en Pb aan in bladeren van platanen op de Kleine Ring, die alle drie gerelateerd zijn aan verkeer. Bovendien presteerden deze bladeren ook beter en vertoonden ze een efficiënter elektronentransport, dat overeenkomt met bevindingen die eerder werden gepubliceerd, en wijzen op een verhoogde prestatie onder invloed van stress. Tot slot wees een correlatieanalyse van de onderzochte parameters op een significante associatie tussen het specifieke bladoppervlakte en warmtedissipatie, en tussen de relatieve hoeveelheid chlorofyl en Cu, Zn en Ni met sommige chlorofylfluorescentie parameters. Deze laatsten zijn allen betrokken in fotosynthese of groei en ontwikkeling van de plant. Wij concluderen dat platanen van de Kleine Ring beter presteren ondanks de hogere depositie van zware metalen gerelateerd aan verkeer.

Deel II: Antioxidatieve responses in *Brassica oleracea* var. *italica* blootgesteld aan dieselemissies

Planten zijn voortdurend blootgesteld aan hun omgeving, en reageren op verscheidene stressfactoren in hun directe omgeving. Het is aangetoond dat luchtvervuilende stoffen verscheidene responsen uitlokken, zoals veranderingen in de groei en prestatie van planten. Effecten op de antioxidatieve verdediging zijn nog maar weinig onderzocht, maar zouden aan de basis kunnen liggen van responsen op hogere organisatieniveaus. Dieselemissies in het bijzonder kunnen schadelijke effecten hebben, omdat ze relatief hoge hoeveelheden van verbrandingsgassen en partikels bevatten. Zodoende kunnen deze emissies een interessant model vormen om de verdedigingsmechanismen van planten tegen verkeersemissies te onderzoeken. Onze veronderstelling was dat broccolibladeren blootgesteld aan dieselemissies, veranderde antioxidatieve responsen vertoonden. Onze resultaten toonden aan dat blootgestelde bladeren een lagere totale antioxidatieve capaciteit vertoonden, wat een indicatie zou kunnen zijn dat antioxidatieve middelen worden uitgeput. Deze bevinding wordt bevestigd door lagere $(NADH + H^+)/NAD^+$ en $FADH_2$/FAD ratio's in blootgestelde bladeren, wat wijst op een veranderde cellulaire redox toestand. Bovendien werd een verhoogde hoeveelheid H_2O_2 gemeten, die de schadelijke impact van dieselemissies aantoont. Tenslotte, een algemeen verlaagde hoeveelheid transcripten van antioxidatieve enzymen werd vastgesteld. Dit wijst op een stress-geïnduceerde downregulatie in tegenstelling tot hogere enzymactiviteit die eerder werd bevonden. Op basis hiervan suggereren wij dat de planten de beschikbare enzymen gebruiken in plaats van er meer te produceren. Wij concluderen dat planten worden aangetast door dieselemissie, wat leidt tot depletie van antioxidatieve middelen, een veranderde cellulaire redoxtoestand, en veranderde genexpressie.

TABLE OF CONTENTS

LIST OF ABBREVIATIONS

ABS	(based on) absorption
APX	Ascorbate peroxidase
BC	Black carbon
CAT	Catalase
CCI	Chlorophyll content index
CCM	Chlorophyll content meter
Chl	Chlorophyll
ChlF	Chlorophyll fluorescence
CS_m	Cross-sectional (based on F_m)
cDNA	Complementary DNA
DI	Dissipation
DTT	1,4-Dithiothreitol
EOM	Electro-optical modulator
ETR	Electron transport rate
FAD	Flavin adenine dinucleotide
FMN	Flavin mononucleotide
FRAP	Ferric reducing antioxidant power
FW	Fresh weight
GPX	Glutathione peroxidase
GR	Glutathione reductase
GuPX	Guaiacol peroxidase
HF	Hydrophilic fraction
ICP-OES	Inductively coupled plasma - optical emission spectrometry
IRCEL	Intergewestelijke cel voor het leefmilieu
LF	Lipophilic fraction
LHC	Light harvesting center
LSM	Laser scanning microscopy
LWC	Leaf water content
MASL	Meters above sea level
NADH	Nicotinamide adenine dinucleotide
NPQ	Non-photochemical quenching
PAM	Pulse amplitude modulation
PEA	Plant efficiency analyzer
PI	Performance index
PM	Particulate matter
PS	Photosystem
$PQ(H_2)$	Plastoquinone
Q_A	Quinone a
Q_B	Quinone b
RC	Reaction center
ROS	Reactive oxygen species
RPM	Rotations per minute
SOD	Superoxide dismutase
SPX	Syringaldazine peroxidase
SLA	Specific leaf area
RT-qPCR	Reverse transcription - quantitative polymerase chain reaction
TAC	Total antioxidative capacity
TPTZ	2,4,6-Tris(2-pyridyl)-*s*-triazine
UV/Vis	Ultraviolet/visible (radiation)

1. INTRODUCTION

1.1 The issue of (urban) air pollution due to increase in traffic density

Air pollution worldwide is getting worse, and at present it is considered the world's single largest environmental health risk. An estimated seven million people die prematurely each year as a result of exposure to air pollution.[1] In particular, the air in cities is becoming more and more polluted, a direct consequence of further urbanization accompanied with an increased traffic load on city roads.[2] Traffic contributes a major fraction to the amount of air pollution in cities and this contribution is estimated to increase as more and more vehicles are congesting city roads.[3] It is therefore important to be able to monitor air pollution and the impact of traffic exposure in urban environments, which could help to take measures and/or precautions to reduce its adverse effects.

Monitoring of air pollution typically relies on data from physical monitoring devices. However, these are often spaced few and far between, allowing only regional average values to be extrapolated. As a result, they do not provide high spatial resolution.[4] Moreover, physical measurements are point measurements; they are limited in their ability to provide a time-integrated (i.e. continuous) analysis of air pollutants. Lastly, physical monitoring is costly, requiring the purchase and maintenance of expensive equipment.[4] Monitoring through plants can serve as an alternative to alleviate these shortcomings. Plants have previously been used to monitor air pollution, and their responses have been linked to exposure to a variety of air pollutants.[5] They can be used to monitor air pollution in any location where vegetation is present. Furthermore, because plants are continuously exposed to their environment, a complete time-integrated exposure assessment is possible. Finally, monitoring is relatively cheap and quick to perform, making large-scale assessments feasible.

1.2 Use of vegetation for early detection of poor air quality

1.2.1 The principle: the chlorophyll fluorescence pathway

Photosynthesis is a process whereby plants use the absorbed light energy to synthesize carbohydrates. Light energy is captured by pigment molecules, chlorophylls and carotenoids, to drive the photosynthetic reactions. These pigments are present as pigment-protein (antenna) complexes in photosystem I and II (PSI and PSII) and as a component of the light harvesting complexes (LHCs) which are tightly associated with the reaction centers (RC) of the PS complexes.[6] Light energy that is absorbed can proceed in three directions: (1) energy can be used for photochemistry, (2) excess energy can be dissipated as heat, and (3) a small fraction can be re-emitted by a process called chlorophyll fluorescence.[7] These three processes are in competition with one another for the amount of energy absorbed by the antenna complexes. Heat dissipation and mechanisms involved in energy use regulation (other than chlorophyll fluorescence) will be given in the section 'other dissipation pathways'. In this section the focus lies entirely on the chlorophyll fluorescence pathway.

Chlorophyll fluorescence (ChlF) is a natural phenomenon which occurs when incident light is re-emitted in the red and far-red spectrum.[8] The signal originates entirely from chlorophyll (Chl) *a* due to rapid energy transfer from Chl *b* in the antenna complexes.[9] The absorbed light energy reaches the RC of PSII and PSI, and is re-emitted as fluorescence at 685 nm and 720-740 nm, respectively (Fig. 1). ChlF is assumed to originate mainly from PSII at room temperature with only a negligible contribution of PSI, and amounts for about 1-2% of energy absorbed.[11] Because ChlF is such a tiny signal to be detected (it cannot be detected with the naked eye), it is hard to separate from ambient light.

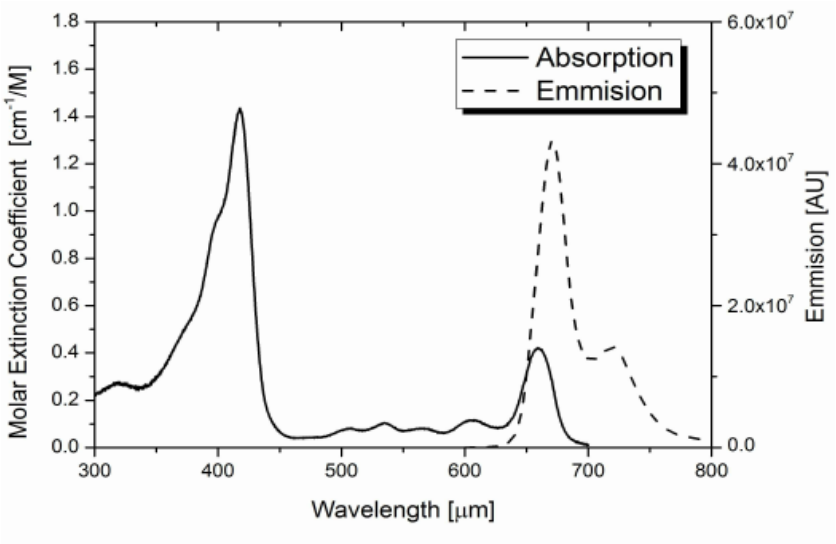

Fig. 1 – General Chl *a* absorption spectrum and ChlF emission spectrum. (From Lee et al. 2012)[10]

Therefore, early measuring systems had to be performed in a dark or a controlled light environment. These shortcomings were addressed by the development of devices which apply controlled light pulses to measure changes in fluorescence kinetics. The earliest work on this was performed by Kautsky and co-workers,[12] who found that when a leaf is exposed to light after a period of dark-adaptation, there is an initial rise in fluorescence over a period of 1s. This rise relates to the reduction of electron acceptors downstream of PSII, namely plastoquinone (PQ) and quinone b (Q_B). As soon as PSII accepts an electron and passes it through to quinone a (Q_A), it is unable to accept a subsequent one until the next electron carrier in line, Q_B, receives the electron from Q_A. The RC are said to be in a 'closed' state during this period. The presence of these closed RC at any instance leads to a maximal fluorescence yield due to saturation of the electron transport chain up till PQH_2.[13-14] The Kautsky curve, also called the fluorescence induction, describes the kinetics of the initial excitation and electron transfer to PQH_2. It is often referred to as the 'OJIP' curve, where each letter represents a subsequent step in the electron transport to PQH_2.[15] The OJIP curve describes the 'fast' ChlF induction kinetics, and an analysis of its transient provides information on plant overall performance and the efficiency of absorption and electron transfer to and in PSII.[16]

Subsequent developments lead to techniques using modulated pulses,[17] such as the PAM (Pulse Amplitude Modulation). The basic principle involves dark-adapting a leaf, followed by directing a measuring light that does not substantially drive photosynthesis to measure basic fluorescence (F_0). Next, a high-intensity pulse is emitted that saturates the electron transport leading to a closed state of all PSII RC to measure maximal fluorescence (F_m). At a regular interval, a high-intensity pulse is emitted to measure maximal fluorescence of a light-adapted leaf (F_m'). The latter unit is lower than F_m due to the partial reduction of the acceptor side of PSII.[13,18] Following the maximal fluorescence yield immediately after administering a high-intensity pulse, the signal is rapidly dampened by two processes that quench the fluorescence signal, namely photochemical and non-photochemical quenching[19] (more on the term quenching in the section 'other dissipation pathways').

Photochemical yield - Y(II) - involves the opening of PSII RC whereby electron transfer starts to direct the incident energy further down the electron pathway. Non-photochemical yield consists of both a regulated - Y(NPQ) - and non-regulated - Y(NO) - component. The regulated component consists of quenching processes such as the xanthophyll cycle, while the non-regulated component exists of

heat dissipation.[20] The three processes are complementary: Y(II) + Y(NO) + Y(NPQ) = 1. Consequently, an analysis of the fluorescence transient following the high-intensity pulses allows to determine the contribution of each component during the quenching process until a steady-state condition is reached.[20] The slope of the slow kinetics curve and the light induction curve reveal information on plant stress recovery. Moreover, an analysis of the quenching processes during the fluorescence transient allows to evaluate how efficient incident light energy is used for photochemistry and to analyze the portions of dissipated excess energy, regulated or non-regulated.[21]

ChlF kinetics have been used in this regard to evaluate if, and to what extent, plants are exposed to stressors in their environment.[22] Furthermore, it can provide a tool to study vegetation using both active and passive techniques. Active techniques include fluorimeters using the modulated pulse method described earlier. These more conventional devices involve labor intensive contact measurements compared to passive techniques.[23] The latter techniques can make use of measuring the fluorescence emission of samples that have reached their steady-state condition, which is termed steady-state fluorescence (Fs). Passive Fs has previously been used to measure effects of a number of stressors, including those of air pollutants.[24] In contrast to active techniques, passive devices do not emit a light pulse but can monitor vegetation from an airborne platform by analyzing the light reflected by earth's surface, such as monitoring through remote sensing using a drone, plane, satellite or specialized spectroradiometers.[25] Remote sensing allows large-scale assessments with high spatial resolution, requiring a lot less time. The use of this passive technique will therefore serve as the future of biomonitoring. A brief explanation of remote sensing follows in the next section.

1.2.2 The future application: remote sensing (hyperspectral measurements)

In remote sensing, energy emanating from earth's surface is analyzed using a sensor mounted on an aircraft or spacecraft platform. Data obtained by these measurements are directly send to a ground station, and are subsequently processed to obtain imagery.[26] There are two types of monitoring: active and passive. In active monitoring, the sensor emits its own signal towards earth's surface and measures the reflection of this signal, while in passive monitoring the sensor measures the emission of the surface in response to incident sunlight.[27] Active sensors include imaging radar and LIDAR (Light Detection and Ranging), while passive sensors include infrared, charge-coupled devices (CCD) and radiometers. Specific wavelengths or certain frequencies are used by passive sensors for measuring the reflected light. The various forms of reflected incident energies with different wavelength ranges are also referred as spectral bands.[28] When multiple different bands (usually 3 to 10) can be measured at once, the process is called multispectral imaging. When many different bands can be analyzed, the process is named hyperspectral imaging.[29] Hyperspectral sensors typically collect 200 or more bands which enables the construction of an almost continuous reflectance spectrum for every pixel in the image they obtain (Fig. 2). These contiguous narrow bands allow for an in-depth investigation of earth surface features, including analysing changes of and responses by vegetation.[31] In this respect, remote sensing using hyperspectral imaging allows for a wide-scale non-invasive method of monitoring the responses of vegetation to different environmental stressors.[32] Several studies successfully produced reliable Chl maps from vegetation reflectance. Recent studies focus on the production of ChlF maps which is only a subtle part of the reflectance signal and sensitive to early stress exposure.[33-34] In the case of air pollution, remote sensing could aid in providing local governments information on which areas are most affected, in order that measures could be taken to reduce its impact on human health.

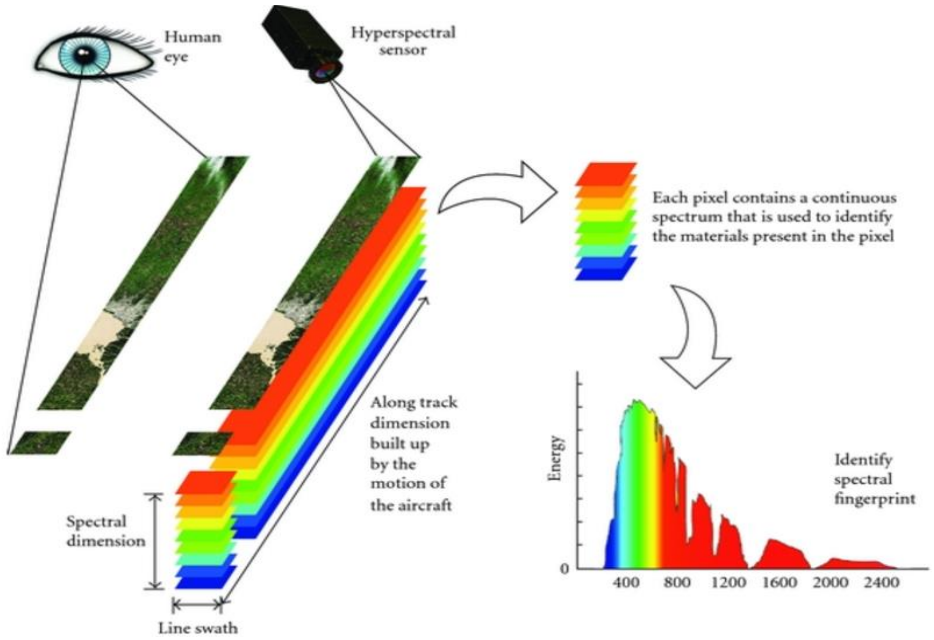

Fig. 2 – Mechanism of hyperspectral imaging using a hyperspectral sensor. (From Aiazzi et al. 2012)[30]

1.2.3 Other dissipation pathways

When a molecule of chlorophyll absorbs incident light energy during photosynthesis, it is elevated to its singlet excited state (^{1}Chl*) from which the three complementary processes of energy dissipation can occur.[35] When the energy stored in Chl in the excited state is rapidly dissipated by excitation transfer or photochemistry, the excited state is said to be quenched.[36-37] If the excited state is not rapidly quenched, it can be converted to its triplet state (^{3}Chl*), and react with molecular oxygen to form an excited state of oxygen known as singlet oxygen ($^1O_2$*), which may react further and cause damage to cellular components.[38-39] Excess excitation energy has the potential to increase the lifetime of ^{1}Chl*, thereby increasing the odds of developing long-lasting Chl triplet states by inter-system crossing with its potential to cause adverse effects to pigments, proteins and lipids in the thylakoid membrane.[39] Plants have a range of photoprotective mechanisms in store to protect them from damage resulting from excess excitation energy. The most notable among these mechanisms is non-photochemical quenching (NPQ), which includes processes involved in transforming and dissipating excess energy into heat.[40] NPQ is thought to prevent photoinhibition from occurring, which is a process that decreases the photosynthetic efficiency and can be triggered by a range of environmental stressors.[41] It includes both slow responses (minutes to hours) and fast responses (seconds to minutes), based on their induction and relaxation kinetics.[42] The former consists of the xanthophyll cycle: three carotenoids (zeaxanthin, violaxanthin and antheraxanthin) present in the LHCs that can be interconverted to favor conformational changes that regulate quenching and heat dissipation.[42] The latter responses happen at the biochemical level and are conventionally thought to consist of two reversible components: the state transitions (qT) and the pH- or energy-dependent component (qE), of which the latter is assumed to be the most prominent in plants.[43] qE involves the buildup of a pH gradient across the thylakoid membrane, and is thought to consist of either a mechanism that regulates the efficiency of energy transfer to the RC, or an altered pathway of electron transfer in the RC.[44] Both slow and fast responses are interrelated in a complex network involving changes in energy

transfer and use in and between antenna complexes to provide a safe-guarding system to regulate excess excitation energy.[45]

1.2.4 **Research objective part I:** Traffic exposure and performance of urban trees in Hasselt

Preliminary data of our research group has indicated changes in leaf physiological parameters of urban vegetation in Antwerp and Valencia, located next to busy traffic roads. Hasselt, the provincial capital of Limburg, has seen increasing urbanization and a resultant increased traffic load in recent years. In particular, the inner ring road is the main intersection for traffic in the center of Hasselt, and has become on the city's busiest roads. Accordingly, it remains to be determined how vegetation in Hasselt is affected by the increasing amount of traffic that the city center is experiencing. This lead to our first research question: 'Are trees located near Hasselt inner ring road affected by increased traffic exposure?' We hypothesize that trees of *Platanus x acerifolia* present near Hasselt inner ring road show altered physiological and structural responses and increased heavy metal deposition compared to trees at a reference site in Kapermolen Park.

1.3 Plant antioxidant responses to stress conditions

1.3.1 Plant responses and the environment

Plants are versatile multicellular organisms that have developed through millions of years to come to dominate the planet by colonizing virtually every environment. Their ability to adapt to any environmental condition which they encounter in their surroundings is the root of this success. Moreover, plants are able to cope with and respond to changes in their environment in a variety of ways, such as adapting leaf sizes, investing in secondary metabolites or regulating nutrient uptake.[46] Though, adapting to changes is inherently stressful for a plant. If these changes are not too drastic, the plant will not experience destructive effects. However, if stress conditions becomes too severe, the plant may not be able to cope anymore, and consequently damage can occur.[47]

1.3.2 Formation of reactive oxygen species

If environmental stress experienced by a plant crosses a certain threshold, damaging events occur at the biochemical level due to the production of excessive amounts of reactive oxygen species (ROS).[48] ROS include both free radicals (e.g. superoxide anion ($O_2^{\bullet -}$), hydroxyl radical ($^{\bullet}OH$)) and non-free radicals (e.g. hydrogen peroxide (H_2O_2), singlet oxygen ($^1O_2$)).[48] The production of ROS is an inevitable result of aerobic metabolism: electron leakage during electron transport activities in the chloroplast, mitochondria and plasma membranes contribute a major part, but byproducts of certain cellular processes (e.g. peroxisomes) may also contribute a significant amount.[49] Furthermore, there is a clear link between the processes involved in photosynthesis and the formation of excessive amounts of ROS (Fig. 3). As mentioned previously, the absorption of sunlight excites a chlorophyll molecule excited to its singlet state by electron transfer. At this point, four pathways are possible: the energy may flow to the complementary mechanisms involved in photosynthesis (photochemistry (1), fluorescence emission (2) and heat dissipation (3)). Yet, if the lifetime of the singlet state is increased, ^{3}Chl* can be produced which can interact with oxygen to form $^1O_2$ (4). Singlet oxygen can react further to create free radicals such as $^{\bullet}OH$. Nonetheless, the presence of ROS is to a certain extent necessary, as they are known to be important secondary messengers for a number of cell processes, including tolerance

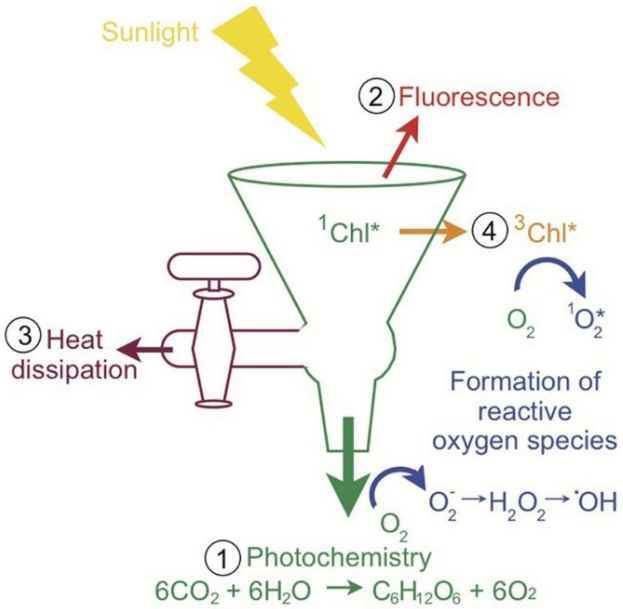

Fig. 3 – Schematic of the relationship of energy usage during photosynthesis and the formation of ROS. (1) energy use for photochemistry, (2) energy emitted as fluorescence, (3) energy lost by heat dissipation, (4) ^{3}Chl* formation through energy transfer by ^{1}Chl*, leading to the formation of ROS. (From Roth 2014)[50]

to environmental stress.[51] However, levels are normally kept in balance to prevent damage occurring. When this balance is offset, the cell is considered to be in a state of oxidative stress.[52] As a result, the presence of excess ROS may cause irreversible damage to lipids, proteins and nucleic acids, due to their reactive behavior towards these cellular components.[53]

1.3.3 Plant antioxidant defense mechanisms

Plants have developed a range of antioxidant defense mechanisms to detoxify and scavenge excess ROS. They can be divided into enzymatic and non-enzymatic antioxidants.[54-55] Enzymatic antioxidants include catalase (CAT), superoxide dismutase (SOD), guaiacol peroxidase (GuPX) and enzymes of the ascorbate-glutathione cycle, mainly ascorbate peroxidase (APX) and glutathione reductase (GR).[56] Non-enzymatic components include the major redox buffer ascorbate and glutathione, together with tocopherols, carotenoids and phenolic compounds.[57] Enzymatic antioxidants actively detoxify ROS and form the primary defense (Fig. 4), while non-enzymatic antioxidants act as scavengers and play a secondary role. Previous studies have indicated increased activities of a number of enzymes of the antioxidant defense system, in cases of oxidative stress induced by exposure to environmental stressors.[58-59] Furthermore, distinct isoforms of these enzymes have been identified: SOD has been shown to consist of three isoforms which have different metal prosthetic groups (Fe, Cu/Zn, Mn) in their active sites as well as a different subcellular localization (mitochondria, cytosol, chloroplast). Likewise, APX has been shown to be localized in cytosol and chloroplasts, whereas CAT isoforms are conventionally thought to reside in cytosol and peroxisomes.[60] Isoforms differ in their abundance as well as their kinetics (substrate affinity and turnover rate). The abundance is a consequence of both transcriptional (gene expression) and translational (protein synthesis and mRNA processing) control mechanisms.[61] Differences in the expression of antioxidant enzymes have been shown in relation to exposure to various environmental stressors,[62-63] while translational effects are less characterized.

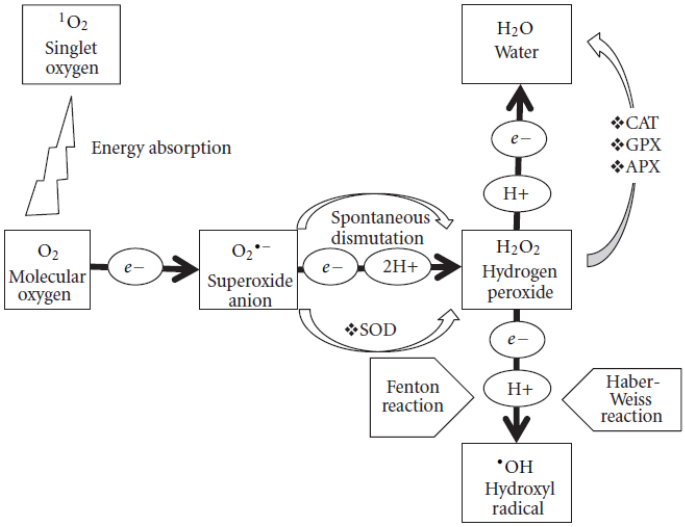

Fig. 4 – Overview of the pathways involved in the generation of ROS and the enzymatic antioxidants. CAT, catalase; GPX, glutathione peroxidase; APX, ascorbate peroxidase; SOD, superoxide dismutase. (From Sharma et al. 2012)[58]

1.3.4 Secondary metabolites and redox coenzymes

Secondary metabolites include more than 200,000 different compounds that can be found in plant tissues.[64] They do not participate directly in growth and development, but rather play a role in protection and competition, and are therefore not essential for survival. Secondary metabolites are conventionally divided into three main groups: phenolics, alkaloids and terpenoids.[64] Detection of secondary metabolites is possible due to a process called autofluorescence. This mechanism detects the fluorescence emission of endogenous molecules when excited by UV/Vis radiation.[65] Excitation in the UV region leads to two distinct types of fluorescence in plant tissues: an emission band in the blue-green region, and one in the red and far-red region[66] consisting almost entirely of ChlF (Fig. 5). The blue-green region is comprised of various fluorophores, molecules that emit a fluorescent signal. Among them are nicotinamide (reduced NADH, free and protein-bound) and flavin (oxidized FMN and FAD) coenzymes, vitamin B derivatives (B_6 and B_9), phenols, alkaloids and terpenoids.[68] The blue-green emission band consists of two shoulders: a shoulder in the blue region consisting of the nicotinamides

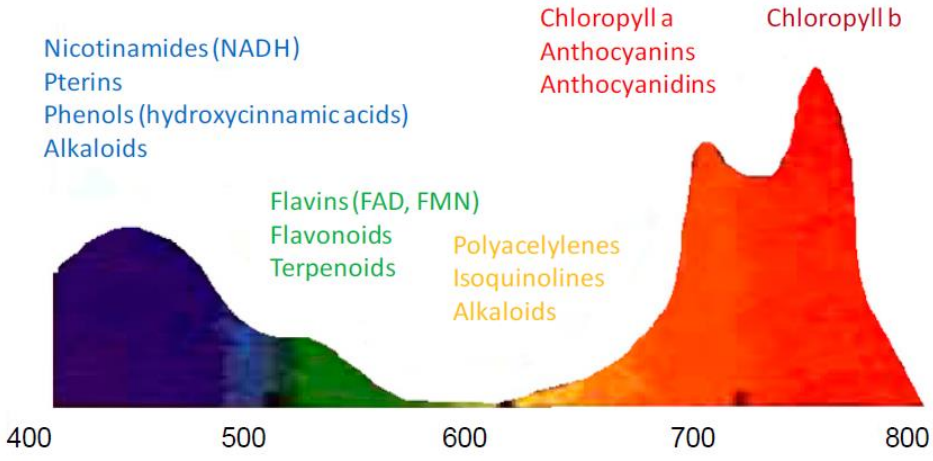

Fig. 5 – Fluorescence emission spectrum of a typical leaf excited by UV-radiation. (From Talamond et al. 2015)[67]

and the phenols and alkaloids, while the shoulder in the green region is comprised of the flavins and the flavonoids and terpenoids.[68] Nicotinamide and flavin coenzymes are involved in many metabolic reactions as carriers of reduction potential. The recycling of these coenzymes requires a series of redox reactions to regenerate their reduced form.[69] Consequently, changes in cellular levels of this reduced form can serve as an indication of the cellular redox state.

1.3.5 **Research objective part II**: Antioxidative responses in broccoli induced by diesel exhaust exposure

Preliminary data of our research group has indicated increased antioxidant enzyme activity in leaves of *Brassica oleracea* var. *italica* exposed to diesel exhaust (Fig. S1, appendix A). This finding suggests that diesel exhaust acts as an environmental stressor and elicits an increased production of ROS to which the plant responds by increasing antioxidant enzyme activity. Though, whether an actual increase in ROS-related products are produced, how the cellular redox state is affected, and whether the altered enzyme activities are a consequence of changes in gene expression levels, remains to be determined. This lead to our second research question: 'Is altered antioxidant gene expression at the root of the changes in antioxidant enzyme activity, and are other antioxidative responses elicited in broccoli plants exposed to diesel exhaust'? We hypothesize that increased antioxidant enzyme activity is caused by increased gene expression of antioxidant enzymes, and additionally that there is an increase in the total antioxidant capacity (TAC) and production of H_2O_2, as well as changes in the amount of NADH and FAD in leaves of *Brassica oleracea* var. *italica* exposed to diesel exhaust.

2. MATERIALS AND METHODS

PART I: The impact of traffic-related air pollution on ChlF kinetics in London Plane

2.1 Sampling site

The city of Hasselt (50.9307°N, 5.3325°E, 44 m MASL and 77.124 inhabitants as of 01/01/2017) is the thirteen largest city in Belgium.[70] Based on traffic density data, sampling points were chosen near Hasselt inner ring road, one of the city's busiest roads. Kapermolen Park was chosen as a reference site. Between August 28th and September 4th 2017, leaves of London planes (*Platanus x acerifolia*) were collected by sampling branches at approximately four meters high from the street side of the trees. In total, 13 trees were sampled (Table S1 and Fig. S2, appendix B), of which 11 in six different locations near Hasselt Inner ring road, and 2 at two time-points (start and end of campaign) at the reference site. The composition and concentration of air pollutants (black carbon, NO_2, $PM_{2.5}$ and PM_{10}) at the sampling points were provided by IRCEL.

2.2 Chlorophyll fluorescence measurements

Fast chlorophyll induction kinetics of the adaxial side of 10 leaves per tree was determined in twofold using a Handy PEA (Hansatech Instruments Ltd.). Slow chlorophyll induction kinetics and the electron transport rate (ETR) of the adaxial side of five randomly chosen leaves of each tree were determined using a PAM-2500 (Heinz Walz, GmbH). PAM data was analyzed at 301s, representing the time-point during the quenching analysis when the steady-state is reached. Steady-state fluorescence (Scanning mode, Excitation = 438nm, range 650-750nm) was simultaneously analyzed on the five randomly chosen leaves using a QuantaMaster™ 340 spectrofluorometer (Horiba, Ltd.).

2.3 Leaf characteristics and relative chlorophyll content

Fresh weight (FW) and dry weight (DW) of all leaves were determined using a standard precision balance. Samples were placed in an oven at 50°C for 3 days prior to measuring the DW. Leaf area was determined by scanning leaves using a copy machine. Images were processed using ImageJ. Relative chlorophyll content of each leaf was determined in fivefold using a CCM-200 (Opti-sciences). The leaf water content (LWC) and specific leaf area (SLA) were calculated using the following equations:

$$\mathrm{LWC} = \frac{(\mathrm{FW}-\mathrm{DW})}{\mathrm{Leaf\ area}} \quad \text{and} \quad \mathrm{SLA} = \frac{\mathrm{Leaf\ area}}{\mathrm{DW}}$$

2.4 Heavy metal deposition

The presence of Cu, Fe, Zn, Pb, Ni, Mn, Cr and Cd were determined in all leaves. Leaves were dried overnight in an oven at 60°C. Next, whole leaves were crumbled (excluding the main nerves), and put in a Mixer Mill MM2000 (Retsch, GmbH) for two minutes. Following homogenization, 100 mg of each sample was transferred to a short heat-resistant tube. Then, 1 ml suprapur 70% HNO_3 was added to each tube, whereupon they were placed in heat blocks at 110°C for four hours until all acid had evaporated. The previous step was repeated. Subsequently, 1 ml of suprapur 37% HCl was added to each tube, vortexed briefly, and placed in heat blocks at 110°C for three hours until all acid had evaporated. Finally, 5 ml 2% HCl was added to each tube, and tubes were gently swirled. Samples were analyzed using an ICP-OES 710 (Agilent Technologies, USA).

2.5 Statistical analysis

One-way ANOVA was used to compare group means of the ChlF parameters, leaf characteristics, heavy metals and air pollutants between leaves sampled at Hasselt Inner ring road and the reference site. Correlations between ChlF parameters, leaf characteristics, heavy metal deposition and air pollutants were evaluated using a linear mixed model, as response variables followed a normal distribution, with samples nested per tree. The statistical analysis was performed using RStudio.

PART II: Antioxidative responses in broccoli induced by diesel exhaust exposure

2.6 Plant material, growth conditions and application of stress

Seeds of broccoli (*Brassica oleracea* var. *italica*) were germinated in plastic trays (30x45cm) containing standard commercial soil until week three of age, upon which they were transferred to stone wool (Grodan© Expert) for the remainder of their growth. The plants were grown for nine weeks in a greenhouse (photoperiod 16 hours light/8 hours dark, light intensity ± 300 µmol m^{-2} s^{-1}, temperature ± 23°C day/16°C night, relative humidity ± 65%), and each plant received 100 ml of a Hoagland solution (composition: Table S2, appendix C) twice a week. In total, 24 plants were used. Of each plant, three leaves (leaves 1-3-5) of decreasing age were chosen in a standardized way, counting from the oldest leaf and excluding the primary leaves. These leaves of different ages were referred to as old (leaf 1), middle (leaf 3) and young (leaf 5) leaves. The treatment included exposing plants during the course of the final two weeks before harvest, twice a day (9 a.m./5 p.m.) for three minutes to diesel engine exhaust (composition: Fig. S3, appendix D). This set-up was optimized from preliminary work by our research group. The two time points were chosen to represent rush hour (morning/evening) with a heavy traffic load. The exhaust was funneled into a climate room where the plants are placed (Fig. 6). The climate room was aerated and cooled to prevent the accumulation of gasses and fluctuating temperatures. An exhaust valve controlled the input of gasses. Control plants were placed in a second climate room (not shown) during the exposure procedure, which was kept at the same constant temperature as the first room, and contained ambient air.

2.7 Harvest and sample collection

Samples were collected close to the main nerve of the leaf and excluding as many nerves as possible. The preparation was performed early in the morning taking into account the plants circadian rhythms. Samples were immediately stored in liquid nitrogen. Approximately 100 mg of samples was collected for each analysis; 75 mg was collected for the gene expression analysis.

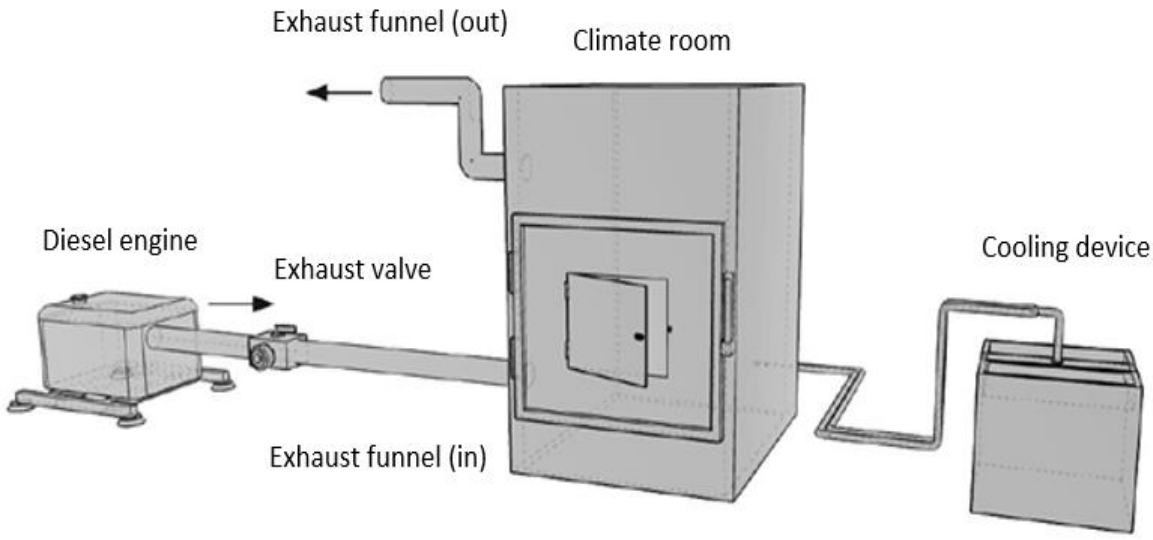

Fig. 6 – Set-up of diesel engine exhaust exposure. See text for description.

2.8 Total antioxidative capacity

The TAC was determined using a modified version of the ferric reducing antioxidant power (FRAP) method as performed by Kerchev and Ivanov.[72] First, the hydrophilic fraction (HF) of antioxidants was extracted: samples were crushed using liquid nitrogen. Then, 1 ml of an extraction buffer ((100x) 0.01N HCl - 1mM Na-EDTA) was added. Samples were mixed, collected in Epps, and centrifuged at 15 000g (4°C) for 30 minutes. Supernatant was collected as the HF. The lipophilic fraction (LF) was collected by resuspension of the pellet in 1 ml 80% acetone by vortexing vigorously. Samples were kept on ice for an hour, followed by centrifugation at 15 000g (4°C) for 15 minutes. The supernatant was collected as the LF. A FRAP reagent (150 µl TPTZ, 150 µl $FeCl_3$ and 17.6 ml of a Na-acetate buffer (pH 3.9)) was added to samples of each fraction before measuring the absorption of a UV 96-well flat-bottom plate (Greiner) using a FLUOstar Omega (BMG LABTECH) plate reader. The TAC was calculated by standard curves prepared with known concentrations of Trolox.

2.9 Hydrogen peroxide and Bradford protein quantification

Hydrogen peroxide was determined using a modified version of the OxiSelect™ Hydrogen Peroxide/Peroxidase Assay Kit (Cell Biolabs, Inc.). Briefly, samples were crushed using liquid nitrogen. Then, 500 µl of 1x assay buffer was added and homogenized samples were collected in Epps. Samples were centrifuged at 13 000g for 10 minutes, and supernatant was collected. Fluorescence intensity of a 1:50 dilution of the samples was determined in a 96-well microplate (polypropylene, f-bottom (chimney well) black (Greiner Bio-One) using a FLUOstar Omega (BMG LABTECH) plate reader. Hydrogen peroxide concentrations were determined using a series of standard dilutions of H_2O_2, as instructed by the manufacturer.

The protein concentration was determined using the Bradford protein assay. Extracts of the hydrogen peroxide analysis were diluted 1:10. Samples were run on a UV 96-well flat-bottom plate (Greiner Bio-One) using a FLUOstar Omega (BMG LABTECH) plate reader.

2.10 RNA extraction, cDNA synthesis and qPCR

Twelve broccoli (*Brassica oleracea* var. *italica*) plants were germinated, grown and exposed as described before. Leaves 1-3-5 were chosen as described before. Leaf samples were harvested as described before, collected in RNase-free Microfuge Tubes (2.0 ml) together with two stainless steel beads, and stored in liquid nitrogen. Total RNA was extracted from leaf samples using the RNeasy Plant Mini kit (Qiagen). Samples were shredded twice for one minute at maximum capacity using a Mixer Mill MM200 (Retsch GmbH). RNA was extracted according to manufacturer's instructions. RNA quality was checked using a NanoDrop ND-1000 spectrophotometer (NanoDrop Technologies).

cDNA synthesis was performed using the TURBO DNA-free™ Kit (Ambion, Inc.) to remove residual DNA, together with the PrimeScript™ RT Reagent Kit (Perfect Real Time) (TaKaRa) to perform reverse transcription. RNA samples were brought to the same concentration (1 µg). Reverse transcription was performed using a C1000 Touch™ Thermal Cycler (Bio-Rad laboratories, Inc.) according to manufacturer's instructions.

Quantitative polymerization chain reaction (qPCR) was performed using the QuantiNova SYBR Green PCR Kit (Qiagen) according to manufacturer's instructions. Samples were run on MicroAmp™ Optical 96-Well Reaction Plates (Applied Biosystems, Inc.) using a 7500 Fast Real-Time PCR System (Applied Biosystems, Inc.). Relative gene expression was calculated as $2^{-\Delta Cq}$ and was normalized with a normalization factor determined by the GrayNorm algorithm.[73] Ten reference genes were previously

investigated in *Brassica oleracea* under stress conditions,[74] and were considered for this research. The stability of seven reference genes was confirmed, and were subsequently tested using the GrayNorm algorithm. Three reference genes were validated and used during this research, including *SAND1*, *TUB6* and *UBQ2*. Gene-specific primers were developed using Phytozome and NCBI databases, and Primer3 (Whitehead Institute/MIT Center for Genome Research). A list of the used primers is provided in Table S3 of appendix E.

2.11 Confocal microscopy of secondary metabolites in leaf cross-sections

Twelve broccoli (*Brassica oleracea* var. *italica*) plants were germinated, grown and exposed as described before. Leaves 1-3-5 were chosen as described before. Fresh leaves were harvested by cutting a piece of approximately 1 cm² containing as few nerves as possible. The sides of the leaf samples were glued between two pieces of 3.5% agarose gel, and placed on a the sample mount, supported by a piece of Styrofoam (Fig. 7). Then, cross-section samples (Ø 1000 µm) of the leaves were made using a Leica VT1200S (Leica Biosystems Nussloch, GmbH), and carefully transferred to a microscope slide. Fluorescence spectra were acquired using a LSM 880 Airyscan installed on an inverted Axio Observer (Carl Zeiss, Jena, Germany) and equipped with a Plan-apochromat 20x/0.8 air objective (Carl Zeiss, Jena, Germany). For all measurements, pixel size was 420 nm with an image resolution of 1024 by 1024. A Z-stack of 9 frames was recorded, spanning a range of 32 µm. The pixel dwell times were 4.1 µs. Excitation was provided by a femtosecond pulsed laser (MaiTai DeepSee, Spectra-Physics, CA, USA) tuned to a central wavelength of 810nm and controlled by an EOM set at 4% transmission. A MBS SP 690 beam splitter directed the 810nm fs-pulsed laser light towards the sample. The autofluorescence was collected by the objective and detected through an open pinhole using a GaAsP spectral detector (QUASAR) with a detection band ranging from 409nm to 592nm and a spectral bin size of 8.9nm. This resulted in 23 channels per pixel.

2.12 Statistical analysis

Group means of treatments were compared using two-way ANOVA. A Tukey-Kramer test was performed to correct for multiple comparison of the different leaf ages. Differences in gene expression were evaluated using one-way ANOVA. Spectra of the leaf cross-sections were analyzed using ARTMO software. Differences between leaf ages and treatments were likewise evaluated using one-way ANOVA. The statistical analysis was performed in RStudio.

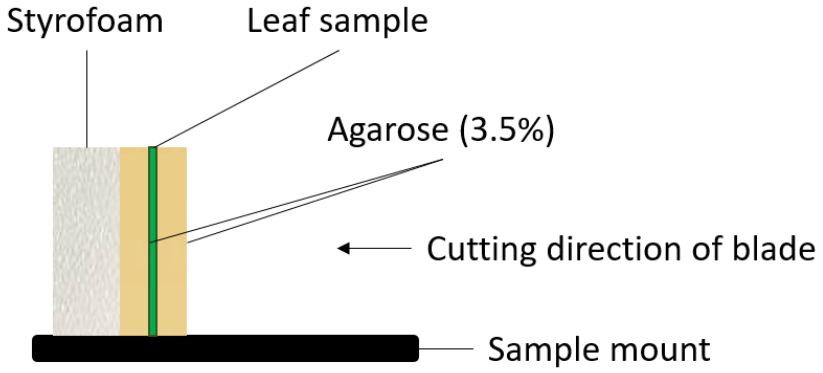

Fig. 7 – Schematic of leaf cross-section sample preparation for confocal microscopy.

3. RESULTS

PART I: The impact of traffic-related air pollution on ChlF kinetics in London Plane

The main goal of the first section of this research was to investigate whether *in situ* traffic exposure leads to altered physiological and structural responses and increased heavy metal deposition in urban vegetation. Leaves of London Planes were collected near a park and a busy road: ChlF induction kinetics and steady-state fluorescence were measured on the sampled leaves. Simultaneously, leaf characteristics and relative chlorophyll content were determined, and heavy metal deposition was analyzed on the sampled leaves.

3.1 Comparison of pollution parameters between Hasselt inner ring road and Kapermolen Park

To determine whether or not London planes near the Hasselt inner ring road are affected by increased traffic exposure, ChlF parameters, leaf characteristics, relative chlorophyll content, heavy metal deposition and presence of air pollutants were compared with the reference site Kapermolen Park. A detailed description of the different ChlF parameters can be found in Table S4 appendix F of the supplemental information.

The concentrations of Cu ($P = 0.020$), Fe ($P = 0.007$) and Pb ($P = 0.010$) are significantly higher in leaves from Hasselt inner ring road compared to those from the reference site (Fig. 8). The concentrations of the other heavy metals are not significantly different (Table 1). Next, there is no significant difference in the leaf water content (LWC, $P = 0.201$), specific leaf area (SLA, $P = 0.463$) and chlorophyll content index (CCI, $P = 0.267$). Subsequently, the concentrations of black carbon (BC, $P > 0.001$), NO_2 ($P > 0.001$) and $PM_{2.5}$ ($P > 0.001$) are significantly higher in leaves from the Hasselt inner ring road. The concentration of PM_{10} is not significantly different ($P = 0.417$).

The OJIP parameters F_m ($P = 0.014$), ϕ_{P0} ($P > 0.001$) and $PI(CS_m)$ ($P = 0.009$) are significantly higher in leaves from Hasselt inner ring road (Fig. 9). The other OJIP parameters are not significantly different (Table 2).

The slow ChlF induction parameters indicate that the electron transport rate (ETR) is significantly higher ($P = 0.046$) in leaves from the Hasselt inner ring road (Fig. 10). The other parameters are not significantly different (Table 3).

The steady-state fluorescence is significantly higher at 685 nm ($P > 0.001$), but not at 725 nm ($P = 0.112$), representing the contribution of photosystem II and I, respectively (Fig. 11).

Together, these findings indicate that Cu, Fe and Zn and the air pollutants BC, NO_2 and PM_{10} are present in higher amounts in trees near Hasselt inner ring road, while leaf characteristics and chlorophyll content are not affected. Furthermore, trees at Hasselt Inner ring road perform better than those at the reference site, as indicated by a higher PI(CSm) and ϕ(P0), as well as a higher ETR. The quenching parameters are not different between the sites, but a higher steady-state fluorescence of PSII is found.

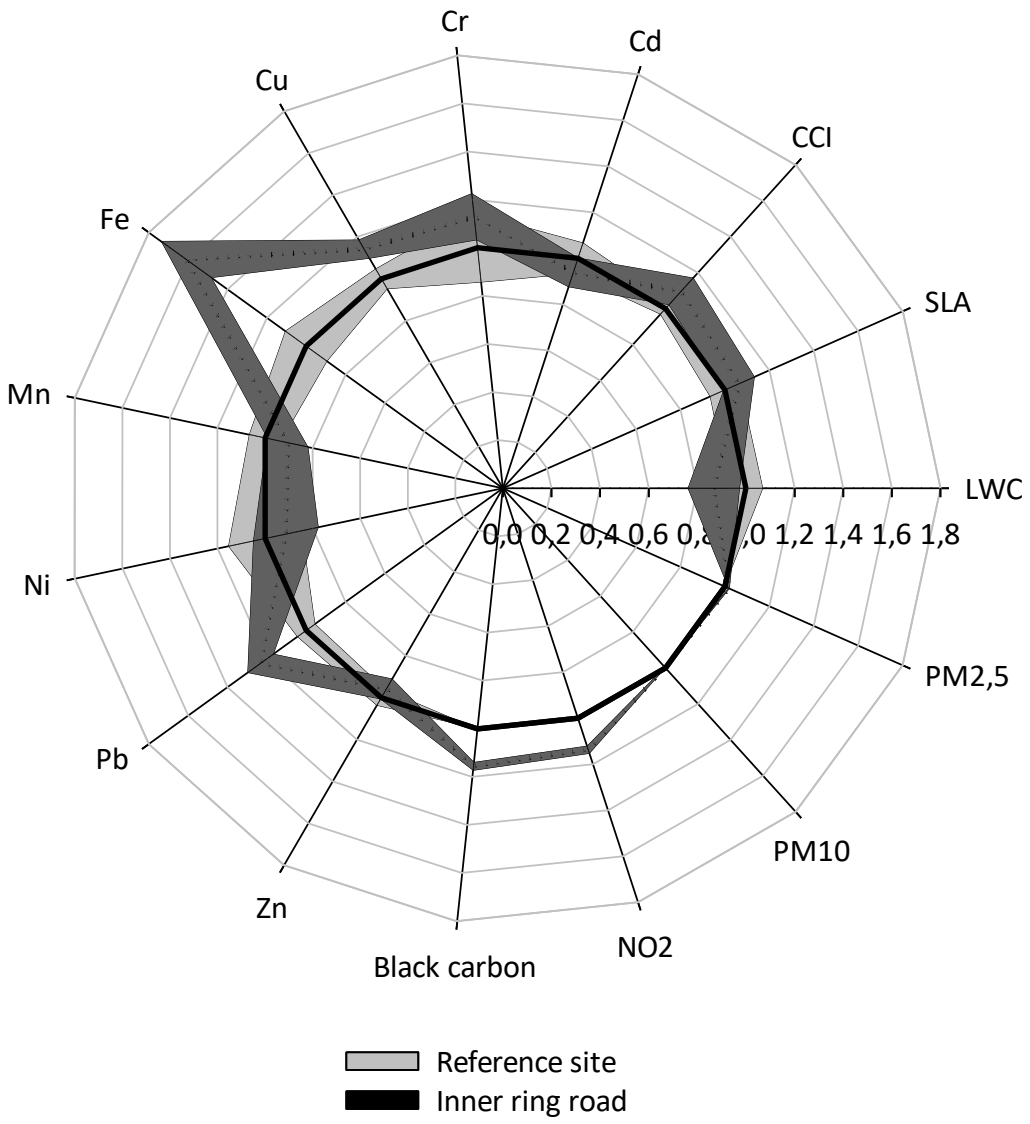

Fig. 8 – Radar plot showing relative changes of mean values of leaf characteristics, heavy metal deposition and presence of air pollutants in leaves of *Platanus x acerifolia* in Hasselt. Data from leaves sampled in Kapermolen Park (reference site) were adjusted to 1.0, and all other parameters were calculated as fold-changes. SLA, specific leaf area; LWC, leaf water content; CCI, chlorophyll content index. Data ± SE. Radar plot created in SigmaPlot.

Table 1 - List of p-values corresponding to the radar plot of Fig. 8. One-way ANOVA.

Parameter	SLA	LWC	CCI	Cd	Cr	Cu	Fe	Mn
p-value	0.463	0.201	0.267	0.402	0.364	0.020	0.007	0.281
Parameter	Ni	Pb	Zn	Black carbon	NO_2	PM_{10}	$PM_{2.5}$	
p-value	0.580	0.010	0.432	> 0.001	> 0.001	0.417	> 0.001	

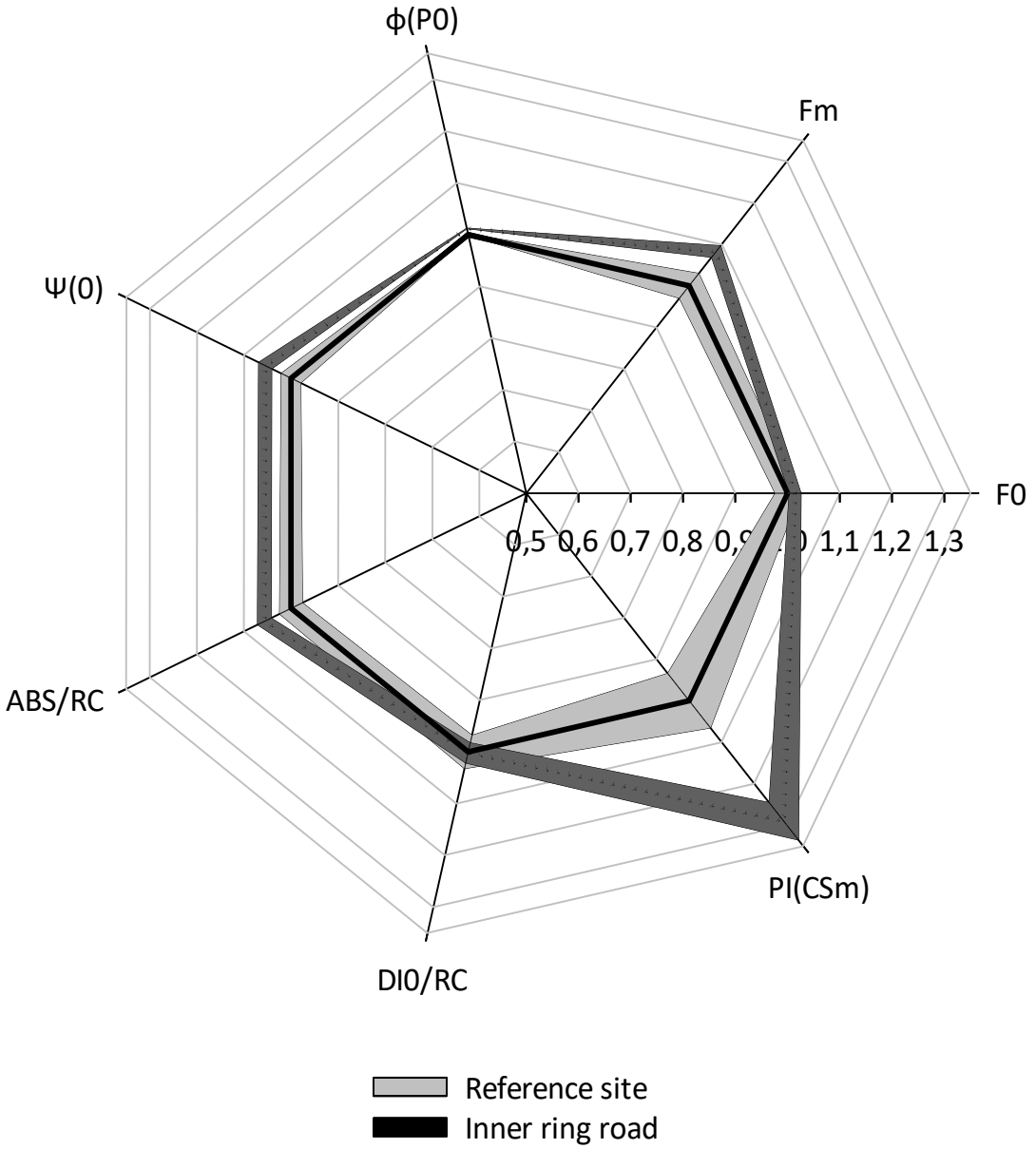

Fig. 9 – Radar plot showing relative changes of mean values of OJIP parameters in leaves of *Platanus x acerifolia* in Hasselt. Data from leaves sampled in Kapermolen Park (reference site) were adjusted to 1.0, and all other parameters were calculated as fold-changes. A detailed list describing the different parameters can be found in Table S4 of appendix F. Data ± SE. Radar plot created in SigmaPlot.

Table 2 - List of p-values corresponding to the radar plot of Fig. 9. One-way ANOVA.

Parameter	F_0	F_m	ϕ_{P0}	Ψ_0	ABS/RC	DI_0/RC	$PI(CS_m)$
p-value	0.574	0.014	> 0.001	0.067	0.074	0.963	0.009

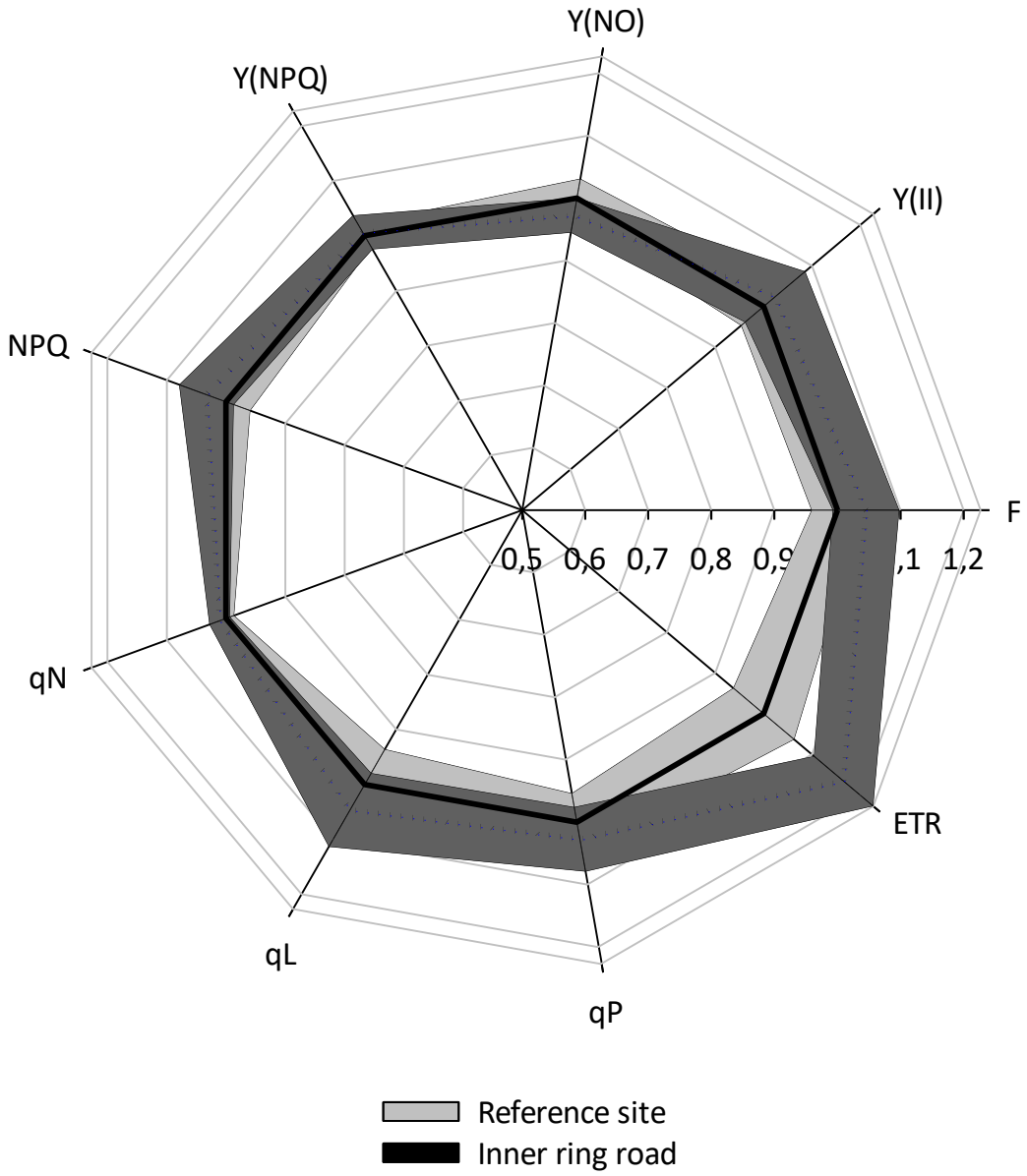

Fig. 10 – Radar plot showing relative changes of mean values of slow chlorophyll fluorescence induction parameters in leaves of *Platanus x acerifolia* in Hasselt. Data from leaves sampled in Kapermolen Park (reference site) were adjusted to 1.0, and all other parameters were calculated as fold-changes. Data ± SE. A detailed list describing the different parameters can be found in Table S4 of appendix F. Radar plot created in SigmaPlot.

Table 3 - List of p-values corresponding to the radar plot of Fig. 10. One-way ANOVA.

Parameter	Y(II)	Y(NO)	Y(NPQ)	NPQ	qN	qL	qP	F	ETR
p-value	0.737	0.408	0.858	0.543	0.588	0.567	0.650	0.458	0.046

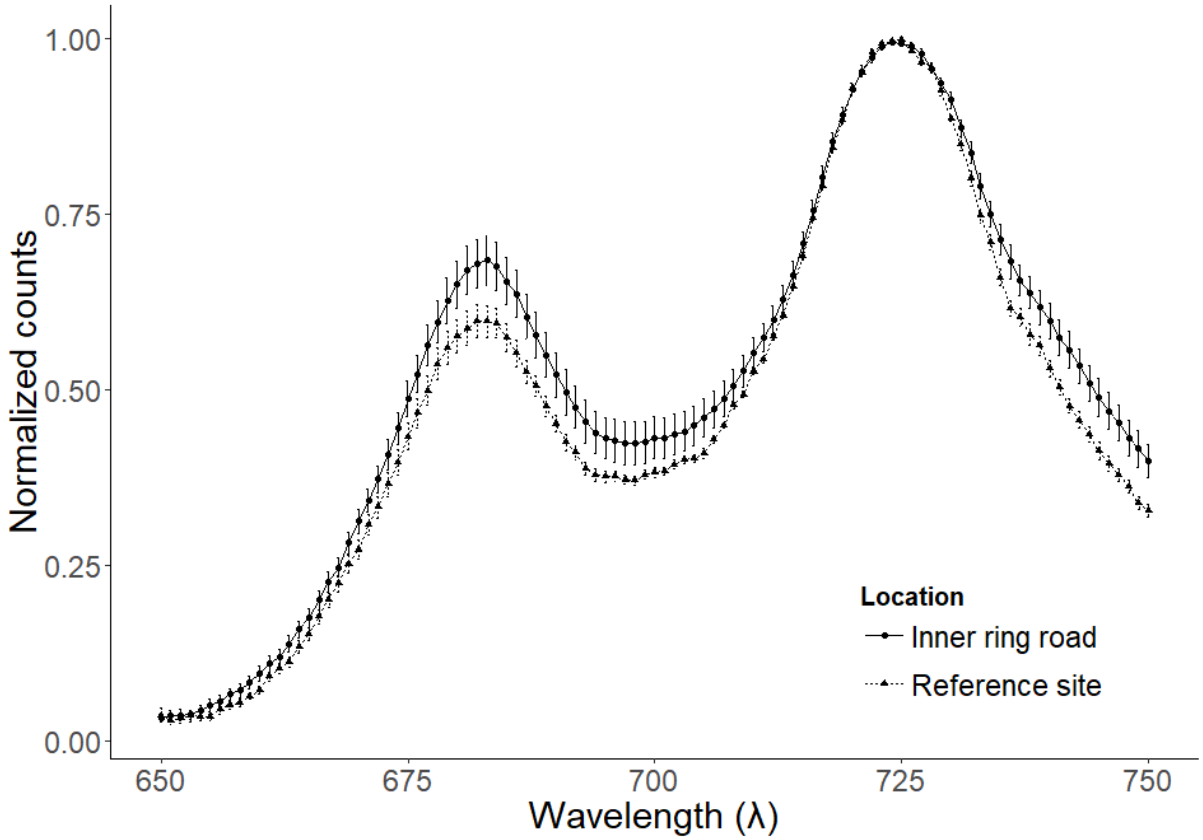

Fig. 11 – **Normalized adaxial steady-state fluorescence in leaves of *Platanus x acerifolia* in Hasselt.** Error bars are ± SE. Line plot created in RStudio using the ggplot2 package. One-way ANOVA was performed to test for significant differences between the two sites.

3.2 Correlation analysis: ChlF parameters, leaf variables, soil and air contamination

To determine whether or not there exist significant correlations between the ChlF parameters, leaf characteristics, heavy metal deposition and air pollutants, the datasets of both sites in Hasselt were combined and analyzed using linear mixed modelling. The main goal was to find out whether traffic exposure has an effect on the physiology and structure of the sampled leaves, as well as if structure could be an indicator of changes of plant physiology (Fig. 12). A prospective study was performed in advance to determine interesting associations between the different parameters considered.

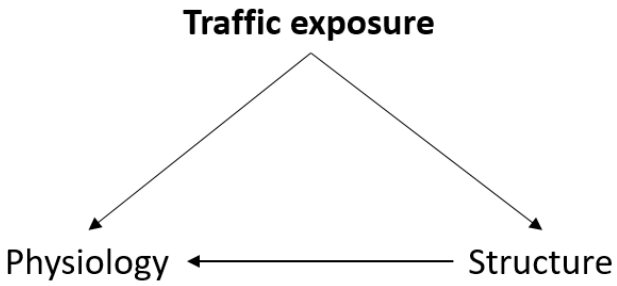

Fig. 12 – Schematic relationship between traffic exposure and effects on plant physiology and structure.

The SLA is significantly associated with Y(NO) (P = 0.020) and the OJIP parameters ABS/RC (P = 0.002), DI_0/RC (P = 0.001) and PI(CSm) (P = 0.048) (Table 4). The LWC is not significantly associated with any ChlF parameter. In contrast, the CCI is significantly associated with most ChlF parameters. When considering correlations between heavy metals, there is a significant correlation of Cu with some of the OJIP parameters. Zn is significantly associated with the steady-state fluorescence at 685nm (P = 0.015) and 700nm (P = 0.009). Ni is significantly associated with some parameters of both the slow ChlF induction kinetics and the OJIP parameters. Cd, Pb and Mn are not associated with any ChlF parameters.

When considering the correlations between the air pollutants and the ChlF induction parameters, a significant correlation is observed between PM_{10} and F (P = 0.036) (Table 5). Finally, when considering the correlation between the leaf characteristics and the presence of heavy metals and air pollutants, there is a significant correlation of the SLA with Fe (P = 0.019). The LWC is not significantly associated with any parameter.

Table 4 - List of p-values of the correlations between the OJIP parameters, slow ChlF induction kinetics, steady-state fluorescence, leaf characteristics and the presence of heavy metals. Significant values (P > 0.05) are marked in red. Correlations were evaluated using nested linear mixed modelling. SLA, specific leaf area; LWC, leaf water content; CCI, chlorophyll content index.

p-value of correlation		Leaf characteristics			Heavy metal deposition					
		LWC	SLA	CCI	Cd	Cu	Mn	Pb	Zn	Ni
OJIP parameters	F_0	0.622	0.262	0.001	0.584	0.192	0.368	0.650	0.512	0.047
	F_m	0.853	0.253	0.001	0.852	0.018	0.319	0.267	0.287	0.028
	ϕ_{P0}	0.742	0.083	0.068	0.845	0.008	0.765	0.098	0.478	0.412
	Ψ_0	0.378	0.091	0.001	0.694	0.047	0.741	0.504	0.479	0.634
	ABS/RC	0.062	0.002	0.681	0.971	0.557	0.825	0.622	0.615	0.002
	DI_0/RC	0.095	0.001	0.555	0.788	0.490	0.762	0.833	0.876	0.017
	PI(CS_m)	0.309	0.048	0.001	0.948	0.025	0.892	0.634	0.332	0.635
Slow ChlF induction parameters	Y(II)	0.628	0.588	0.015	0.743	0.936	0.601	0.334	0.201	0.350
	Y(NO)	0.907	0.020	0.388	0.115	0.908	0.371	0.858	0.221	0.011
	Y(NPQ)	0.754	0.694	0.001	0.311	0.994	0.815	0.497	0.357	0.128
	NPQ	0.825	0.125	0.004	0.107	0.949	0.273	0.652	0.207	0.032
	qN	0.776	0.234	0.001	0.158	0.819	0.304	0.745	0.378	0.043
	qL	0.821	0.167	0.846	0.905	0.109	0.794	0.849	0.861	0.179
	qP	0.659	0.282	0.571	0.777	0.258	0.670	0.753	0.604	0.642
	ETR	0.256	0.341	0.004	0.915	0.289	0.302	0.342	0.245	0.312
	F	0.519	0.294	0.011	0.463	0.607	0.646	0.539	0.329	0.044
Steady-state fluorescence	λ685	0.645	0.355	0.523	0.297	0.254	0.572	0.683	0.015	0.296
	λ700	0.688	0.165	0.011	0.141	0.996	0.069	0.441	0.009	0.918
	λ725	0.972	0.740	0.920	0.529	0.286	0.539	0.376	0.289	0.974
	λ685/700	0.529	0.883	0.001	0.714	0.052	0.330	0.847	0.359	0.041

Together, these findings indicate that the SLA and the presence of Cu, Zn and Ni are correlated with some of the ChlF parameters, while the CCI shows a correlation with most parameters. In addition, F is significantly correlated with PM_{10} and the SLA with Fe.

Table 5 - List of p-values of the correlations between ChlF induction kinetics, steady-state fluorescence and air pollutants (left), and the presence of heavy metals, air pollutants and leaf characteristics (right). Significant values ($P > 0.05$) are marked in red. Correlations were evaluated using nested linear mixed modelling. BC, black carbon. SLA, specific leaf area; LWC, leaf water content; CCI, chlorophyll content index.

p-value of correlation		BC	NO_2	PM_{10}	$PM_{2.5}$	p-value of correlation		LWC	SLA	CCI
OJIP parameters	F_0	0.776	0.806	0.494	0.705	Heavy metal deposition	Cd	0.497	0.163	0.902
	F_m	0.729	0.750	0.416	0.990		Cr	0.450	0.643	0.629
	ϕ_{P0}	0.308	0.380	0.842	0.556		Cu	0.289	0.685	0.567
	Ψ_0	0.754	0.789	0.697	0.675		Fe	0.676	0.019	0.254
	ABS/RC	0.306	0.288	0.776	0.489		Mn	0.147	0.471	0.050
	DI_0/RC	0.609	0.554	0.890	0.691		Ni	0.170	0.852	0.487
	PI(CSm)	0.583	0.626	0.808	0.609		Pb	0.598	0.143	0.928
Slow ChlF induction parameters s	Y(II)	0.997	0.916	0.806	0.923		Zn	0.755	0.692	0.355
	Y(NO)	0.136	0.165	0.153	0.170	Air pollutants	BC	0.759	0.282	0.929
	Y(NPQ)	0.271	0.247	0.470	0.259		NO_2	0.804	0.282	0.937
	NPQ	0.122	0.136	0.214	0.151		PM_{10}	0.490	0.321	0.936
	qN	0.097	0.107	0.157	0.115		$PM_{2.5}$	0.956	0.251	0.998
	qL	0.492	0.585	0.386	0.590					
	qP	0.631	0.728	0.479	0.729					
	ETR	0.381	0.444	0.549	0.470					
	F	0.200	0.236	0.036	0.179					
Steady-state fluorescence	λ685	0.219	0.213	0.301	0.508					
	λ700	0.245	0.232	0.370	0.529					
	λ725	0.293	0.331	0.919	0.437					
	λ685/700	0.766	0.785	0.925	0.809					

PART II: Antioxidative responses in broccoli induced by diesel exhaust exposure

The main goal of the second part of this research was to investigate whether broccoli plants exposed to diesel exhaust show altered antioxidative responses. First, the TAC was investigated to determine changes in the cellular redox state. Then, the amount of H_2O_2 was quantified to examine whether there is an increase in ROS-related products. Simultaneously, the amount of protein was quantified to consider changes in total protein levels. Subsequently, the expression of genes related to antioxidative pathways were investigated to consider whether altered levels of transcripts of antioxidant enzymes were present. Finally, fluorescence emission spectra were analyzed to examine whether there are changes in the amount of secondary metabolites and the presence of coenzymes NADH and FAD.

3.3 Total antioxidant capacity

To determine whether exposure to diesel exhaust leads to an altered redox state at the cellular level, the TAC was investigated in homogenized leaf samples. A significantly lower TAC is apparent in exposed plants for middle and young leaves (both $P > 0.001$) (Fig. 13). The difference between treatments in old leaves is not significant ($P = 0.228$). When considering the difference between the leaf ages, there is a significantly lower TAC in old compared to middle and young leaves ($P > 0.001$ for both).

We also examined the contribution of both fractions (Fig. S4, appendix G). The HF/LF ratio is not significantly different between treatments (old: $P = 0.802$; middle: $P = 0.792$; young: $P = 0.864$). When considering the difference between leaf ages, old leaves show a significantly higher HF/LF ratio compared to middle and young leaves (both $P > 0.001$). The difference between middle and young leaves is not significantly different ($P = 0.946$). Together, these findings show that the TAC is lower in exposed leaves, and lower in older compared to young leaves. The ratio HF/LF is significantly higher in old leaves, but not in middle and young leaves, nor between treatments.

3.4 Hydrogen peroxide quantification

To find out whether diesel exhaust exposure leads to an increase in ROS-related products, the amount of H_2O_2 present in homogenized leaf samples was quantified. In general, exposed leaves show a higher presence of H_2O_2 compared to control leaves. The amount of H_2O_2 is not significantly different between treatments (old: $P = 0.992$; middle: $P = 0.999$; young: $P = 0.999$) (Fig. 14). Old leaves contain significantly more H_2O_2 compared to middle and young leaves (both $P > 0.001$). The amount of H_2O_2 between middle and young leaves is not significantly different ($P = 0.177$). Together, these findings indicate that a higher amount of H_2O_2 was found in exposed leaves, and that older leaves contain a significantly higher amount of H_2O_2 compared to middle and young leaves.

3.5 Bradford protein determination

To find out whether diesel exhaust exposure leads to changes in total protein levels, a Bradford protein assay was conducted on the extracts of the hydrogen peroxide assay. In general, protein levels are slightly higher in middle and young leaves, and lower in old leaves (Fig. 15). The difference between treatments is not significant (old: $P = 0.082$; middle: $P = 0.994$; young: $P = 0.960$). When considering the difference between the leaf ages, there is a significantly higher amount of protein in old compared to middle and young leaves (both $P > 0.001$). Moreover, young leaves show a significantly higher amount of protein compared to middle leaves ($P > 0001$). Together, these results indicate that there is only a marginal difference in the amount of protein between treatments in middle and young leaves,

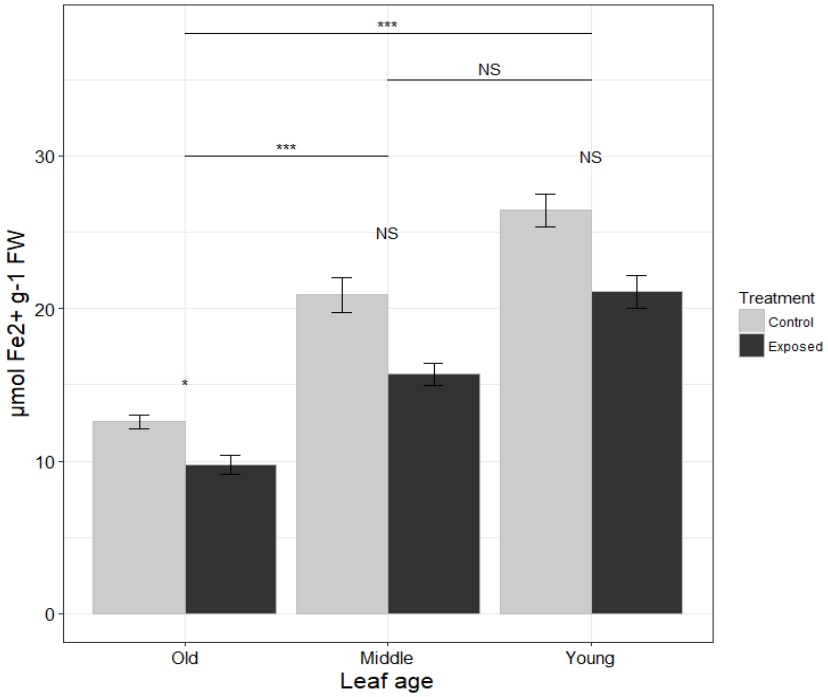

Fig. 13 – TAC in leaves of *Brassica oleracea* var. *italica* exposed to diesel exhaust. Data is a sum of both HF and LP fractions and is expressed in µmol Fe^{2+} per gram FW. Error bars are ± SE. Significant findings are denoted by an asterisk (* = $P < 0.05$, ** = $P < 0.01$, *** = $P < 0.001$, two-way ANOVA with Tukey-Kramer correction for multiple comparison). NS, Not Significant. Bar plots created in RStudio using the ggplot2 package.

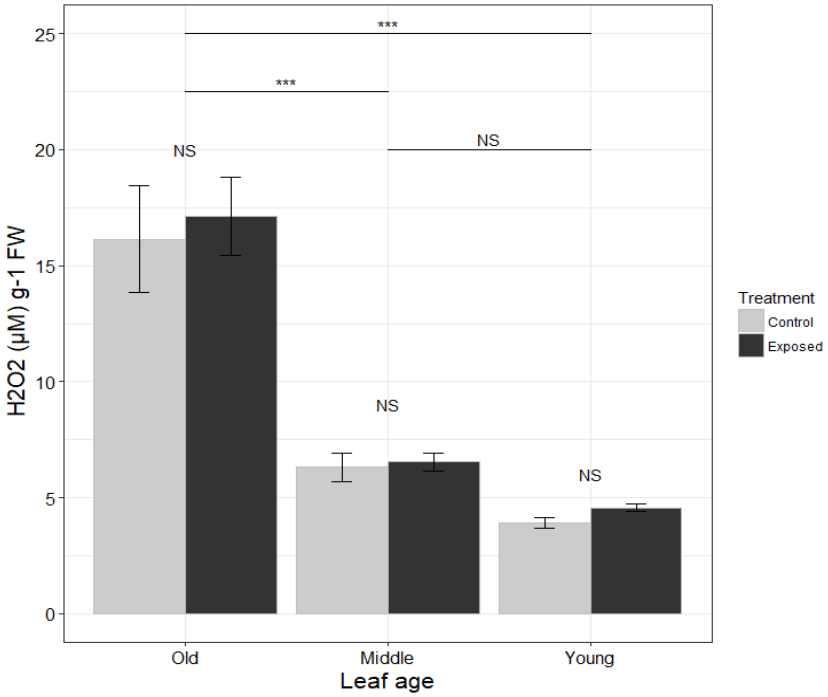

Fig. 14 – H_2O_2 in leaves of *Brassica oleracea* var. *italica* exposed to diesel exhaust. Data is expressed in µM H_2O_2 per gram FW. Error bars are ± SE. Significant findings are denoted by an asterisk (* = $P < 0.05$, ** = $P < 0.01$, *** = $P < 0.001$, two-way ANOVA with Tukey-Kramer correction for multiple comparison). NS, Not Significant. Bar plots created in RStudio using the ggplot2 package.

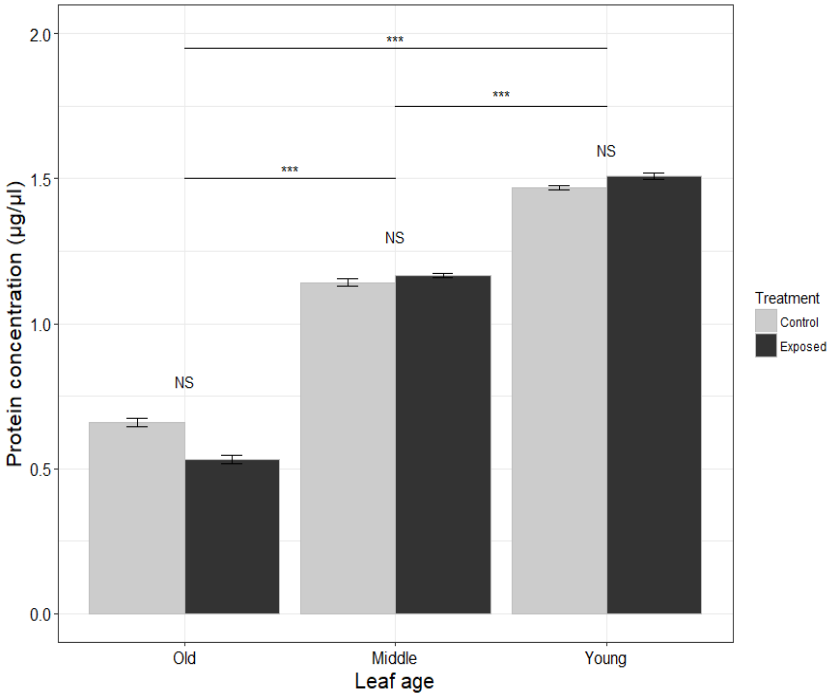

Fig. 15 – **Protein concentration of leaves of *Brassica oleracea* var. *italica* exposed to diesel exhaust.** n=12**.** Error bars are ± SE. Significant findings are denoted by an asterisk (* = $P < 0.05$, ** = $P < 0.01$, *** = $P < 0.001$, two-way ANOVA with Tukey-Kramer correction for multiple comparison). NS, Not Significant. Bar plot created in RStudio using the ggplot2 package.

and a lower amount in exposed plants of old leaves. Young leaves contain a higher amount of protein compared to old leaves.

3.5 Gene expression of antioxidant enzymes

To determine whether diesel exhaust exposure alters the expression of genes involved in antioxidative pathways, leaf samples were analyzed using RT-qPCR. Normalized expression data is shown in Table 6 and 7. Appendix H contains a list of p-values corresponding to the expression data (Table S5 and S6), and the non-normalized expression data (Table S7 and S8). In general, most genes are downregulated in exposed plants for middle and young leaves (Table 6). However, this finding is significant only for *CAT2* ($P > 0.001$), *MnSOD2* ($P = 0.002$), *APXS* ($P = 0.005$) in young leaves, and for *GPX3* ($P = 0.033$) in middle leaves. In general, expression in old leaves does not differ between treatments. In contrast, there exists ($P > 0.001$), *MnSOD2* ($P = 0.002$), *APXS* ($P = 0.005$) in young leaves, and for *GPX3* ($P = 0.033$) in middle leaves.

In general, expression in old leaves does not differ between treatments. In contrast, there exists a general trend of upregulation for *CAT1*, *CAT3*, *GR1 (Chl)*, and *APXT*. This finding is significant for *CAT3* for all ages (old: $P = 0.002$; middle: $P = 0.003$; young: $P = 0.002$), and for *GR1 (Chl)* ($P = 0.003$) and *APXT* ($P = 0.041$) in old and middle leaves, respectively. When considering the expression patterns between leaves of different ages, there exist a significant upregulation for most genes in older leaves (Table 7). In contrast, younger leaves indicate a general trend of downregulation. A notable exception to this rule is *APXT*, which shows a significant upregulation ($P > 0.001$) in young leaves of control plants.

Table 6 - Expression patterns of genes related to antioxidative pathways in leaves of *Brassica oleracea* var. *italica* exposed to diesel exhaust. n=9. Data ± SE. (significant upregulation in green, significant downregulation in red of exposed relative to control leaves for each leaf age separate; one-way ANOVA, $P < 0.05$, analysis performed in RStudio). Genes: catalase (*CAT1*, *CAT2*, and *CAT3*), iron superoxide dismutase (*Fe-SOD1*), copper/zinc superoxide dismutase (*Cu/Zn-SOD1*), manganese superoxide dismutase (*MnSOD2*), glutathione reductase (*GR1 (Chl)* (chloroplastic) and *GR1 (Cyt)* (cytosolic)), ascorbate peroxidase (*APX1*, *APX3*, *APX6*, *APXS* (stromal), *APXT* (thylakoid)), glutathione peroxidase (*GPX1*, *GPX2*, and *GPX3*).

Treatment	Leaf age			Genes
	Old	Middle	Young	
Control	1.00 ± 0.12	1.00 ± 0.12	1.00 ± 0.14	***CAT1***
Exposed	1.03 ± 0.14	1.17 ± 0.12	1.29 ± 0.10	
Control	1.00 ± 0.19	1.00 ± 0.17	1.00 ± 0.09	***CAT2***
Exposed	0.77 ± 0.08	0.73 ± 0.18	0.57 ± 0.05	
Control	1.00 ± 0.17	1.00 ± 0.17	1.00 ± 0.17	***CAT3***
Exposed	2.79 ± 0.49	2.26 ± 0.37	2.75 ± 0.46	
Control	1.00 ± 0.08	1.00 ± 0.10	1.00 ± 0.15	***Fe-SOD1***
Exposed	0.97 ± 0.05	0.88 ± 0.09	0.87 ± 0.09	
Control	1.00 ± 0.11	1.00 ± 0.16	1.00 ± 0.12	***Cu/Zn-SOD1***
Exposed	0.92 ± 0.08	0.86 ± 0.21	1.47 ± 0.31	
Control	1.00 ± 0.22	1.00 ± 0.25	1.00 ± 0.35	***MnSOD2***
Exposed	0.90 ± 0.13	0.64 ± 0.14	0.16 ± 0.06	
Control	1.00 ± 0.07	1.00 ± 0.08	1.00 ± 0.08	***GR1 (Chl)***
Exposed	1.41 ± 0.14	1.00 ± 0.08	1.00 ± 0.06	
Control	1.00 ± 0.11	1.00 ± 0.07	1.00 ± 0.06	***GR1 (Cyt)***
Exposed	1.02 ± 0.09	0.91 ± 0.06	0.84 ± 0.08	
Control	1.00 ± 0.10	1.00 ± 0.09	1.00 ± 0.11	***APX1***
Exposed	1.06 ± 0.14	0.85 ± 0.05	0.91 ± 0.07	
Control	1.00 ± 0.06	1.00 ± 0.06	1.00 ± 0.07	***APX3***
Exposed	1.18 ± 0.10	0.88 ± 0.04	0.93 ± 0.09	
Control	1.00 ± 0.19	1.00 ± 0.12	1.00 ± 0.08	***APX6***
Exposed	0.83 ± 0.15	0.88 ± 0.08	1.09 ± 0.11	
Control	1.00 ± 0.12	1.00 ± 0.10	1.00 ± 0.07	***APXS***
Exposed	0.98 ± 0.10	0.80 ± 0.09	0.72 ± 0.06	
Control	1.00 ± 0.15	1.00 ± 0.10	1.00 ± 0.09	***APXT***
Exposed	1.46 ± 0.23	1.34 ± 0.19	0.90 ± 0.09	
Control	1.00 ± 0.07	1.00 ± 0.06	1.00 ± 0.05	***GPX1***
Exposed	1.04 ± 0.10	0.91 ± 0.08	0.95 ± 0.12	
Control	1.00 ± 0.08	1.00 ± 0.06	1.00 ± 0.08	***GPX2***
Exposed	1.10 ± 0.08	0.92 ± 0.05	0.93 ± 0.10	
Control	1.00 ± 0.06	1.00 ± 0.05	1.00 ± 0.08	***GPX3***
Exposed	1.11 ± 0.08	0.85 ± 0.05	0.88 ± 0.10	

Table 7 - Expression patterns of genes related to antioxidative pathways in leaves of *Brassica oleracea* var. *italica* exposed to diesel exhaust. n=9. Data ± SE. (significant upregulation in green, significant downregulation in red of old and young leaves relative to middle leaves; one-way ANOVA, $P < 0.05$, analysis performed in RStudio). Genes: catalase (*CAT1*, *CAT2*, and *CAT3*), iron superoxide dismutase (*Fe-SOD1*), copper/zinc superoxide dismutase (*Cu/Zn-SOD1*), manganese superoxide dismutase (*MnSOD2*), glutathione reductase (*GR1 (Chl)* (chloroplastic) and *GR1 (Cyt)* (cytosolic)), ascorbate peroxidase (*APX1*, *APX3*, *APX6*, *APXS* (stromal), *APXT* (thylakoid)), glutathione peroxidase (*GPX1*, *GPX2*, and *GPX3*).

Treatment	Leaf age			Genes
	Old	Middle	Young	
Control	2.12 ± 0.26	1.00 ± 0.12	0.64 ± 0.09	***CAT1***
Exposed	1.88 ± 0.26	1.00 ± 0.10	0.71 ± 0.06	
Control	1.83 ± 0.36	1.00 ± 0.17	0.65 ± 0.06	***CAT2***
Exposed	1.94 ± 0.21	1.00 ± 0.25	0.51 ± 0.05	
Control	0.85 ± 0.14	1.00 ± 0.17	060 ± 0.10	***CAT3***
Exposed	1.05 ± 0.18	1.00 ± 0.17	0.73 ± 0.12	
Control	1.52 ± 0.13	1.00 ± 0.10	0.58 ± 0.09	***Fe-SOD1***
Exposed	1.68 ± 0.09	1.00 ± 0.11	0.57 ± 0.06	
Control	1.83 ± 0.20	1.00 ± 0.16	0.53 ± 0.07	***Cu/Zn-SOD1***
Exposed	1.96 ± 0.18	1.00 ± 0.25	0.91 ± 0.19	
Control	0.84 ± 0.19	1.00 ± 0.25	0.76 ± 0.26	***MnSOD2***
Exposed	1.19 ± 0.17	1.00 ± 0.22	0.19 ± 0.07	
Control	1.07 ± 0.07	1.00 ± 0.08	0.85 ± 0.07	***GR1 (Chl)***
Exposed	1.52 ± 0.15	1.00 ± 0.08	0.85 ± 0.05	
Control	1.71 ± 0.18	1.00 ± 0.07	0.68 ± 0.04	***GR1 (Cyt)***
Exposed	1.90 ± 0.17	1.00 ± 0.07	0.63 ± 0.06	
Control	1.59 ± 0.16	1.00 ± 0.09	0.61 ± 0.06	***APX1***
Exposed	1.98 ± 0.26	1.00 ± 0.06	0.65 ± 0.05	
Control	0.94 ± 0.06	1.00 ± 0.06	0.80 ± 0.05	***APX3***
Exposed	1.27 ± 0.11	1.00 ± 0.05	0.85 ± 0.08	
Control	5.97 ± 1.11	1.00 ± 0.12	0.51 ± 0.04	***APX6***
Exposed	5.59 ± 1.00	1.00 ± 0.09	0.63 ± 0.06	
Control	1.23 ± 0.15	1.00 ± 0.10	0.73 ± 0.05	***APXS***
Exposed	1.51 ± 0.16	1.00 ± 0.11	0.65 ± 0.06	
Control	0.84 ± 0.13	1.00 ± 0.10	1.46 ± 0.13	***APXT***
Exposed	0.92 ± 0.15	1.00 ± 0.14	0.97 ± 0.10	
Control	1.16 ± 0.08	1.00 ± 0.06	0.71 ± 0.03	***GPX1***
Exposed	1.34 ± 0.12	1.00 ± 0.09	0.74 ± 0.09	
Control	1.08 ± 0.09	1.00 ± 0.06	0.82 ± 0.07	***GPX2***
Exposed	1.30 ± 0.09	1.00 ± 0.05	0.84 ± 0.09	
Control	1.08 ± 0.06	1.00 ± 0.05	0.77 ± 0.06	***GPX3***
Exposed	1.41 ± 0.10	1.00 ± 0.06	0.80 ± 0.09	

Consequently, old leaves show a significant upregulation for most genes investigated compared to young leaves (Table S6, appendix H).

Together, these findings show a general trend of downregulation for most genes in exposed leaves, with some notable exceptions. Subsequently, older leaves show a significant upregulation for most genes, while expression in younger leaves is generally downregulated.

3.6 Fluorescence emission spectra of secondary metabolites

To determine whether diesel exhaust exposure alters the relative abundance of secondary metabolites and the (NADH + H^+)/NAD^+ and $FADH_2$/FAD ratios in the blue-green emission region (400-600nm), spectra of fresh leaf cross-sections were analyzed using confocal microscopy. The normalized data is shown in Fig. 16-20 and Table 8. The non-normalized data can be found in appendix I.

The emission is higher in young compared to old leaves for both treatments in the blue emission region (400-500nm) (Fig. 16-17). This trend is seemingly reversed in the green emission region (500-600nm). The emission is significantly higher at 468nm in old compared to young leaves in exposed plants (P = 0.044) (Table 8). There is no significant difference at the other wavelengths.

When considering the differences between treatments, a similar trend is visible in all leaf ages: exposed plants show a lower emission in the blue region, while a higher emission is indicated in the green region (Fig. 18-20). The difference between the treatments is not significantly different. Finally, distinct peaks are visible: a peak at 468nm in the blue region, a peak at 503nm at the transition of the blue to green region, and a shoulder at 521nm in the green region.

Together, these findings indicate that the fluorescence emission is lower in the blue region in exposed plants and in old compared to young leaves, but this trend is reversed in the green region. Emission peaks are visible at 468nm, 503nm and 521nm.

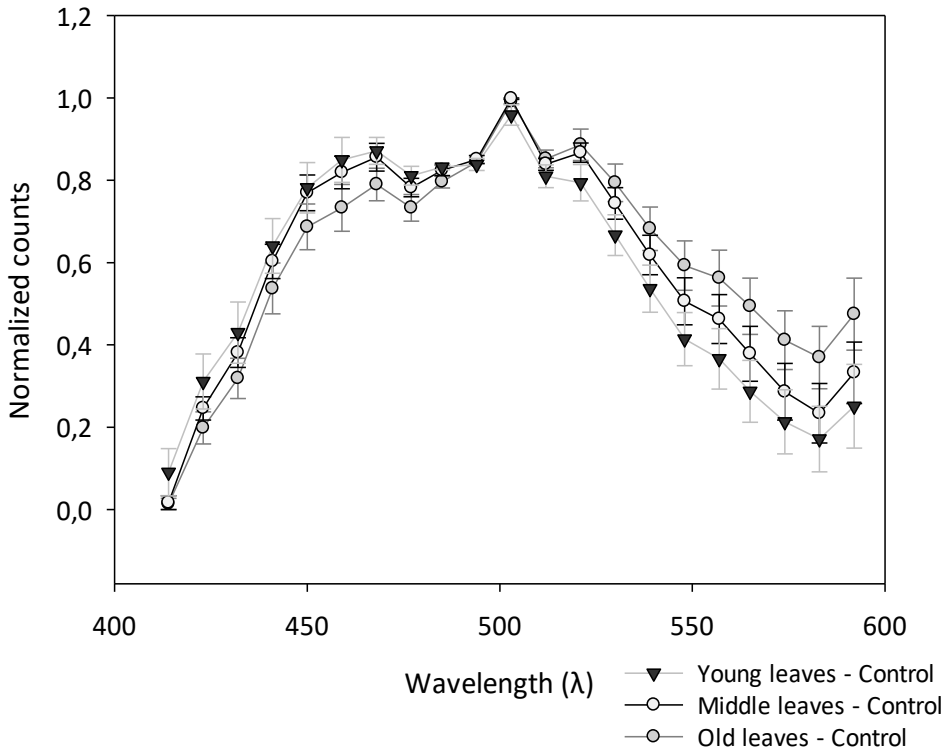

Fig. 16 – **Normalized cross-section fluorescence emission spectra in the blue-green region of control leaves of *Brassica oleracea* var. *italica***. Data ± SE**.** Line graph created in SigmaPlot**.**

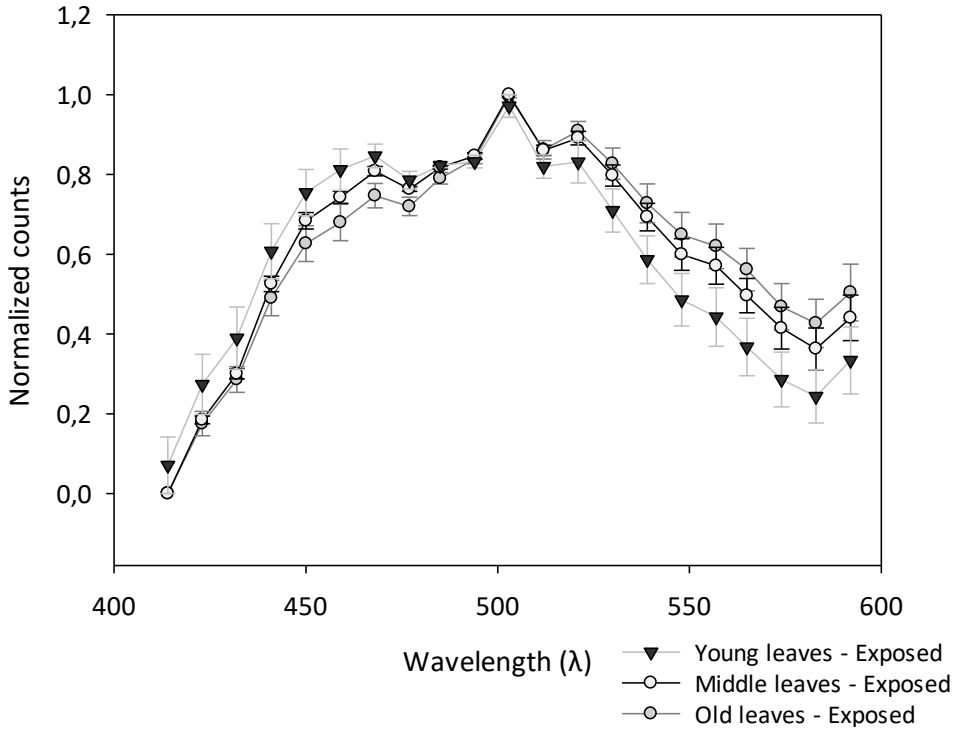

Fig. 17 – **Normalized cross-section fluorescence emission spectra in the blue-green region of leaves of *Brassica oleracea* var. *italica* exposed to diesel exhaust**. Data ± SE**.** Line graph created in SigmaPlot**.**

Table 8 - List of p-values of differences in fluorescence emission in leaves of *Brassica oleracea* var. *italica* exposed to diesel exhaust. One-way ANOVA. Significant values ($P > 0.05$) are marked in red. Control leaves corresponds to data of Fig. 16. Exposed leaves corresponds to data of Fig. 17. O-M, old versus middle leaves; M-Y, middle versus young leaves; O-Y, old versus young leaves. Between treatments, control versus exposed leaves.

Wavelength (nm)	Control leaves			Exposed leaves			Between treatments		
	O-M	M-Y	O-Y	O-M	M-Y	O-Y	Old	Middle	Young
414	0.998	0.331	0.304	1.000	0.482	0.513	0.389	0.341	0.834
432	0.711	0.812	0.358	0.980	0.442	0.374	0.613	0.058	0.717
441	0.704	0.891	0.434	0.878	0.481	0.271	0.576	0.123	0.738
450	0.538	0.986	0.446	0.664	0.507	0.159	0.448	0.105	0.753
459	0.473	0.906	0.287	0.560	0.465	0.105	0.508	0.101	0.629
468	0.407	0.950	0.266	0.256	0.540	0.044	0.439	0.211	0.584
477	0.404	0.722	0.123	0.279	0.673	0.072	0.763	0.438	0.443
485	0.280	0.900	0.140	0.120	0.918	0.062	0.785	0.644	0.288
494	0.912	0.696	0.912	0.916	0.705	0.929	0.678	0.749	0.776
503	0.938	0.174	0.295	0.988	0.486	0.605	0.491	0.341	0.740
512	0.910	0.624	0.387	0.999	0.443	0.451	0.766	0.298	0.805
521	0.926	0.354	0.204	0.938	0.475	0.329	0.650	0.423	0.601
530	0.713	0.462	0.144	0.881	0.327	0.175	0.613	0.276	0.572
539	0.676	0.532	0.160	0.884	0.300	0.162	0.564	0.235	0.563
548	0.583	0.543	0.127	0.818	0.337	0.148	0.532	0.209	0.453
557	0.558	0.557	0.130	0.848	0.314	0.150	0.552	0.181	0.477
565	0.493	0.637	0.128	0.732	0.286	0.094	0.482	0.168	0.459
574	0.462	0.762	0.166	0.821	0.316	0.139	0.575	0.168	0.500
583	0.437	0.831	0.189	0.758	0.370	0.138	0.593	0.180	0.502
592	0.507	0.796	0.208	0.823	0.556	0.276	0.812	0.276	0.544

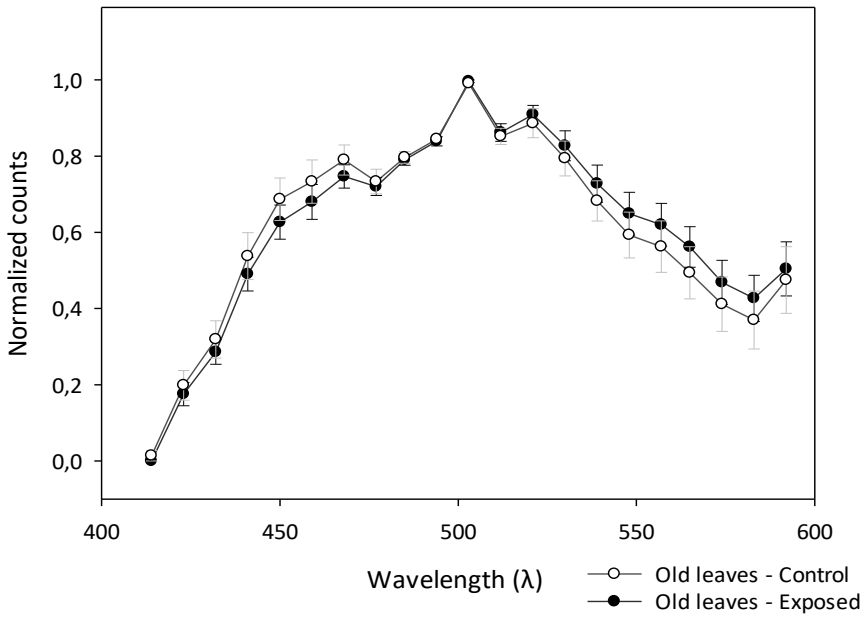

Fig. 18 – Normalized cross-section fluorescence emission spectra in the blue-green region of old leaves of *Brassica oleracea* var. *italica* exposed to diesel exhaust. Data ± SE. Line graph created in SigmaPlot.

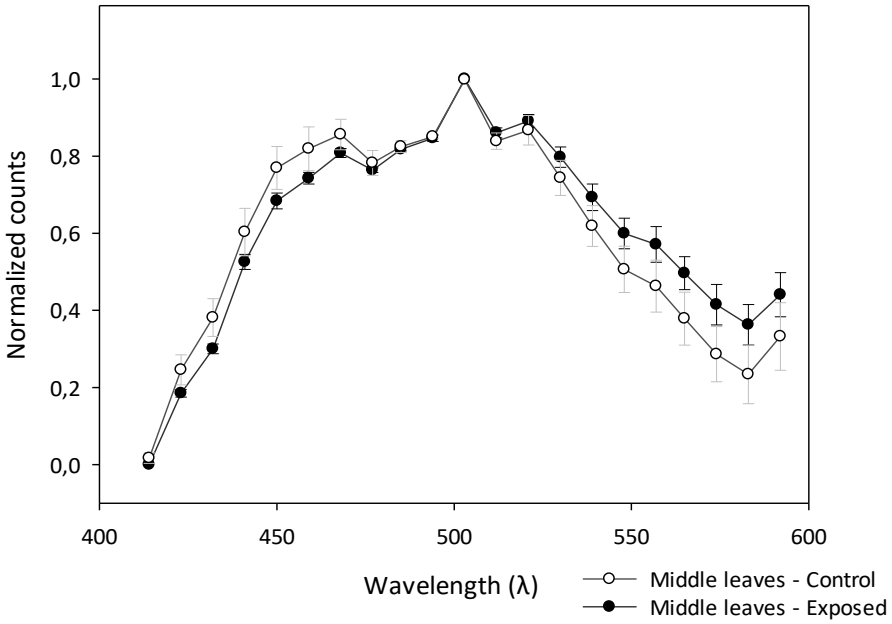

Fig. 19 – **Normalized cross-section fluorescence emission spectra in the blue-green region of middle leaves of *Brassica oleracea* var. *italica* exposed to diesel exhaust**. Data ± SE. Line graph created in SigmaPlot.

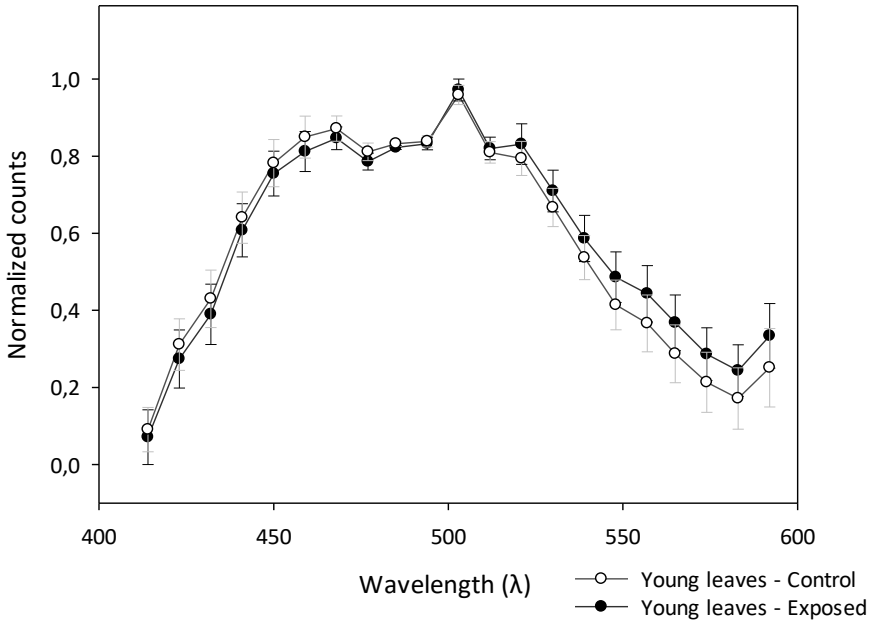

Fig. 20 – **Normalized cross-section fluorescence emission spectra in the blue-green region of young leaves of *Brassica oleracea* var. *italica* exposed to diesel exhaust**. Data ± SE. Line graph created in SigmaPlot.

4. DISCUSSION

PART I: The impact of traffic-related air pollution on ChlF kinetics in London Plane

ChlF kinetics in urban vegetation have previously been investigated in a number of cities[24,75], although these studies generally focus on the use of either active or passive techniques. We made use of both destructive (PTI) and non-destructive (PEA and PAM) active techniques to investigate how urban vegetation in Hasselt, one of Belgium's larger urban centres, is affected by traffic exposure. We hypothesized that leaves of *Platanus x acerifolia* near Hasselt inner ring road showed altered ChlF kinetics and more heavy metal deposition compared to those at a reference site in Kapermolen Park.

4.1 Traffic exposure near Hasselt Inner ring road

Our data showed a significantly higher presence of Fe, Cu and Pb in leaves of London Planes near Hasselt inner ring road compared to Kapermolen Park. The presence of Fe, Cu and Pb are linked to both traffic exhaust related (byproducts of combustion processes) and non-exhaust related sources (brake disk wear, tire abrasion).[76-77] These sources likely account for the majority of the higher concentrations that we found in leaves near Hasselt inner ring road, and therefore indicate a higher traffic exposure in this location. On a side note, it should be emphasized that a higher presence of Cu and Pb in these leaves could also be a consequence of higher uptake and presence in the soil as a result of traffic-related sources.[78]

Furthermore, the data on the air pollutants showed a significantly higher presence of BC, NO_2 and $PM_{2.5}$ near Hasselt inner ring road. BC is a byproduct of incomplete combustion processes, both anthropogenic and natural. In perspective of traffic, diesel exhaust is a major source of BC.[79] NO_2 is an air pollutant that is likewise formed during combustion processes, and proved to be a valuable indicator of traffic exposure.[80] $PM_{2.5}$ is ubiquitous in ambient air due to both anthropogenic and natural sources, though local levels in the vicinities of roads may rise steeply due to its strong correlation with exhaust emissions.[81]

In conclusion, the higher presence of these heavy metals and the air pollutants confirm that trees near Hasselt inner ring road experience a higher traffic exposure compared to trees near Kapermolen Park.

4.2 Plant performance under air pollution stress

Exposure to different stressors has in many cases shown to reduce the performance and overall health in different plant species.[82-83] Our results showed the opposite, a significantly higher ϕ_{P0} and PI(CS_m) indicate higher leaf performance near Hasselt inner ring road. These findings suggest that traffic exposure in Hasselt acts as a mild environmental stressor that optimizes plant overall performance. This is confirmed by a stable LWC, SLA and CCI, as leaf morphology and chlorophyll content are altered only in case of severe stress.[84] A higher Ψ_0 and ABS/RC was also detected in leaves from Hasselt inner ring road, indicating that both more electrons are captured per RC, and that the ones captured are more efficiently transported through the electron transport chain. Moreover, a significantly higher ETR further supports this result. Additionally, Cu-eutrophication could enhance the ETR as it is a crucial element of plastocyanin which is involved in electron transfer from PSII to PSI.[85] Furthermore, the higher NO_2 presence could serve as a N source (N-fertilizing), which is usually the limiting element for vegetation growth and development. This might also have a positive effect on plant performance.[86]

Our data did not indicate a significant change in the complementary yield parameters - Y(II), Y(NO) and Y(NPQ)) - nor in the processes involved in NPQ. This result suggests that photochemical processes are not overwhelmed by stress, but instead the trees seem to be performing optimally. A slightly higher Y(II) and lower Y(NO) confirm the higher ϕ_{P0} and PI(CS_m) observed earlier on.

Interestingly, a significant increase in steady-state fluorescence at 685 nm, corresponding to PSII, was noticed in leaves from Hasselt inner ring road. This result was unexpected considering a higher steady-state fluorescence generally indicates that plants are performing worse due to stress, while we found an increased performance and overall health of the trees. This seeming contradiction could be explained by a change in the ratio of LHCII/LHCI (thylakoid stacking) due to dephosphorylation of PSII-LHCII proteins, which promotes energy flow to PSII.[87-88] Consequently, a higher flow of energy might explain the increased overall performance and more efficient electron transport and the higher ETR, while at the same time the higher input to PSII implies a higher fluorescence emission in absolute counts due to more PSII complexes being activated.

Although each of the three applied devices used in this research (PEA, PAM and PTI) approach the fluorescence kinetics differently, they all seem to back this explanation. In the PEA data we found a significantly higher F_m correlated with a significantly higher ABS/RC. PAM produced a higher F and ETR after quenching until steady-state (Fs observed after 301s). These findings by both fluorimeters could be a probe for the higher steady-state fluorescence emission from the PTI. In conclusion, this implies that passive remote sensing techniques that produce spectral data (similar to PTI) alone are not sufficient to analyze the physiological state of the vegetation. As remote sensing platforms would have observed higher fluorescence at Hasselt ring road – indicating stress exposure – and would therefore conclude that the vegetation is in suboptimal condition, while this is contradicted by the active measurements that provide more detailed information on the plants physiology.

4.3 Correlation analysis of investigated parameters

We also examined the possibility of correlated parameters between all samples taken in Hasselt. Our data indicated significant correlations between the CCI and SLA and ChlF parameters. Fluorimeters are designed to normalize data for the CCI, and therefore are unlikely to explain this correlation. Moreover, there was no significant difference in both parameters between the two sites, which indicates that traffic exposure is also not likely to explain this finding. We also demonstrated that the CCI and SLA are not affected by heavy metals or by air pollutants, and therefore have to look for other elements that might influence these parameters. One possible explanation could be that the sampled leaves show changes in light adaptation, as it has been shown that leaves from different parts of a canopy which receive different amounts of light, show morphological adaptations to cope with the available light energy they receive. Even though we sampled at approximately the same height in each tree, changes in infrastructure near the trees and the sampling orientation can have an effect on the ability of leaves to adapt to the available light conditions.

The correlation between the SLA, Y(NO) and DI_0/RC is interesting, and indicates the importance of leaf surface area in leaf thermoregulation. It has previously been noted that thinner leaves may promote heat dissipation through improved convective heat loss.[89-90] Next, the correlation of Cu with some of the OJIP parameters can be a result of its role in the electron transport chain, as mentioned before. Subsequently, the correlation of Zn with steady-state fluorescence could be an indication of its role in

the Calvin-Benson cycle as part of the carbonic anhydrases that convert CO_2 and H_2O into HCO^-, thereby supplying the enzyme ribulose 1,5-bisphosphate carboxylase/oxygenase (Rubisco) with a ready source of carbon to drive photosynthetic CO_2 fixation.[91] Steady-state fluorescence is dependent on the interplay between reactions of the Calvin-Benson cycle and processes involved in non-photochemical quenching.

Ni is an essential micronutrient for plants as it is an integral part of the active site of urease, an enzyme that hydrolyzes urea and consequently plays an important role in N recycling.[92] Moreover, Ni has also been implicated to play a role in activating glyoxalases, which are enzymes involved in degrading methylglyoxal (MG).[93] MG is a toxic product formed during glycolysis, and its formation is increased under stressful conditions.[93] Cellular respiration is intimately linked to the processes involved in photosynthesis, and therefore establishes a link between the formation of MG during glycolysis and the role of Ni in affecting ChlF parameters. In this respect, the correlation of Ni with some the ChlF parameters may relate to its role in providing nitrogen for plant growth and development, or due to its role in reducing the toxic effects of MG production in the cell under stress conditions.

Interestingly, our analysis also found a correlation between PM_{10} and F. A correlation between F and PM_{10} but not $PM_{2.5}$ or BC demonstrates that only larger particles have an effect on F. Larger particles are carried for shorter distances before they deposit, and therefore act as a higher local source of air pollution. $PM_{2.5}$ and BC are carried longer distances due to their size, while NO_2 diffuses rapidly due to its volatility and therefore is a better indicator at a larger scale. PM_{10} is a stressor and could therefore lead to a higher fluorescence emission, though elucidating its role in influencing fluorescence emission will require further research.

Finally, the correlation between the SLA and Fe could be explained by the importance of Fe in biochemical and physiological processes, including chlorophyll synthesis and reduction steps of important biological events, such as respiration and photosynthesis.[94]

PART II: Antioxidative responses in broccoli induced by diesel exhaust exposure

The effects of air pollution on plant antioxidant defenses have been studied for a number of individual air pollutants (e.g. ozone, SO_2).[95-96] However, there has not yet been a comprehensive study whereby traffic exhaust, specifically diesel emissions, are simulated in a controlled environment to investigate effects on plant antioxidative responses. We hypothesized that leaves of *Brassica oleracea* var. *italica* exposed to diesel exhaust showed altered antioxidative responses.

4.4 Total antioxidant capacity

Exposure to stress generally leads to a higher antioxidant capacity in plants due to an increased production of antioxidants and increased antioxidant enzyme activity.[97] Preliminary data of our research group indicated increased enzymatic activities of CAT, SOD, APX and GR. We therefore expected an increase in the TAC in leaves exposed to diesel exhaust compared to control leaves. Although we applied the same cultivation and exposure procedures, our data showed the opposite. This indicates that our analysis took place after the initial rise in the amount of antioxidants had occurred, and that antioxidant resources in general are being depleted as result of a prolonged state of oxidative stress.[98] In other words, it is assumed that initially there is an increase in the TAC in exposed leaves to cope with an increasing amount of ROS, but that the available antioxidant resources to scavenge these ROS are depleted over the course of the exposure. On the other hand, it is also possible that the exposure acts in a destructive way to inhibit the synthesis of antioxidants, or interferes with reactions involved in antioxidative pathways.[99] This is investigated by means of a gene expression study later on, including several of the most prominent antioxidative enzymes.

Furthermore, we found a lower HF/LF ratio in exposed leaves compared to control leaves, which is caused mostly by a lower HF in exposed leaves. This fraction contains the water-soluble antioxidants, including the major cellular redox buffers glutathione and ascorbate. A lower HF could indicate that these antioxidants have been reduced in number, and therefore confirm that antioxidant resources are being depleted.

Studies examining the difference in the TAC between leaves of different ages are rather scarce, however the available literature indicates that the TAC decreases when leaf age increases.[100] Our data confirms this finding by indicating that older leaves have a significantly lower TAC compared to younger leaves. The processes involved in senescence have been shown to lower the antioxidant capacity in the aging leaf due to an increased production of ROS which deplete available antioxidant resources.[101] Moreover, this would also account for the lower TAC found in older leaves of control plants. Additionally, we found a higher HF/LF ratio in old leaves. This result of which is caused by a much lower LF in these leaves, which includes fat-soluble components such as tocopherols, carotenoids and phenolic compounds. It is possible that the increased ROS production in relation to leaf senescence in old leaves facilitates the depletion of the fat-soluble antioxidant as well.

4.5 Hydrogen peroxide quantification

We also investigated the amount of H_2O_2 present in the leaf samples. Our data indicated a higher amount of H_2O_2 in leaves exposed to diesel exhaust. The higher presence of H_2O_2 indicates an increase in ROS-related products a result of a state of oxidative stress.[102] Below a certain threshold, H_2O_2 has been shown to act as a signaling molecule to strengthen antioxidant defense when under stress, such

as by enhancing antioxidant enzyme activities,[103] which would correspond to the previous findings of our research group.

Old leaves contain a significantly higher amount of H_2O_2 compared to middle and young leaves, while the difference between middle and young leaves is not significant. This finding relates to processes involved in leaf senescence, as leaf aging is associated with the degradation of Chl and membranes and a decrease in total RNA and protein count,[100] ultimately leading to the production of free radicals, including the formation of H_2O_2. Moreover, we investigated the relative Chl content (data not shown) and total protein count and confirmed that both were decreased in older leaves. The difference between treatments was not significantly different for both analyses, indicating that the exposure did not act in a destructive way.

4.6 Gene expression of antioxidant enzymes

We examined the expression of genes related to antioxidative pathways. Exposed plants indicated a general trend of downregulation for most genes in middle and young leaves, while expression in old leaves is generally slightly upregulated. Exceptions to this trend are *CAT1*, *CAT3*, and *APXT* which are upregulated for all leaf ages. Antioxidant gene expression has previously been investigated by Rhizsky and coworkers in tobacco under different stress conditions.[104] They found that differential expression of antioxidant enzymes appeared to correlate to some extent between different stressors, although stressor-specific responses were noted as well.

CAT: the authors found that heat stress decreases the expression of *CAT1* and *CAT2*, while drought showed the opposite. *CAT3* was significantly upregulated for both. We found an upregulation for *CAT1* and *CAT3*, and a downregulation for *CAT2*. Enzymatic CAT has a high specificity and a high turnover rate for H_2O_2, and operate mostly in peroxisomes to convert H_2O_2 formed during photorespiratory oxidation, although its presence in other organelles has been noted as well.[105] The contrast between upregulation in *CAT3* and downregulation in *CAT2* can be a consequence of plant circadian rhythms. *CAT2* transcript abundance in *Arabidopsis* is typically at its lowest at night-day transition. However, *CAT3* shows an inverse circadian rhythm and therefore has its highest abundance at the night-day transition.[106-107] ***SOD***: a downregulation of *Fe-SOD* and *Cu/Zn-SOD* was found by the authors during heat stress. Our data confirmed these findings, with the exception of upregulation in young leaves for *Cu/Zn-SOD*. Additionally, we found a downregulation in *MnSOD* as well. SOD enzymes convert $O_2^{\bullet -}$ to O_2 and H_2O_2, and are present in most subcellular compartments where activated oxygen is produced.[108] ***GR***: the authors noted a significant downregulation of *GR* under both heat and drought stress. Our data showed an upregulation of *GR (Chl)* in old leaves. Enzymatic GR catalyzes the reduction of oxidized glutathione (GSSG) to its reduced form (GSH) using NAD(P)H, thereby maintaining the cellular GSH/GSSG ratio.[109] ***APX***: the authors investigated both *APX1* and the thylakoid (*APXT*) and stromal (*APXS*) isozymes, and found that *APX1* and *APXT* were upregulated, while *APXS* was downregulated. Enzymatic APX is localized in most cellular compartments where it plays the same role as CAT, though it has a much higher affinity for H_2O_2, and therefore acts as a competent scavenger of H_2O_2 under stress.[110] ***GPX***: *GPX* was downregulated under both heat and drought stress. We found the same result for middle and young leaves, while old leaves show an upregulation. GPX enzymes utilize GSH to convert H_2O_2 into GSSH and H_2O, but play only a minor role in peroxide metabolism.[111]

Previous data of our research group indicated increased enzyme activities of CAT, SOD, GR and APX. With regard to the link between gene expression and enzymatic activity, we could not indicate a direct

correlation. *CAT2* and *CAT3* are much more abundant than *CAT1*,[106-107] and therefore have a much higher effect on overall enzyme abundance of CAT. Our data indicated a downregulation of *CAT2* and an upregulation of *CAT3*, which suggests that the enzymatic activity of CAT is regulated by higher turnover rates or other translational mechanisms, rather than by a higher expression. The same could be the case for SOD, as we found a downregulation for all three isozymes. For GR and APX, we could not indicate a direct role of gene expression either.

When considering the differential expression between the different leaf ages, we found that old leaves show a significant upregulation for most genes investigated compared to middle leaves, while young leaves show a general trend of downregulation. Leaf aging has been shown to upregulate several genes involved in antioxidative pathways,[100] most likely to combat the increased presence of ROS as a consequence of processes involved in senescence. Our data suggests that this event of upregulated antioxidant gene expression already takes place in middle leaves, as expression levels overall are increased compared to young leaves.

4.7 Fluorescence emission spectra of secondary metabolites

Finally, we investigated the relative abundance of secondary metabolites and the $(NADH + H^+)/NAD^+$ and $FADH_2/FAD$ ratios in cross-sectional leaf samples. Our data showed that both exposed plants and older leaves show a lower emission in the blue emission band (400-500nm), but a higher emission in the green emission band (500-600nm). Distinct peaks are visible at 468nm, 503nm and 521nm. The peak at 468nm corresponds to the emission of free NADH at 460nm, whereas the emission maximum of protein-bound NADH relates to the region 430-435nm,[112] next to phenolic compounds among others. The peak at 521nm corresponds to the emission of the oxidized flavins (FMN and FAD) at 515-520nm,[113] next to flavonoids among others. The peak at 503nm is most likely an artefact due to the analysis capturing a technical spectrum rather than an absolute spectrum, with the former being susceptible to creating imaging artefacts.

A lower emission in the blue region together with a higher emission in the green region corresponds to a lower abundance of reduced coenzymes, and a higher abundance of oxidized coenzymes. We found this to be the case for leaves exposed to diesel exhaust and older compared to younger leaves, which corresponds to the reduced TAC that we found in relation to increased ROS production with regard to diesel exhaust exposure and leaf senescence, respectively. Moreover, phenolics have been shown to have antioxidant properties as well. In particular, flavonoids have been implicated to act as potent H_2O_2 scavengers.[114] There is some evidence that phenolic metabolism can be induced when a plant experiences stress.[115] In this respect, it is possible that the higher emission in the green band correlates to a higher presence of phenolics, perhaps induced due to the higher presence of H_2O_2 caused by both the exposure and processes involved in leaf senescence.

5. CONCLUSION AND FUTURE PERSPECTIVES

In the first part of this research we hypothesized that trees of *Platanus x acerifolia* present near Hasselt inner ring road indicate altered physiological responses and increased heavy metal deposition compared to trees at a reference site in Kapermolen Park.

Leaves of *Platanus x acerifolia* near Hasselt inner ring road contain a significantly higher amount of Cu, Fe and Pb compared to those from Kapermolen Park, which are derived primarily from traffic-related sources. Moreover, a significantly higher presence of BC, NO_2 and $PM_{2.5}$ near Hasselt Inner ring road confirms a higher traffic exposure. A significantly higher ϕ_{P0} and PI(CS_m) in leaves from Hasselt inner ring road indicates that these trees have an overall higher performance, likely due to mild stress induced by traffic exposure. A higher Ψ_0 and ABS/RC indicates more efficient electron capture and transport, which is confirmed by a significantly higher ETR. No significant differences in the quenching mechanisms suggest that photochemical processes are not overwhelmed, though an increased steady-state fluorescence of PSII was found. The latter could be explained by change in the ratio of LHCII/LHCII, thereby promoting a higher energy flow to PSII. The correlation analysis revealed significant associations between most of the ChlF parameters and the CCI, and between some of the ChlF parameters and the metals Cu, Zn and Ni. The correlation with CCI could relate to processes involved in light adaptation, while the metals are all in some way related to processes involved in photosynthesis. The correlation between the SLA, Y(NO) and DI_0/RC signifies a role of leaf surface area in heat dissipation, while the correlation between SLA and Fe could point to the role of Fe in several biochemical and physiological processes.

In the second part of this research, we hypothesized that increased antioxidant enzyme activity is caused by altered gene expression levels, and additionally that there is an increase in the TAC, production of H_2O_2, and changes in the $(NADH + H^+)/NAD^+$ and $FADH_2$/FAD ratios in leaves of *Brassica oleracea* var. *italica* exposed to diesel exhaust.

Exposed leaves have a lower TAC compared to control leaves, which indicates that antioxidants are being depleted. Moreover, an increased production of H_2O_2 indicates an increase in ROS-related products, which can explain the antioxidant depletion in the long run. Alternatively, a role as signaling molecule in relation to a cellular state of oxidative stress is possible as well. The fluorescence emission data supports the association of ROS production and antioxidant depletion by indicating that the cellular redox state is affected, as is evident by lower $(NADH + H^+)/NAD^+$ and $FADH_2$/FAD ratios. Antioxidant gene expression does not indicate a direct link to antioxidant enzyme activities, but suggests a role of translational control mechanisms in regulating activity levels.

Older leaves have a lower TAC compared to younger leaves, which is a result of processes involved in leaf senescence. These processes are responsible for an increased production of H_2O_2, thereby depleting available antioxidant resources, which translates into a lower TAC. The depletion of these resources is evident by an altered cellular redox state in the form of lower $(NADH + H^+)/NAD^+$ and $FADH_2$/FAD ratios. At the same time, the increased production of ROS-related products leads to an upregulation of antioxidant gene expression, which can ultimately lead to increased antioxidant enzyme activities to combat the excess ROS.

Many unanswered questions remain at the conclusion of this research. There is a need to further advance our knowledge on what the mechanisms are behind the higher steady-state fluorescence signal emitted in leaves which are paradoxically performing better and have a more efficient electron transport. The route from energy absorption to CO_2 fixation consists of a long and complex series of events, whereby complex interactions happen at every step. There is still a lot of research required to begin to understand how the different processes involved in photosynthesis interact with one another and how external influences can have an effect on each stage of the photosynthetic reactions. In particular, the contribution of PSI to the ChlF signal has still been little studied. Augmenting the current active devices (e.g. including gas exchange measurements) or combining different devices (e.g. PAM and PTI) would allow one to study the simultaneous effects on and contribution by PSI as well. This would improve the current knowledge and models on how plants respond to their environment. Furthermore, the role of heavy metals related to traffic exposure and their effects on plant performance remain to be elucidated. Moreover, the correlation analysis revealed some interesting associations between certain heavy metals and the fluorescence kinetics, as well as an unexpected association, such as that of F with PM_{10}, of which the biological meaning is currently unclear.

With regard to the antioxidative analysis, it would interesting to advance on whether the presence of H_2O_2 or other ROS-related products can be linked directly to traffic exposure. Subsequently, there is a need to further elucidate the link between antioxidant gene expression and enzyme activities in relation to traffic exposure, for example by including analyses of translational mechanisms, such a proteomics analysis. Finally, the fluorescence emission spectra obtained by confocal microscopy provided interesting trends, which require further elucidation. The contribution of different secondary metabolites to the emissions peaks in the blue-green emission region is still largely unknown. Life-time measurements could be performed to distinguish between different metabolites, however this is a very challenging task since there a lot of spectral overlap, but recent technologies allow to advance in this perspective.

6. REFERENCES

(1) World Health Organization. Ambient (outdoor) air quality and health. Fact sheet. 2014 Mar 13;313

(2) Sundvor I, Balaguer N, Viana M, Querol X, Reche C, Amato F, et al. Road traffic's contribution to air quality in European cities. ETC/ACM technical paper. 2012;14(2012):1-74.

(3) Mayer H (1999) Air pollution in cities. Atmospheric environment 33 (24-25):4029-4037

(4) Kulshrestha U, Saxena P (2016) Plant Responses to Air Pollution. Springer

(5) Woo, S., D. Lee and Y. Lee (2007). "Net photosynthetic rate, ascorbate peroxidase and glutathione reductase activities of *Erythrina orientalis* in polluted and non-polluted areas." Photosynthetica 45(2): 293-295.

(6) Papageorgiou GC (2004) Fluorescence of photosynthetic pigments *in vitro* and *in vivo*. In: Chlorophyll a Fluorescence. Springer

(7) Harbinson J, Rosenqvist E (2003) An introduction to chlorophyll fluorescence. In: Practical Applications of Chlorophyll Fluorescence in Plant Biology. Springer, pp 1-29

(8) McCree KJ (1971) The action spectrum, absorptance and quantum yield of photosynthesis in crop plants. Agricultural Meteorology

(9) Papageorgiou G (1975) Chlorophyll fluorescence: an intrinsic probe of photosynthesis. Bioenergetics of photosynthesis:319-371

(10) Lee K-H, Lee S-H (2012) Monitoring of floating green algae using ocean color satellite remote sensing. Journal of the Korean Association of Geographic Information Studies 15 (3):137-147

(11) Govindjee (1995) 63 years since kautsky - chlorophyll-a fluorescence. Australian Journal of Plant Physiology 22 (2):131-160. doi:10.1071/pp9950131

(12) Kautsky H, Appel W, Amann H (1960) Chlorophyll fluorescence and carbon assimilation. Part XIII. The fluorescence and the photochemistry of plants. Biochemische Zeitschrift 332:277-292

(13) Stirbet A, Govindjee (2011) On the relation between the Kautsky effect (chlorophyll a fluorescence induction) and photosystem II: basics and applications of the OJIP fluorescence transient. Journal of Photochemistry and Photobiology B: Biology 104 (1):236-257

(14) Strasser Rj, Tsimilli-Michael M, Srivastava A (2004) Analysis of the chlorophyll a fluorescence transient. In: Chlorophyll a Fluorescence. Springer, pp 321-362

(15) Maxwell K, Johnson GN (2000) Chlorophyll fluorescence - a practical guide. Journal of experimental botany 51 (345):659-668

(16) Strasser RJ, Srivastava A, Tsimilli-Michael M (2000) The fluorescence transient as a tool to characterize and screen photosynthetic samples. Probing photosynthesis: mechanisms, regulation and adaptation:445-483

(17) Schreiber U, Schliwa U, Bilger W (1986) Continuous recording of photochemical and non-photochemical chlorophyll fluorescence quenching with a new type of modulation fluorometer. Photosynthesis research 10 (1-2):51-62

(18) Misra AN, Misra M, Singh R (2012) Chlorophyll fluorescence in plant biology. In: Biophysics. InTech,

(19) Kramer DM, Johnson G, Kiirats O, Edwards GE (2004) New fluorescence parameters for the determination of QA redox state and excitation energy fluxes. Photosynthesis Research 79 (2):209-218

(20) Roháček K, Soukupová J, Barták M (2008) Chlorophyll fluorescence: a wonderful tool to study plant physiology and plant stress. Plant Cell Compartments-Selected Topics Research Signpost, Kerala, India:41-104

(21) Bradbury M, Baker NR (1981) Analysis of the slow phases of the *in vivo* chlorophyll fluorescence induction curve. Changes in the redox state of photosystem II electron acceptors and fluorescence emission from photosystems I and II. Biochimica et Biophysica Acta (BBA)-Bioenergetics 635 (3):542-551

(22) Guidi L, Calatayud A (2014) Non-invasive tools to estimate stress-induced changes in photosynthetic performance in plants inhabiting Mediterranean areas. Environmental and experimental botany 103:42-52

(23) Cendrero-Mateo MP, Moran MS, Papuga SA, Thorp K, Alonso L, Moreno J, Ponce-Campos G, Rascher U, Wang G (2015) Plant chlorophyll fluorescence: active and passive measurements at canopy and leaf scales with different nitrogen treatments. Journal of experimental botany 67 (1):275-286

(24) Van Wittenberghe S, Alonso L, Verrelst J, Hermans I, Delegido J, Veroustraete F, Valcke R, Moreno J, Samson R (2013) Upward and downward solar-induced chlorophyll fluorescence yield indices of four tree species as indicators of traffic pollution in Valencia. Environmental Pollution 173:29-37

(25) Magney TS, Frankenberg C, Fisher JB, Sun Y, North GB, Davis TS, Kornfeld A, Siebke K (2017) Connecting active to passive fluorescence with photosynthesis: a method for evaluating remote sensing measurements of Chl fluorescence. New Phytologist 215 (4):1594-1608

(26) Schowengerdt, R. A. (2006). *Remote sensing: models and methods for image processing*. Elsevier.

(27) Liu, J. G., & Mason, P. J. (2013). *Essential image processing and GIS for remote sensing*. John Wiley & Sons.

(28) Schott, J. R. (2007). *Remote sensing: the image chain approach*. Oxford University Press on Demand.

(29) Aiazzi B, Alparone L, Baronti S, Lastri C, Selva M (2012) Spectral distortion in lossy compression of hyperspectral data. Journal of Electrical and Computer Engineering 2012:3

(30) Ran L, Zhang Y, Wei W, Zhang Q (2017) A Hyperspectral Image Classification Framework with Spatial Pixel Pair Features. Sensors 17 (10):2421

(31) Meroni M, Rossini M, Guanter L, Alonso L, Rascher U, Colombo R, Moreno J (2009) Remote sensing of solar-induced chlorophyll fluorescence: Review of methods and applications. Remote Sensing of Environment 113 (10):2037-2051

(32) Campbell P, Middleton E, McMurtrey J, Chappelle E (2007) Assessment of vegetation stress using reflectance or fluorescence measurements. Journal of environmental quality 36 (3):832-845

(33) Rossini M, Meroni M, Celesti M, Cogliati S, Julitta T, Panigada C, Rascher U, van der Tol C, Colombo R (2016) Analysis of red and far-red sun-induced chlorophyll fluorescence and their ratio in different canopies based on observed and modeled data. Remote sensing 8 (5):412

(34) Smorenburg K, Courreges-Lacoste GB, Berger M, Buschman C, Del Bello U, Langsdorf G, Lichtenthaler HK, Sioris C, Stoll M-P, Visser H Remote sensing of solar-induced fluorescence of vegetation. In: Remote Sensing for Agriculture, Ecosystems, and Hydrology III, 2002. International Society for Optics and Photonics, pp 178-191

(35) Müller P, Li X-P, Niyogi KK (2001) Non-photochemical quenching. A response to excess light energy. Plant physiology 125 (4)

(36) Mozzo M, Dall'Osto L, Hienerwadel R, Bassi R, Croce R (2008) Photoprotection in the antenna complexes of photosystem II Role of individual xanthophylls in chlorophyll triplet quenching. Journal of Biological Chemistry 283 (10):6184-6192

(37) Peterman E, Dukker FM, Van Grondelle R, Van Amerongen H (1995) Chlorophyll a and carotenoid triplet states in light-harvesting complex II of higher plants. Biophysical journal 69 (6):2670-2678

(38) Telfer A (2005) Too much light? How β-carotene protects the photosystem II reaction centre. Photochemical & Photobiological Sciences 4 (12):950-956

(39) Barber J, Andersson B (1992) Too much of a good thing: light can be bad for photosynthesis. Trends in biochemical sciences 17 (2):61-66
(40) Derks A, Schaven K, Bruce D (2015) Diverse mechanisms for photoprotection in photosynthesis. Dynamic regulation of photosystem II excitation in response to rapid environmental change. Biochimica et Biophysica Acta (BBA)-Bioenergetics 1847 (4-5):468-485
(41) Aro E-M, Virgin I, Andersson B (1993) Photoinhibition of photosystem II. Inactivation, protein damage and turnover. Biochimica et Biophysica Acta (BBA)-Bioenergetics 1143 (2):113-134
(42) Gilmore AM (1997) Mechanistic aspects of xanthophyll cycle-dependent photoprotection in higher plant chloroplasts and leaves. Physiologia Plantarum 99 (1):197-209
(43) Walters RG, Ruban AV, Horton P (1994) Higher Plant Light-Harvesting Complexes LHCIIa and LHCIIc are Bound by Dicyclohexylcarbodiimide During Inhibition of Energy Dissipation. The FEBS Journal 226 (3):1063-1069
(44) Rochaix J-D (2014) Regulation and dynamics of the light-harvesting system. Annual review of plant biology 65:287-309
(45) Demmig-Adams B, Adams WW (1996) Xanthophyll cycle and light stress in nature: Uniform response to excess direct sunlight among higher plant species. Planta 198 (3):460-470. doi:10.1007/bf00620064
(46) Bohnert HJ, Nelson DE, Jensen RG (1995) Adaptations to environmental stresses. The plant cell 7 (7):1099
(47) Ahanger MA, Akram NA, Ashraf M, Alyemeni MN, Wijaya L, Ahmad P (2017) Plant responses to environmental stresses—from gene to biotechnology. AoB Plants 9 (4)
(48) Sharma P, Jha AB, Dubey RS, Pessarakli M. Reactive oxygen species, oxidative damage, and antioxidative defense mechanism in plants under stressful conditions. Journal of botany. 2012 Apr 24;2012.
(49) Foyer, C. H. and J. Harbinson (1994). "Oxygen metabolism and the regulation of photosynthetic electron transport." Causes of photooxidative stress and amelioration of defense systems in plants: 1-42.
(50) Roth MS (2014) The engine of the reef: photobiology of the coral–algal symbiosis. Frontiers in microbiology 5:422
(51) Neill, S. O., K. S. Gould, P. A. Kilmartin, K. A. Mitchell and K. R. Markham (2002). "Antioxidant capacities of green and cyanic leaves in the sun species, *Quintinia serrata*." Functional Plant Biology 29(12): 1437-1443.
(52) Mullineaux PM, Baker NR (2010) Oxidative stress: antagonistic signaling for acclimation or cell death? Plant physiology 154 (2)
(53) Shah, K., R. G. Kumar, S. Verma and R. Dubey (2001). "Effect of cadmium on lipid peroxidation, superoxide anion generation and activities of antioxidant enzymes in growing rice seedlings." Plant Science 161(6): 1135-1144.
(54) Mittler R (2002) Oxidative stress, antioxidants and stress tolerance. Trends in plant science 7 (9):405-410
(55) Mittler R, Vanderauwera S, Gollery M, Van Breusegem F (2004) Reactive oxygen gene network of plants. Trends in plant science 9 (10):490-498
(56) Noctor, G. and C. H. Foyer (1998). "Ascorbate and glutathione: keeping active oxygen under control." Annual review of plant biology 49(1): 249-279
(57) Chen, Q., M. Zhang and S. Shen (2011). "Effect of salt on malondialdehyde and antioxidant enzymes in seedling roots of Jerusalem artichoke (*Helianthus tuberosus* L.)." Acta physiologiae plantarum 33(2): 273-278.
(58) Zaefyzadeh, M., R. A. Quliyev, S. M. Babayeva and M. A. Abbasov (2009). "The effect of the interaction between genotypes and drought stress on the superoxide dismutase and chlorophyll content in durum wheat landraces." Turkish Journal of biology 33(1): 1-7.
(59) Foyer CH, Noctor G (2005) Oxidant and antioxidant signalling in plants: a re-evaluation of the concept of oxidative stress in a physiological context. Plant, Cell & Environment 28 (8):1056-1071
(60) Gill SS, Tuteja N (2010) Reactive oxygen species and antioxidant machinery in abiotic stress tolerance in crop plants. Plant physiology and biochemistry 48 (12):909-930
(61) Møller IM, Jensen PE, Hansson A (2007) Oxidative modifications to cellular components in plants. Annu Rev Plant Biol 58:459-481
(62) Baek K-H, Skinner DZ (2003) Alteration of antioxidant enzyme gene expression during cold acclimation of near-isogenic wheat lines. Plant Science 165 (6):1221-1227
(63) Bian S, Jiang Y (2009) Reactive oxygen species, antioxidant enzyme activities and gene expression patterns in leaves and roots of Kentucky bluegrass in response to drought stress and recovery. Scientia Horticulturae 120 (2):264-270
(64) Buschmann C, Lichtenthaler HK (1998) Principles and characteristics of multi-colour fluorescence imaging of plants. Journal of Plant Physiology 152 (2-3):297-314.
(65) Zimmermann T, Rietdorf J, Pepperkok R (2003) Spectral imaging and its applications in live cell microscopy. FEBS letters 546 (1):
(66) Meyer S, Cartelat A, Moya I, Cerovic Z (2003) UV-induced blue-green and far-red fluorescence along wheat leaves: a potential signature of leaf ageing. Journal of experimental botany 54 (383):757-769
(67) Talamond P, Verdeil J-L, Conéjéro G (2015) Secondary metabolite localization by autofluorescence in living plant cells. Molecules 20 (3):5024-5037
(68) Buschmann C, Langsdorf G, Lichtenthaler H (2000) Imaging of the blue, green, and red fluorescence emission of plants: an overview. Photosynthetica 38 (4):483-491
(69) Skala MC, Riching KM, Gendron-Fitzpatrick A, Eickhoff J, Eliceiri KW, White JG, Ramanujam N (2007) *In vivo* multiphoton microscopy of NADH and FAD redox states, fluorescence lifetimes, and cellular morphology in precancerous epithelia. Proceedings of the National Academy of Sciences 104 (49):19494-19499
(70) Fgovbe. (2018). Fgovbe. 'Population per municipality as of 1 January 2017', from http://statbel.fgov.be/en
(71) Reşitoğlu İA, Altinişik K, Keskin A (2015) The pollutant emissions from diesel-engine vehicles and exhaust aftertreatment systems. Clean Technologies and Environmental Policy 17 (1):15-27
(72) Kerchev P, Ivanov S (2008) Influence of extraction techniques and solvents on the antioxidant capacity of plant material. Biotechnology & Biotechnological Equipment 22 (1):556-559
(73) Remans T, Keunen E, Bex GJ, Smeets K, Vangronsveld J, Cuypers A (2014) Reliable gene expression analysis by reverse transcription-quantitative PCR: reporting and minimizing the uncertainty in data accuracy. The Plant Cell 26 (10):3829-38375.
(74) Brulle F, Bernard F, Vandenbulcke F, Cuny D, Dumez S (2014) Identification of suitable qPCR reference genes in leaves of *Brassica oleracea* under abiotic stresses. Ecotoxicology 23 (3):459-471
(75) Paoletti E (2009) Ozone and urban forests in Italy. Environmental Pollution 157 (5):1506-1512
(76) Adamiec E, Jarosz-Krzemińska E, Wieszała R (2016) Heavy metals from non-exhaust vehicle emissions in urban and motorway road dusts. Environmental monitoring and assessment 188 (6):369
(77) Penkała M, Ogrodnik P, Rogula-Kozłowska W (2018) Particulate Matter from the Road Surface Abrasion as a Problem of Non-Exhaust Emission Control. Environments 5 (1):9

(78) Wiseman CL, Zereini F, Püttmann W (2013) Traffic-related trace element fate and uptake by plants cultivated in roadside soils in Toronto, Canada. Science of the Total Environment 442:86-9
(79) Miguel AH, Kirchstetter TW, Harley RA, Hering SV (1998) On-road emissions of particulate polycyclic aromatic hydrocarbons and black carbon from gasoline and diesel vehicles. Environmental Science & Technology 32 (4):450-455
(80) Perez P, Trier A (2001) Prediction of NO and NO_2 concentrations near a street with heavy traffic in Santiago, Chile. Atmospheric Environment 35 (10):1783-1789
(81) Pérez N, Pey J, Cusack M, Reche C, Querol X, Alastuey A, Viana M (2010) Variability of particle number, black carbon, and PM_{10}, $PM_{2.5}$, and PM_1 levels and speciation: influence of road traffic emissions on urban air quality. Aerosol Science and Technology 44 (7):487-499
(82) Oukarroum A, Schansker G, Strasser RJ (2009) Drought stress effects on photosystem I content and photosystem II thermotolerance analyzed using Chl a fluorescence kinetics in barley varieties differing in their drought tolerance. Physiologia Plantarum 137 (2):188-199
(83) Živčák M, Brestič M, Olšovská K, Slamka P (2008) Performance index as a sensitive indicator of water stress in *Triticum aestivum* L. Plant Soil Environ 54 (4):133-13
(84) Bolat I, Dikilitas M, Ercisli S, Ikinci A, Tonkaz T (2014) The effect of water stress on some morphological, physiological, and biochemical characteristics and bud success on apple and quince rootstocks. The Scientific World Journal 2014
(85) Schöttler MA, Kirchhoff H, Weis E (2004) The role of plastocyanin in the adjustment of the photosynthetic electron transport to the carbon metabolism in tobacco. Plant physiology 136 (4):4265-4274
(86) Ammann M, Siegwolf R, Pichlmayer F, Suter M, Saurer M, Brunold C (1999) Estimating the uptake of traffic-derived NO_2 from ^{15}N abundance in Norway spruce needles. Oecologia 118 (2):124-131
(87) Tikkanen M, Aro E-M (2012) Thylakoid protein phosphorylation in dynamic regulation of photosystem II in higher plants. Biochimica et Biophysica Acta (BBA)-Bioenergetics 1817 (1):232-238
(88) Haldrup A, Jensen PE, Lunde C, Scheller HV (2001) Balance of power: a view of the mechanism of photosynthetic state transitions. Trends in plant science 6 (7):301-305
(89) Leigh A, Sevanto S, Close J, Nicotra A (2017) The influence of leaf size and shape on leaf thermal dynamics: does theory hold up under natural conditions? Plant, cell & environment 40 (2):237-248
(90) Liu M, Xin Z, Xu J, Sun F, Dou L, Li Y (2013) Influence of leaf size of plant on leaf transpiration and temperature in arid regions. Chinese Journal of Plant Ecology 37 (5):436-442
(91) DiMario RJ, Clayton H, Mukherjee A, Ludwig M, Moroney JV (2017) Plant carbonic anhydrases: structures, locations, evolution, and physiological roles. Molecular plant 10 (1):30-46
(92) Eskew DL, Welch RM, Cary EE (1983) Nickel: an essential micronutrient for legumes and possibly all higher plants. Science (New York, NY) 222 (4624):621-623
(93) Kalapos MP (2008) The tandem of free radicals and methylglyoxal. Chemico-biological interactions 171 (3):251-271
(94) Incesu M, Yeşiloğlu T, Cimen B, Yilmaz B (2015) Influences of different iron levels on plant growth and photosynthesis of *W. Murcott* mandarin grafted on two rootstocks under high pH conditions. Turkish Journal of Agriculture and Forestry 39 (5):838-844
(95) Langebartels C, Schraudner M, Heller W, Ernst D, Sandermann H (2002) Oxidative stress and defense reactions in plants exposed to air pollutants and UV-B radiation. Oxidative stress in plants Taylor and Francis, London:105-135
(96) Sharma YK, Davis KR (1997) The effects of ozone on antioxidant responses in plants. Free Radical Biology and Medicine 23 (3):480
(97) Reddy AR, Chaitanya KV, Vivekanandan M (2004) Drought-induced responses of photosynthesis and antioxidant metabolism in higher plants. Journal of plant physiology 161 (11):1189-1202
(98) Scandalios J (2005) Oxidative stress: molecular perception and transduction of signals triggering antioxidant gene defenses. Brazilian Journal of Medical and Biological Research 38 (7):995-1014
(99) Ali A, Alqurainy F (2006) Activities of antioxidants in plants under environmental stress. The lutein-prevention and treatment for diseases:187-256
(100) Zimmermann PZ, Ulrike (2005) The correlation between oxidative stress and leaf senescence during plant development. Cellular and Molecular Biology Letters 10 (3):51
(101) Padda MS, Picha D (2007) Antioxidant activity and phenolic composition in 'Beauregard'sweetpotato are affected by root size and leaf age. Journal of the American Society for Horticultural Science 132 (4):447-451
(102) Quan LJ, Zhang B, Shi WW, Li HY (2008) Hydrogen peroxide in plants: a versatile molecule of the reactive oxygen species network. Journal of Integrative Plant Biology 50 (1):2-1
(103) Gechev T, Gadjev I, Van Breusegem F, Inzé D, Dukiandjiev S, Toneva V, Minkov I (2002) Hydrogen peroxide protects tobacco from oxidative stress by inducing a set of antioxidant enzymes. Cellular and Molecular Life Sciences CMLS 59 (4):708-714
(104) Rizhsky L, Liang H, Mittler R (2002) The combined effect of drought stress and heat shock on gene expression in tobacco. Plant physiology 130 (3):1143-1151
(105) Scandalios JG, Guan L, Polidoros AN (1997) Catalases in plants: gene structure, properties, regulation, and expression. Cold Spring Harbor Monograph Series 34:343-406
(106) McClung CR (1997) Regulation of catalases in *Arabidopsis*. Free Radical Biology and Medicine 23 (3):489-496
(107) Zhong HH, Young JC, Pease EA, Hangarter RP, McClung CR (1994) Interactions between light and the circadian clock in the regulation of *CAT2* expression in *Arabidopsis*. Plant physiology 104 (3):889-898
(108) Scandalios JG (1993) Oxygen stress and superoxide dismutases. Plant physiology 101 (1):7
(109) Ghisla S, Massey V (1989) Mechanisms of flavoprotein-catalyzed reactions. In: EJB Reviews 1989. Springer, pp 29-45
(110) Wang J, Zhang H, Allen RD (1999) Overexpression of an *Arabidopsis* peroxisomal ascorbate peroxidase gene in tobacco increases protection against oxidative stress. Plant and Cell Physiology 40 (7):725-732
(111) Milla MAR, Maurer A, Huete AR, Gustafson JP (2003) Glutathione peroxidase genes in *Arabidopsis* are ubiquitous and regulated by abiotic stresses through diverse signaling pathways. The Plant Journal 36 (5):602-615
(112) Lakowicz JR, Szmacinski H, Nowaczyk K, Johnson ML (1992) Fluorescence lifetime imaging of free and protein-bound NADH. Proceedings of the National Academy of Sciences 89 (4):1271-1275
(113) Barile M, Anna Giancaspero T, Brizio C, Panebianco C, Indiveri C, Galluccio M, Vergani L, Eberini I, Gianazza E (2013) Biosynthesis of flavin cofactors in man: implications in health and disease. Current pharmaceutical design 19 (14):2649-2675
(114) Grace SC, Logan BA (2000) Energy dissipation and radical scavenging by the plant phenylpropanoid pathway. Philosophical Transactions of the Royal Society of London B: Biological Sciences 355 (1402):1499-1510
(115) Michalak A (2006) Phenolic compounds and their antioxidant activity in plants growing under heavy metal stress. Polish Journal of Environmental Studies 15 (4)

SUPPLEMENTAL INFORMATION

Content

Appendix A

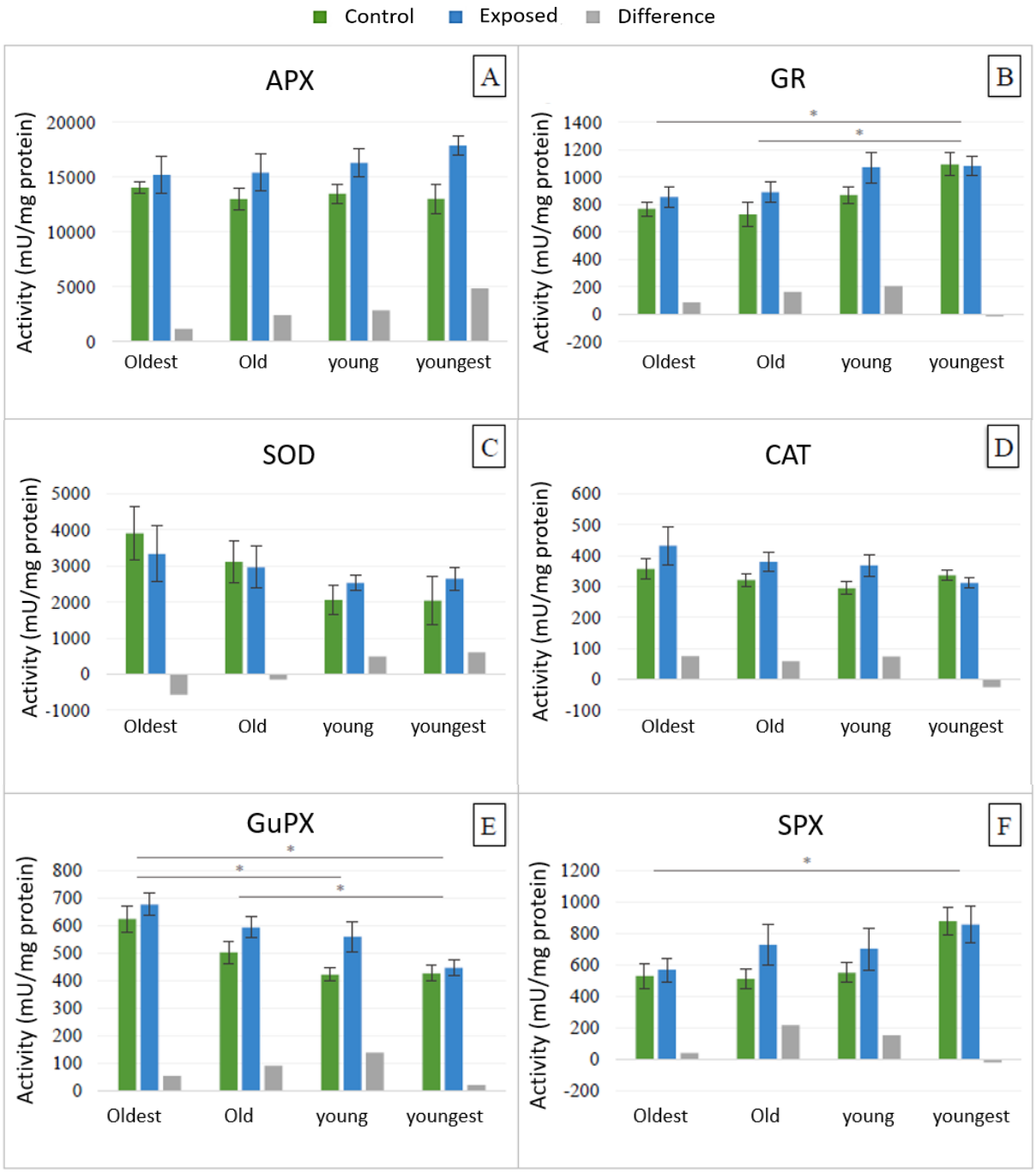

Fig. S1 – Activities of enzymes related to antioxidative pathways in leaves of *Brassica oleracea* var. *italica* exposed to diesel exhaust. n= 9. Data ± SE. Significant findings are denoted by an asterisk (* = $P < 0.05$). Horizontal bars represent comparisons between leaf age groups. (A) ascorbate peroxidase (APX), (B) glutathione reductase (GR), (C) superoxide dismutase (SOD), (D) catalase (CAT), (E) guaiacol peroxidase (GuPX), (F) syringaldazine peroxidase (SPX).

Appendix B

Table S1 - List of the sampling points in Hasselt.

Location of sampling point	Tree number	Coordinates of sampled trees
Schiervellaan 1	1	50°55'49.8"N, 5°19'57.5"E
	2	50°55'50.2"N, 5°19'57.7"E
Vrijwilligersplein 14	3	50°56'01.5"N, 5°19'53.4"E
Rozenstraat 1	4	50°56'01.7"N, 5°19'54.1"E
Thonissenlaan 81	5	50°56'02.6"N, 5°20'21.7"E
Martelarenlaan 2	6	50°56'02.4"N, 5°20'22.6"E
Martelarenlaan 17	7	50°55'57.7"N, 5°20'32.6"E
Maastrichtersteenweg 1	8	50°55'49.9"N, 5°20'40.8"E
Guldensporenplein 4	9	50°55'49.7"N, 5°20'40.5"E
Guffenslaan 84	10	50°55'43.5"N, 5°20'32.2"E
	11	50°55'43.0"N, 5°20'31.6"E
Kapermolen Park (reference site)	12[a]	50°56'08.4"N, 5°20'54.3"E
	13[a]	50°56'08.0"N, 5°20'53.9"E

a. Tree number 12 and 13 in Kapermolen Park were sampled both at the start and the end of the campaign.

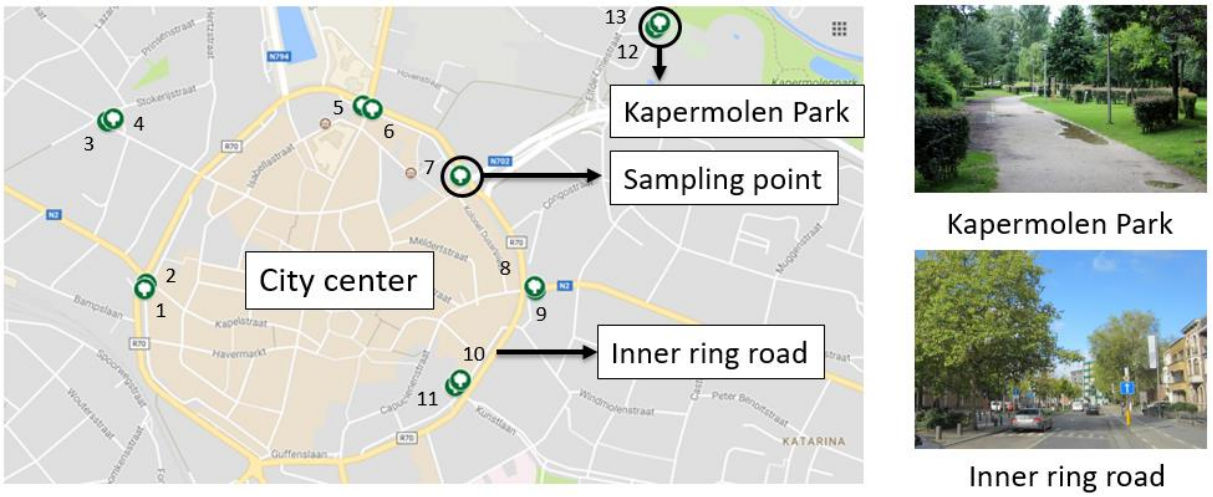

Fig. S2 – **Map of the city center of Hasselt with the location of the sampling points indicated.** The green icons with a white tree represent the locations of the sampled trees. The numbers correspond with the tree numbers of Table S1.

Appendix C

Table S2 - Composition of the Hoagland solution.

Macro-elements
0.1 M KNO_3
0.3 M $Ca(NO_3)_2.4H_2O$
0.2 M $NH_4H_2PO_4$
0.2 M $MgSO_4.7H_2O$

Micro-elements
0.05 M H_3BO_3
0.01 M $MnCl_2.4H_2O$
3 µM $CuSO_4.5H_2O$
0.5 µM $H_2MoO_4.H_2O$
0.77 µM $ZnSO_4.7H_2O$
0.03 M Fe-EDTA

Appendix D

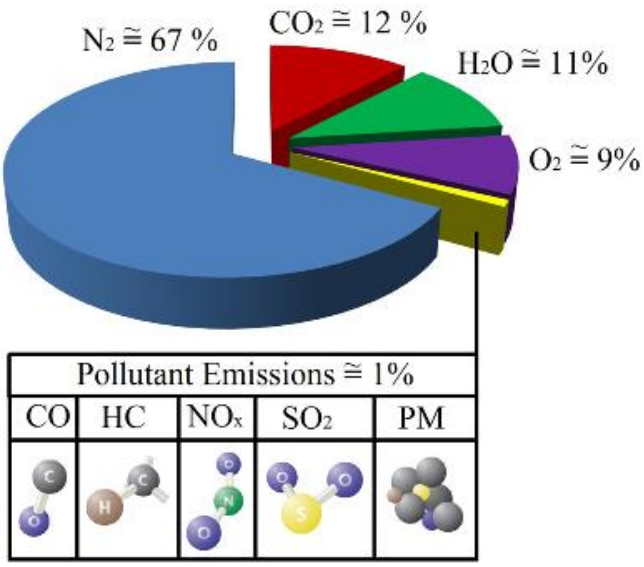

Fig. S3 – **Composition of diesel exhaust emission.** Harmful pollutants represent approximately 1% of total emissions, and are comprised of carbon monoxide (CO), hydrocarbons (HC), nitrogen oxides (NO_x), sulphur dioxide (SO_2) and particulate matter (PM). (From Reşitoğlu et al. 2014)[70]

Appendix E

Table S3 - Primer list and details of investigated genes in this study (part 1).

Database Genome Species	Database	Gene	Annotation	Subcellular localization
Brassica oleracea var. *capitata*	Phytozome	*CAT-1*	Catalase isozyme 1	Peroxisome/cytosol
Brassica oleracea var. *capitata*	Phytozome	*CAT-2*	Catalase isozyme 2	Peroxisome/cytosol
Brassica oleracea var. *capitata*	Phytozome	*CAT-3*	Catalase isozyme 3	Peroxisome/cytosol
Brassica oleracea var. *capitata*	Phytozome	*Fe-SOD 1*	Superoxide dismutase [Fe] 1, chloroplastic	Chloroplast
Brassica oleracea var. *capitata*	Phytozome	*Cu/Zn-SOD 1*	Superoxide dismutase [Cu-Zn] 1, chloroplastic	Chloroplast
Brassica oleracea var. *capitata*	Phytozome	*Mn-SOD 2*	Superoxide dismutase [Mn] 2, mitochondrial	Mitochondrion
Brassica oleracea var. *oleracea* (wild cabbage)	NCBI	*APX 1*	L-ascorbate peroxidase 1, cytosolic	Cytosol
Brassica oleracea var. *oleracea* (wild cabbage)	NCBI	*APX 3*	L-ascorbate peroxidase 3, peroxisomal	Peroxisome
Brassica oleracea var. *oleracea* (wild cabbage)	NCBI	*APX 6*	L-ascorbate peroxidase 6, chloroplastic	Chloroplast
Brassica oleracea var. *oleracea* (wild cabbage)	NCBI	*APX S*	L-ascorbate peroxidase S, chloroplastic-mitochondrial	Chloroplast/ Mitochondrion
Brassica oleracea var. *oleracea* (wild cabbage)	NCBI	*APX T*	L-ascorbate peroxidase T, chloroplastic	Chloroplast
Brassica oleracea var. *oleracea* (wild cabbage)	NCBI	*GR 1*	Glutathione reductase, chloroplastic	Chloroplast
Brassica oleracea var. *oleracea* (wild cabbage)	NCBI	*GR 1*	Glutathione reductase, cytosolic	Cytosol
Brassica oleracea var. *oleracea* (wild cabbage)	NCBI	*GPX 1*	Phospholipid hydroperoxide glutathione peroxidase 1, chloroplastic	Chloroplast
Brassica oleracea var. *oleracea* (wild cabbage)	NCBI	*GPX 2*	Probable glutathione peroxidase 2, cytosolic	Cytosol
Brassica oleracea var. *oleracea* (wild cabbage)	NCBI	*GPX 3*	Probable glutathione peroxidase 3, mitochondria	Mitochondrion

Table S3 - Primer list and details of investigated genes in this study (continued).

Forward sequence	Reverse sequence	Primer efficiency (%)	Amplicon size (bp)
TGGAAACCGTGAGAAGTGCA	CACGAACCTCTCTTGCCTGT	96.44	100
CACAGGGACGAGGAGGTAAAC	TCACGTTTCCCAGAGCAGAC	103.74	101
CCACAGCCACGCAACTAAAG	TCACATCAAGCGGGTCGAAA	87.70	128
ATCTCGACTTCCAGAACCGC	TCAGGAAGAAGCAGCCTTGG	94.62	113
ACTCTATTGTCGGAAGGGCC	ATAATACCACAAGCAACACGGC	98.54	118
CACGCCTACTATCCACAGTACA	TCACGAATATGTCCGAAGCGT	93.25	97
AGCAGTTCCCTACCATCTCCT	GCTTGTCCTCTCTTCCAGGG	94.44	111
GGATATTGTAGCACTCTCAGGGG	TCTCCTTTTAGCAGTTCCACG	94.90	132
CAGGTGGCATCAATGGGTCT	CGATCATATCCGCCCAAGACA	93.55	138
AAGTACACGAAAGAGGGGCC	CATCAGTGGGCAGGACAAGA	93.90	133
TGTAGAGGAGGCTGGTGGTC	ATGATCCGCTGGTGAAGGTG	90.45	118
GCTGTTGGGGATGTCACTGA	GGGAACAGCTCTATAATCAGGCT	100.44	120
CATCCATGTGCGGTCCAGAT	GTATCCCAACCGTGCTGTCA	96.55	102
CGCGAATCTGAGTAATGGGC	ACCATCAATGTCCTTTACGGTGA	105.32	139
GGGACAAGAACCAGGAAACAATG	CCCGTTCACATCTACCTTGTCA	90.04	97
CAACGTAGCCTCTAAGTGTGGT	AATTGGTTGCAGGGGAAACGC	92.11	114

Appendix F

Table S4 - List of selected parameters of chlorophyll fluorescence induction kinetics used in this research.

PARAMETER	DESCRIPTION
OJIP PARAMETERS	
F_0	Minimal fluorescence when all PSII reaction centers are open (at t=0)
F_M	Maximal fluorescence when all PSII reaction centers are closed
ϕ_{P0}	Maximal yield of primary photochemistry (=TR_0/RC: Trapped energy flux at t=0 (TR_0) per reaction center (RC))
Ψ_0	Probability that a trapped exciton moves an electron into the electron transport chain beyond Q_A^- (=ET_0/TR_0)
ABS/RC	Light absorption flux for PSII antenna chlorophylls (ABS) per reaction center (RC)
DI_0/RC	Dissipated energy flux (DI_0) per reaction center (RC) (at t=0)
PI(CSm)	Performance Index (PI) on cross-section basis (approximated by F_m)
SLOW CHLOROPHYLL INDUCTION KINETICS	
Y(II)	Effective photochemical quantum yield of PSII
Y(NO)	Quantum yield of non-photochemical energy conversion in PSII other than that caused by down-regulation of the light-harvesting function
Y(NPQ)	Quantum yield of non-photochemical energy conversion in PSII due to down-regulation of the light-harvesting function
NPQ	Non-photochemical fluorescence quenching: quantification of non-photochemical quenching alternative to qN calculations
qN	Coefficient of non-photochemical fluorescence quenching
qL	Coefficient of photochemical fluorescence quenching assuming that all reaction centres share a common light-harvesting antenna (lake model)
qP	Coefficient of photochemical fluorescence quenching, based on a model of separate photosynthetic units (puddle model)
ETR	Electron transport rate in µmol electrons/(m^2.s)
F	Continuously recorded fluorescence (steady-state)

Appendix G

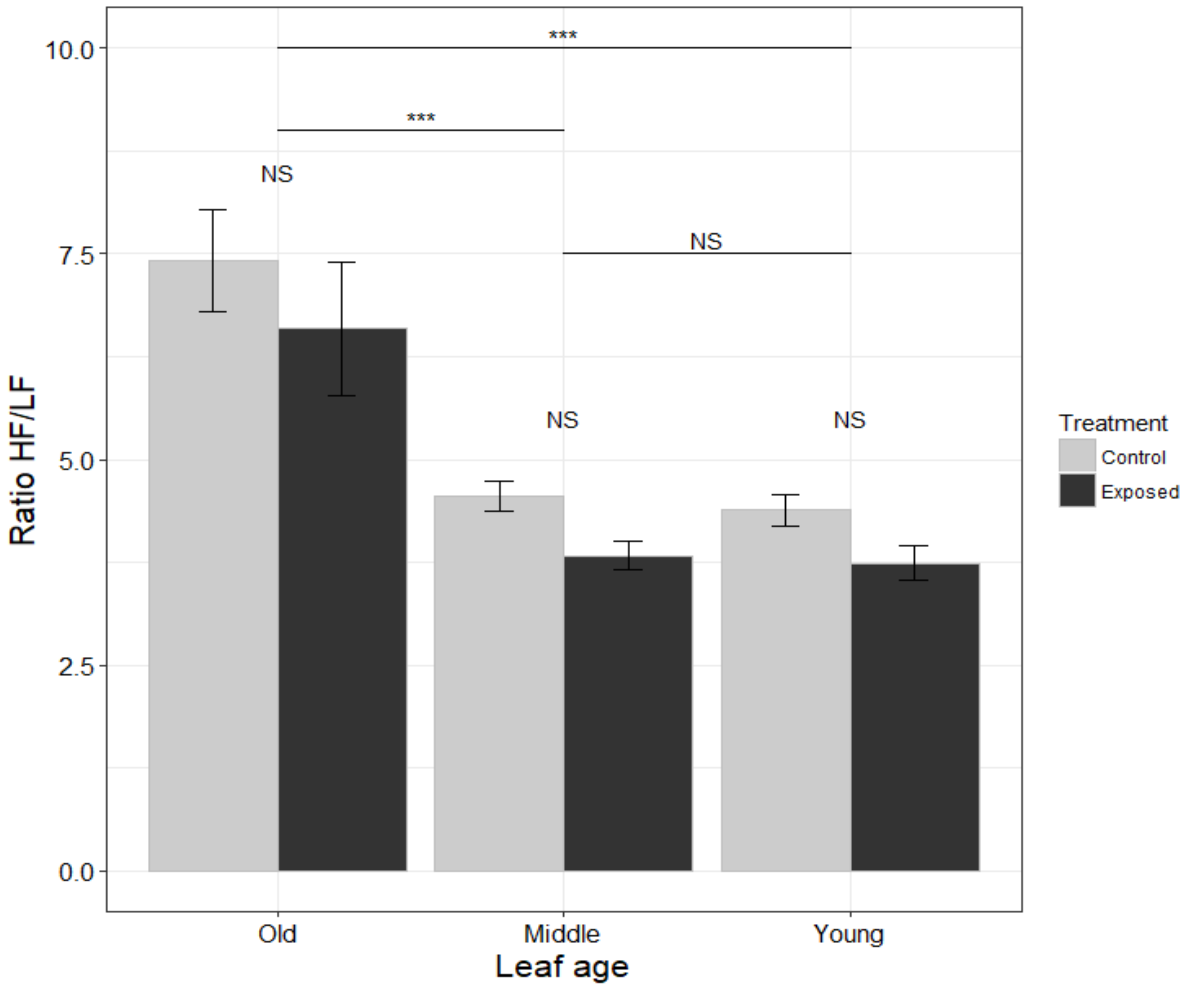

Fig. S4 – HF/LF ratio of the TAC of leaves of *Brassica oleracea* var. *italica* exposed to diesel exhaust. Error bars are ± SE. Significant findings are denoted by an asterisk (* = $P < 0.05$, ** = $P < 0.01$, *** = $P < 0.001$, two-way ANOVA with Tukey-Kramer correction for multiple comparison). NS, Not Significant. Bar plot created in RStudio using the ggplot2 package.

Appendix H

Table S5 - List of p-values of differentially expressed genes related to antioxidative pathways in leaves of *Brassica oleracea* var. *italica* exposed to diesel exhaust. n=9. (data corresponding to expression data of Table 6, one-way ANOVA, analysis performed in RStudio). Genes: catalase (*CAT1*, *CAT2*, and *CAT3*), iron superoxide dismutase (*Fe-SOD1*), copper/zinc superoxide dismutase (*Cu/Zn-SOD1*), manganese superoxide dismutase (*MnSOD2*), glutathione reductase (*GR1 (Chl)* (chloroplastic) and *GR1 (Cyt)* (cytosolic)), ascorbate peroxidase (*APX1*, *APX3*, *APX6*, *APXS* (stromal), *APXT* (thylakoid)), glutathione peroxidase (*GPX1*, *GPX2*, and *GPX3*).

Treatment	Leaf age			Genes
	Old	Middle	Young	
Control	Reference	Reference	Reference	***CAT1***
Exposed	0.963	0.294	0.096	
Control	Reference	Reference	Reference	***CAT2***
Exposed	0.573	0.180	$3.5*10^{-4}$	
Control	Reference	Reference	Reference	***CAT3***
Exposed	0.002	0.003	0.002	
Control	Reference	Reference	Reference	***Fe-SOD1***
Exposed	0.871	0.541	0.661	
Control	Reference	Reference	Reference	***Cu/Zn-SOD1***
Exposed	0.722	0.368	0.169	
Control	Reference	Reference	Reference	***MnSOD2***
Exposed	0.969	0.731	0.002	
Control	Reference	Reference	Reference	***GR1 (Chl)***
Exposed	0.003	0.706	0.677	
Control	Reference	Reference	Reference	***GR1 (Cyt)***
Exposed	0.845	0.597	0.164	
Control	Reference	Reference	Reference	***APX1***
Exposed	0.816	0.324	0.736	
Control	Reference	Reference	Reference	***APX3***
Exposed	0.271	0.344	0.577	
Control	Reference	Reference	Reference	***APX6***
Exposed	0.756	0.531	0.357	
Control	Reference	Reference	Reference	***APXS***
Exposed	0.919	0.192	0.005	
Control	Reference	Reference	Reference	***APXT***
Exposed	0.076	0.041	0.476	
Control	Reference	Reference	Reference	***GPX1***
Exposed	0.938	0.520	0.689	
Control	Reference	Reference	Reference	***GPX2***
Exposed	0.215	0.865	0.578	
Control	Reference	Reference	Reference	***GPX3***
Exposed	0.293	0.033	0.310	

Table S6 - List of p-values of differentially expressed genes related to antioxidative pathways in leaves of *Brassica oleracea* var. *italica* exposed to diesel exhaust. n=9. (data corresponding to expression data of Table 7, one-way ANOVA, analysis performed in RStudio). Genes: catalase (*CAT1*, *CAT2*, and *CAT3*), iron superoxide dismutase (*Fe-SOD1*), copper/zinc superoxide dismutase (*Cu/Zn-SOD1*), manganese superoxide dismutase (*MnSOD2*), glutathione reductase (*GR1 (Chl)* (chloroplastic) and *GR1 (Cyt)* (cytosolic)), ascorbate peroxidase (*APX1*, *APX3*, *APX6*, *APXS* (stromal), *APXT* (thylakoid)), glutathione peroxidase (*GPX1*, *GPX2*, and *GPX3*). Old-Young, old and young leaves compared.

Treatment	Leaf age				Genes
	Old	Middle	Young	Old-Young	
Control	0.003	Reference	0.433	$1.4*10^{-4}$	***CAT1***
Exposed	0.014	Reference	0.740	0.002	
Control	0.063	Reference	0.790	0.015	***CAT2***
Exposed	0.004	Reference	0.367	$1.2*10^{-4}$	
Control	0.812	Reference	0.442	0.810	***CAT3***
Exposed	0.997	Reference	0.851	0.889	
Control	0.038	Reference	0.069	$1.3*10^{-4}$	***Fe-SOD1***
Exposed	0.012	Reference	0.108	$6.6*10^{-5}$	
Control	0.009	Reference	0.080	$3.3*10^{-5}$	***Cu/Zn-SOD1***
Exposed	0.008	Reference	0.868	0.025	
Control	0.990	Reference	0.961	0.914	***MnSOD2***
Exposed	0.783	Reference	$9.6*10^{-5}$	$1.8*10^{-5}$	
Control	0.754	Reference	0.856	0.999	***GR1 (Chl)***
Exposed	$1.0*10^{-4}$	Reference	0.694	$8.1*10^{-4}$	
Control	$3.7*10^{-4}$	Reference	0.310	$8.7*10^{-6}$	***GR1 (Cyt)***
Exposed	$3.2*10^{-4}$	Reference	0.058	$8.0*10^{-7}$	
Control	0.026	Reference	0.136	$2.0*10^{-4}$	***APX1***
Exposed	$3.1*10^{-4}$	Reference	0.163	$2.9*10^{6}$	
Control	0.641	Reference	0.983	0.748	***APX3***
Exposed	0.518	Reference	0.997	0.559	
Control	0.001	Reference	0.165	0.001	***APX6***
Exposed	0.001	Reference	0.206	0.001	
Control	0.321	Reference	0.800	0.107	***APXS***
Exposed	0.011	Reference	0.140	$8.5*10^{-5}$	
Control	0.421	Reference	0.005	$2.0*10^{-4}$	***APXT***
Exposed	0.575	Reference	0.521	0.107	
Control	0.387	Reference	0.450	0.043	***GPX1***
Exposed	0.319	Reference	0.714	0.080	
Control	0.527	Reference	0.903	0.776	***GPX2***
Exposed	0.290	Reference	0.966	0.194	
Control	0.680	Reference	0.714	0.252	***GPX3***
Exposed	0.033	Reference	0.789	0.007	

Table S7 - Non-normalized data of differentially expressed genes related to antioxidative pathways in leaves of *Brassica oleracea* var. *italica* exposed to diesel exhaust. n=9. Data ± SE. Data corresponding to expression data of Table 6. Genes: catalase (*CAT1*, *CAT2*, and *CAT3*), iron superoxide dismutase (*Fe-SOD1*), copper/zinc superoxide dismutase (*Cu/Zn-SOD1*), manganese superoxide dismutase (*MnSOD2*), glutathione reductase (*GR1 (Chl)* (chloroplastic) and *GR1 (Cyt)* (cytosolic)), ascorbate peroxidase (*APX1*, *APX3*, *APX6*, *APXS* (stromal), *APXT* (thylakoid)), glutathione peroxidase (*GPX1*, *GPX2*, and *GPX3*).

Treatment	Leaf age			Genes
	Old	Middle	Young	
Control	1.00 ± 0.14	1.00 ± 0.14	1.00 ± 0.15	***CAT1***
Exposed	0.99 ± 0.13	1.23 ± 018	1.33 ± 0.15	
Control	1.00 ± 0.18	1.00 ± 0.16	1.00 ± 0.06	***CAT2***
Exposed	0.78 ± 0.09	0.73 ± 0.14	0.60 ± 0.06	
Control	1.00 ± 0.23	1.00 ± 0.17	1.00 ± 0.20	***CAT3***
Exposed	2.59 ± 0.51	2.39 ± 0.38	2.76 ± 0.53	
Control	1.00 ± 0.07	1.00 ± 0.11	1.00 ± 0.13	***Fe-SOD1***
Exposed	0.97 ± 0.06	0.93 ± 0.12	0.90 ± 0.10	
Control	1.00 ± 0.11	1.00 ± 0.11	1.00 ± 0.13	***Cu/Zn-SOD1***
Exposed	0.91 ± 0.09	0.92 ± 0.23	1.56 ± 0.38	
Control	1.00 ± 0.17	1.00 ± 0.25	1.00 ± 0.32	***MnSOD2***
Exposed	0.97 ± 0.14	0.63 ± 0.12	0.17 ± 0.05	
Control	1.00 ± 0.06	1.00 ± 0.10	1.00 ± 0.08	***GR1 (Chl)***
Exposed	1.35 ± 0.08	1.01 ± 0.05	1.02 ± 0.04	
Control	1.00 ± 0.09	1.00 ± 0.07	1.00 ± 0.04	***GR1 (Cyt)***
Exposed	1.00 ± 0.05	0.95 ± 0.06	0.86 ± 0.08	
Control	1.00 ± 0.11	1.00 ± 0.09	1.00 ± 0.07	***APX1***
Exposed	1.03 ± 0.12	0.89 ± 0.05	0.97 ± 0.08	
Control	1.00 ± 0.04	1.00 ± 0.06	1.00 ± 0.06	***APX3***
Exposed	1.17 ± 0.11	0.92 ± 0.07	0.96 ± 0.09	
Control	1.00 ± 0.19	1.00 ± 0.08	1.00 ± 0.06	***APX6***
Exposed	0.81 ± 0.11	0.93 ± 0.07	1.11 ± 0.07	
Control	1.00 ± 0.31	1.00 ± 0.10	1.00 ± 0.05	***APXS***
Exposed	0.96 ± 0.06	0.83 ± 0.07	0.74 ± 0.05	
Control	1.00 ± 0.19	1.00 ± 0.09	1.00 ± 0.06	***APXT***
Exposed	1.34 ± 0.14	1.35 ± 0.13	0.93 ± 0.11	
Control	1.00 ± 0.06	1.00 ± 0.07	1.00 ± 0.10	***GPX1***
Exposed	1.02 ± 0.08	0.95 ± 0.10	0.98 ± 0.15	
Control	1.00 ± 0.06	1.00 ± 0.05	1.00 ± 0.06	***GPX2***
Exposed	1.08 ± 0.04	0.99 ± 0.07	0.97 ± 0.12	
Control	1.00 ± 0.07	1.00 ± 0.03	1.00 ± 0.06	***GPX3***
Exposed	1.07 ± 0.04	0.88 ± 0.04	0.90 ± 0.08	

Table S8 - Non-normalized data of differentially expressed genes related to antioxidative pathways in leaves of *Brassica oleracea* var. *italica* exposed to diesel exhaust. n=9. Data ± SE. Data corresponding to expression data of Table 7. Genes: catalase (*CAT1*, *CAT2*, and *CAT3*), iron superoxide dismutase (*Fe-SOD1*), copper/zinc superoxide dismutase (*Cu/Zn-SOD1*), manganese superoxide dismutase (*MnSOD2*), glutathione reductase (*GR1 (Chl)* (chloroplastic) and *GR1 (Cyt)* (cytosolic)), ascorbate peroxidase (*APX1*, *APX3*, *APX6*, *APXS* (stromal), *APXT* (thylakoid)), glutathione peroxidase (*GPX1*, *GPX2*, and *GPX3*).

Treatment	Leaf age			Genes
	Old	Middle	Young	
Control	2.09 ± 0.29	1.00 ± 0.14	0.79 ± 0.12	***CAT1***
Exposed	1.69 ± 0.22	1.00 ± 0.14	0.86 ± 0.10	
Control	1.79 ± 0.32	1.00 ± 0.16	0.79 ± 0.04	***CAT2***
Exposed	1.92 ± 0.21	1.00 ± 0.19	0.65 ± 0.06	
Control	0.91 ± 0.21	1.00 ± 0.17	0.77 ± 0.15	***CAT3***
Exposed	0.99 ± 0.20	1.00 ± 0.16	0.89 ± 0.17	
Control	1.49 ± 0.11	1.00 ± 0.11	0.72 ± 0.09	***Fe-SOD1***
Exposed	1.56 ± 0.09	1.00 ± 0.13	0.69 ± 0.08	
Control	1.86 ± 0.21	1.00 ± 0.11	0.68 ± 0.09	***Cu/Zn-SOD1***
Exposed	1.84 ± 0.17	1.00 ± 0.25	1.16 ± 0.28	
Control	0.77 ± 0.13	1.00 ± 0.25	0.87 ± 0.28	***MnSOD2***
Exposed	1.19 ± 0.17	1.00 ± 0.19	0.23 ± 0.07	
Control	1.06 ± 0.06	1.00 ± 0.10	1.05 ± 0.09	***GR1 (Chl)***
Exposed	1.42 ± 0.08	1.00 ± 0.05	1.05 ± 0.04	
Control	1.67 ± 0.15	1.00 ± 0.07	0.84 ± 0.04	***GR1 (Cyt)***
Exposed	1.76 ± 0.10	1.00 ± 0.07	0.77 ± 0.08	
Control	1.58 ± 0.17	1.00 ± 0.09	0.74 ± 0.05	***APX1***
Exposed	1.84 ± 0.21	1.00 ± 0.06	0.80 ± 0.07	
Control	0.93 ± 0.04	1.00 ± 0.06	0.99 ± 0.06	***APX3***
Exposed	1.18 ± 0.11	1.00 ± 0.08	1.03 ± 0.10	
Control	5.21 ± 0.74	1.00 ± 0.07	0.77 ± 0.05	***APX6***
Exposed	5.96 ± 1.12	1.00 ± 0.08	0.64 ± 0.04	
Control	1.21 ± 0.12	1.00 ± 0.10	0.89 ± 0.04	***APXS***
Exposed	1.41 ± 0.09	1.00 ± 0.09	0.80 ± 0.06	
Control	0.87 ± 0.17	1.00 ± 0.09	1.78 ± 0.12	***APXT***
Exposed	0.86 ± 0.09	1.00 ± 0.10	1.23 ± 0.14	
Control	1.15 ± 0.07	1.00 ± 0.07	0.89 ± 0.09	***GPX1***
Exposed	1.24 ± 0.10	1.00 ± 0.11	0.92 ± 0.14	
Control	1.10 ± 0.06	1.00 ± 0.05	1.04 ± 0.06	***GPX2***
Exposed	1.20 ± 0.04	1.00 ± 0.07	1.02 ± 0.13	
Control	1.08 ± 0.07	1.00 ± 0.03	0.95 ± 0.06	***GPX3***
Exposed	1.32 ± 0.05	1.00 ± 0.04	0.97 ± 0.09	

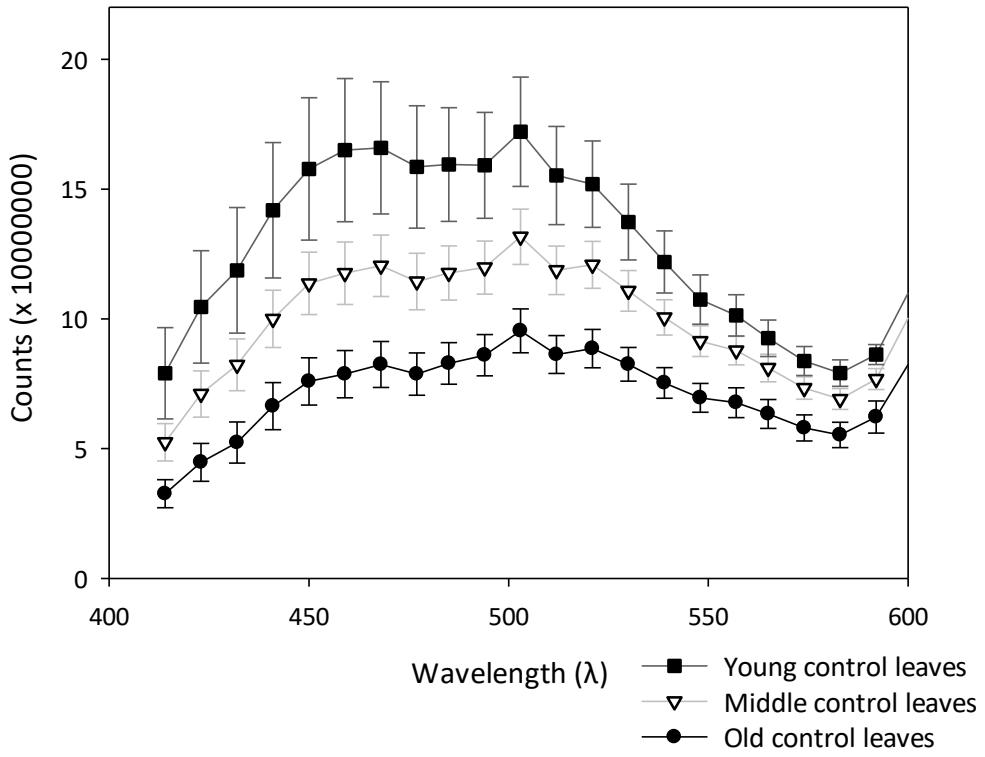

Fig. S5 – Non-normalized cross-section fluorescence emission spectra in the blue-green region of control leaves of *Brassica oleracea* var. *italica*. Error bars are ± SE. Line graph created in SigmaPlot.

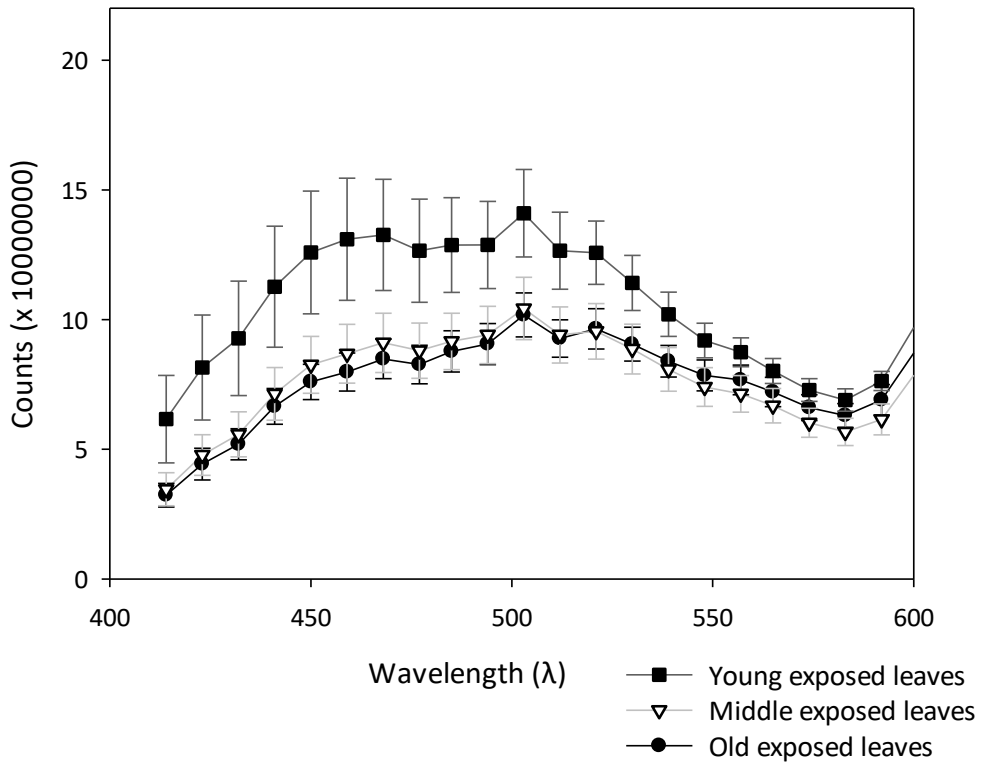

Fig. S6 – Non-normalized cross-section fluorescence emission spectra in the blue-green region of leaves of *Brassica oleracea* var. *italica* exposed to diesel exhaust. Error bars are ± SE. Line graph created in SigmaPlot.

Table S9 - List of p-values of non-normalized fluorescence emission spectra in leaves of *Brassica oleracea* var. *italica* exposed to diesel exhaust. One-way ANOVA. Significant values ($P > 0.05$) are marked in red. Control leaves corresponds to Fig. S5. Exposed leaves corresponds to Fig. S6. O-M, old versus middle leaves; M-Y, middle versus young leaves; O-Y, old versus young leaves. Between treatments, control versus exposed leaves.

Wavelength (nm)	Control leaves			Exposed leaves			Between treatments		
	O-M	M-Y	O-Y	O-M	M-Y	O-Y	Old	Middle	Young
432	0.459	0.324	0.040	0.620	0.074	0.010	0.173	0.056	0.275
441	0.435	0.286	0.031	0.589	0.061	0.007	0.169	0.057	0.278
450	0.391	0.286	0.027	0.532	0.058	0.005	0.156	0.052	0.260
459	0.373	0.242	0.020	0.516	0.047	0.003	0.159	0.054	0.261
468	0.344	0.229	0.016	0.503	0.043	0.003	0.168	0.058	0.261
477	0.333	0.200	0.013	0.514	0.038	0.003	0.188	0.065	0.277
485	0.307	0.194	0.011	0.526	0.036	0.003	0.203	0.067	0.275
494	0.290	0.196	0.011	0.542	0.037	0.003	0.208	0.064	0.253
503	0.269	0.202	0.010	0.533	0.037	0.003	0.226	0.071	0.268
512	0.266	0.194	0.009	0.531	0.037	0.003	0.229	0.072	0.261
521	0.210	0.233	0.009	0.514	0.045	0.003	0.257	0.077	0.253
530	0.210	0.251	0.010	0.535	0.054	0.004	0.330	0.087	0.260
539	0.177	0.278	0.009	0.528	0.068	0.006	0.330	0.102	0.269
548	0.159	0.347	0.011	0.577	0.091	0.010	0.423	0.132	0.311
557	0.149	0.393	0.012	0.589	0.117	0.014	0.466	0.150	0.317
565	0.174	0.454	0.018	0.682	0.157	0.030	0.581	0.195	0.356
574	0.150	0.393	0.012	0.674	0.132	0.023	0.560	0.179	0.344
583	0.170	0.376	0.013	0.752	0.119	0.028	0.603	0.180	0.352
592	0.156	0.431	0.014	0.788	0.117	0.031	0.519	0.129	0.278

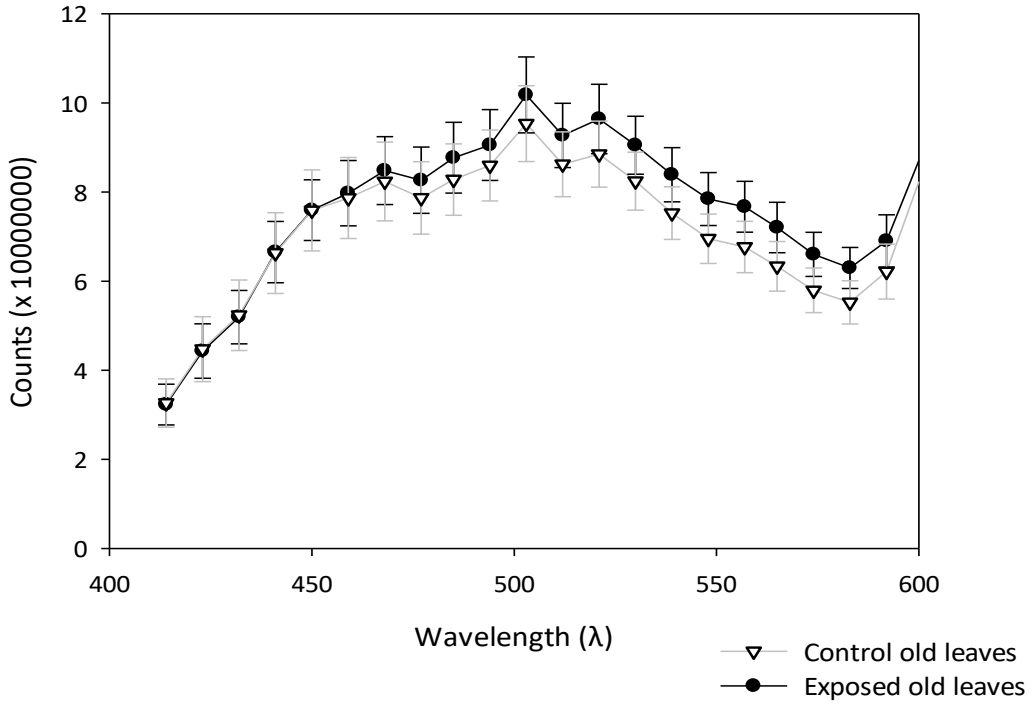

Fig. S7 – Non-normalized cross-section fluorescence emission spectra in the blue-green region of old leaves of *Brassica oleracea* var. *italica* exposed to diesel exhaust. Error bars are ± SE. Line graph created in SigmaPlot.

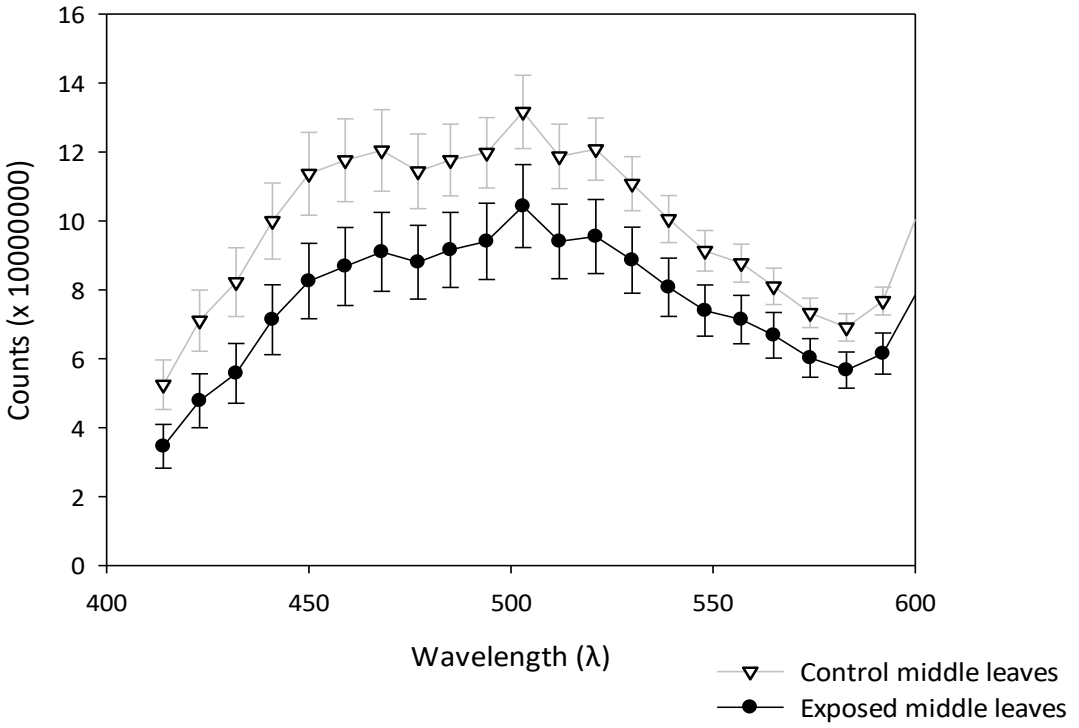

Fig. S8 – Non-normalized cross-section fluorescence emission spectra in the blue-green region of middle leaves of *Brassica oleracea* var. *italica* exposed to diesel exhaust. Error bars are ± SE. Line graph created in SigmaPlot.

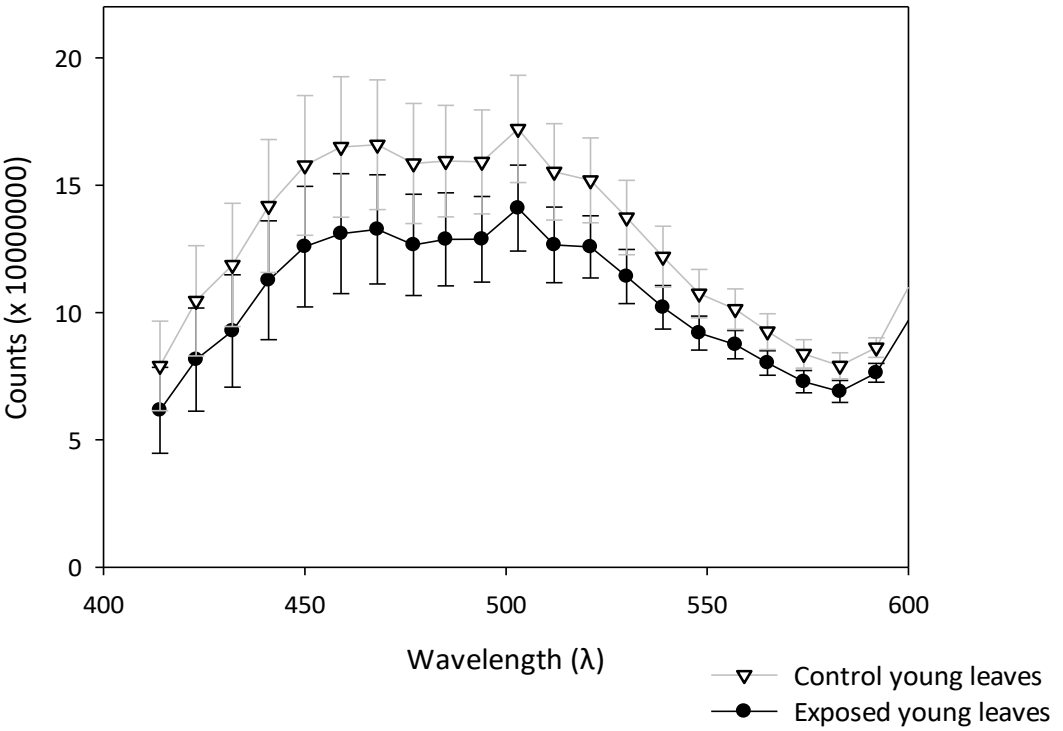

Fig. S9 – Non-normalized cross-section fluorescence emission spectra in the blue-green region of young leaves of *Brassica oleracea* var. *italica* exposed to diesel exhaust. Error bars are ± SE. Line graph created in SigmaPlot.

Auteursrechtelijke overeenkomst

Ik/wij verlenen het wereldwijde auteursrecht voor de ingediende eindverhandeling:
**Vegetation exposed to traffic exhaust: a dual study of chlorophyll fluorescence kinetics in Platanus x acerifolia and antioxidative responses in Brassica oleracea var. italica

**

Richting: **master in de biomedische wetenschappen-milieu en gezondheid**
Jaar: **2018**

in alle mogelijke mediaformaten, - bestaande en in de toekomst te ontwikkelen - , aan de Universiteit Hasselt.

Niet tegenstaand deze toekenning van het auteursrecht aan de Universiteit Hasselt behoud ik als auteur het recht om de eindverhandeling, - in zijn geheel of gedeeltelijk -, vrij te reproduceren, (her)publiceren of distribueren zonder de toelating te moeten verkrijgen van de Universiteit Hasselt.

Ik bevestig dat de eindverhandeling mijn origineel werk is, en dat ik het recht heb om de rechten te verlenen die in deze overeenkomst worden beschreven. Ik verklaar tevens dat de eindverhandeling, naar mijn weten, het auteursrecht van anderen niet overtreedt.

Ik verklaar tevens dat ik voor het materiaal in de eindverhandeling dat beschermd wordt door het auteursrecht, de nodige toelatingen heb verkregen zodat ik deze ook aan de Universiteit Hasselt kan overdragen en dat dit duidelijk in de tekst en inhoud van de eindverhandeling werd genotificeerd.

Universiteit Hasselt zal mij als auteur(s) van de eindverhandeling identificeren en zal geen wijzigingen aanbrengen aan de eindverhandeling, uitgezonderd deze toegelaten door deze overeenkomst.

Voor akkoord,

Lenaers, Mathias